*Department of Civil and*

*Environmental Engineering,*

*University College Cork.*


# *Rainfall Analysis and Flood Hydrograph Determination in the Munster Blackwater Catchment*

By

Paul Guéro

*A Thesis submitted for the*

*Degree of Master of Engineering Science*

***October 2006***

# Acknowledgements

The author wishes to express his thanks to the following people:

**Prof. Ger Kiely**, my supervisor, for his guidance and his encouragement.

**Prof. J.P.J. O'Kane**, for the use of the facilities of the Department of Civil and Environmental Engineering, U.C.C.

**Dr. Micheal Creed**, for his warm welcoming and administrative support.

**Cecile Delolme**, for help and encouragement to come to Ireland.

**The helpful staff at Met Éireann,** particularly Mr. Niall Brooks and Ms. Mary Curley.

**The helpful staff at the Office of Public Work,** particularly Mr. Mark Hayes and Mr. Peter Newport.

**The helpful staff at the Environmental Protection Agency,** particularly Mr. Micheal McCarthaigh.

**Paul Leahy**, for his patience, his more than grateful help throughout the year and his friendship.

**Julien Gillet**, for his wise advices and his friendship.

**Ken Byrne, Matteo Sottocornola, Adrian Birkby, Anna Laine, James Eaton, Sylvia , Anne Brune and Micheal Fenton** for their permanent help and their friendship throughout the year.

**Barbara Orellana,** for her precious help

**Cedric Besairie and his friend D.G. Pah**

# Abstract

The Munster Blackwater catchment, in the South West of Ireland, is regularly subject to flooding, particularly in the towns of Mallow and Fermoy where it causes many disturbances for its inhabitants and sometimes severe economic losses. A good understanding of rainfall-runoff processes is therefore important in order to prevent such situations.

In the first part of this project, particular attention was given to rainfall data. The installation of a 32 tipping buckets network in the catchment, ranging in both longitude and elevation provides precise time-scaled information. Detailed analysis of spatial and temporal variation over the catchment was examined. The existence of an intensity gradient from West to East, and a neat correlation between elevation and rainfall depth were highlighted. It explains the higher runoff over catchment area observed in the West, which are responsible for rising of water level downstream in the East. Particular attention was also given to the 2006 spring and summer that appeared to be a significantly dry period. A drought assessment showed that 2006 was comparable to 1976, when the most important dry period was recorded in Ireland.

The Unit Hydrograph is the surface runoff hydrograph resulting from one unit of rainfall excess uniformly distributed spatially and temporally over a watershed for a specified duration. In the second part of the project, three different approaches of this concept (the synthetic Nash Instantaneous Unit Hydrograph, the analysis-based Ordinates Method and the "in between" Geomorphological Unit Hydrograph of Reservoirs) were studied. The Unit Hydrograph concept was incorporated in a rainfall-runoff model structure, which was applied at the outlet of the three nested sub-catchments along the river: Duarrigle (245 $km^2$), Dromcummer (861 $km^2$) and Killavulen (1265 $km^2$). A comparison of the simulation results using several storms identified the Nash Instantaneous Unit Hydrograph as being the more efficient method, and the approach providing the best flood hydrograph determination. The model efficiency appears to be dependent on the catchment size and the model should not be applied to drainage areas greater than about 500 $km^2$.

# Table of contents

# Chapter 1 Introduction

## 1.1 Introduction

The natural feature of flooding occurs when excess rainfall can not be absorbed by the receiving soils or discharged fast enough by the stream network. In these conditions, the river sees its depth rising until the water can overtop its banks and spread throughout the adjacent flood plains. In areas were the river bed is surrounded by relatively flat lands, the flood plain can therefore be rapidly covered with a vast expanse of shallow water. After the water retreats, flooding deposits silt on the flood plain and improves its fertility over decades. As a consequence, frequently flooded area used to attract agriculture and therefore human developments near the river, where soils are rich. Nowadays, human activities have changed, agriculture not at the centre of our society anymore, and flooding is now only seen as a natural disaster when water spreads throughout urban areas, where population and economic activities are usually concentred.

Flooding, when reaching particular threshold, can have disastrous consequences in both term of life and money. In poor rural countries extreme events can indeed cause many deaths like for example in Venezuela (December 1999), where approximately 10,000 people died and 150,000 became homeless. In developed countries, where rivers prone to flooding are managed carefully, damages are usually more economic than human. Unfortunately, tragedy can also happen where people feel safer, and the last example was the terrible flooding caused by Hurricane Katrina in New Orleans (August 2005), where overtopping of the banks caused about one thousand of deaths and $200 billion worth of damage.

The frequency and magnitude of floods appear to have increased in the last decades. Climatic changes, which are more and more noticeable all over the world, are often held responsible for changes in storms patterns and therefore in flood frequency increases. Another contributing factor is the constant spreading of urbanization areas over the rural lands, with the construction of concrete where soil once was, which contributes to increase the vulnerability of the river catchments.

Solutions to flooding problems have been introduced, with for example the structural solutions that attempt to eliminate flooding in specific areas using engineering work such as flood control dams, dikes, widening of river beds, etc. This could however often result in unwanted environmental, hydrologic, economic and ecological consequences. On the other hand, non-structural solutions aim at lowering the vulnerability of an area, and include land use regulation, flood warning systems and flood forecasting systems.

Flooding and river rising problems, which are mainly driven by the excessive rainfall patterns on given catchments, are indeed more easily predictable that other natural disasters

(earthquakes, tsunamis, volcanic eruptions, etc.). It has therefore became important to gain a good understanding of rainfall variations in the different areas where flooding are recurrent, and to asses how the excess rainfall will be drained to the stream network. In past decades, many rainfall-runoff models have been developed with this goal.

As with many other catchments in Ireland, the Munster Blackwater is subject to frequent flooding problems. This project deals with the understanding of rainfall patterns over this area and the modelling of the hydrological processes that occur when heavy precipitation cause important volumes of excess rainfall.

## *1.2 Flood context in the Munster Blackwater catchment*

### 1.2.1 A frequently flooded area

The Munster Blackwater catchment suffers from flooding when the Blackwater River overflows its banks in or near the towns of Mallow and Fermoy. Records are showing that major floods occurred in 1853, 1875, 1916, 1946, 1948, 1969 and 1980. The railway bridge over the Blackwater at Ballymaquirke (near Kanturk) was washed away in the flood of August 12, 1946 (Doheny, 1997). On November 2$^{nd}$ 1980, a flood with a return period of about 30 years occurred on the Blackwater. Flood damage and losses in the catchment on this occasion were estimated at over £2.5 million (Doheny, 1997).

The town of Mallow experiences some flooding every year, due to the River Blackwater, or due to the Spa Glen stream, which is a small tributary of the Blackwater that flows through Mallow Town Center. Serious flooding affecting properties and roads in Bridge Street and in the Spa Walk occurred in 1986, 1988, 1990, 1995 and 1998. The Town Park and the Park Road in Mallow are flooded on a regular basis, as much as six times every year. In 1999, two floods occurred in the month of December (Steinmann, 2004). According to records, the most disastrous flood occurred in 1853 leaving the lowest street under 3.6 m of water. In 1980 the fourth largest recorded flood occurred where the water level reached 2.5 m in some houses. In November 1998, Bridge Street, Mallow was flooded to a depth of 0.4 m and as much as 2.2 m in the town park (Steinmann, 2004). These many inundations cause major traffic problems and appear to be very dangerous for the street user and Mallow inhabitants. Figure 1.1 shows an example of a flood in Mallow.

**Figure 1.1 Flooding at the Town Park Road, Mallow 14:30 December 30, 1998 (EPA, 1998)**

Fermoy town is also threatened as it is at risk from some scale of flood event almost every year. One particular flood in October 1988 had a 50 years return period (Kiely *et al*, 2000). Flooding in Fermoy is exacerbated by the fact that flooding of the streets and property has on occasions lasted for up to two days. Minor floods also occur in smaller towns in the catchment, causing similar kind of issues, both financial and linked to the security.

Even if some subsequent flood alleviation scheme in Kanturk appeared to be effective, the rising level of the river can not be totally controlled by physical means and flood forecasting and warning scheme is therefore vital.

### 1.2.2 Flood warning system

Some different attempts were made in order to provide the Munster Blackwater Valley with a proper flood warning system. The first one was set up as a consequence of the major 1980 flood, but failed to be reliable due to a lack of locally available expertise and maintenance. Even if a more robust system was installed in the summer of 2003, its reliability still appeared to be questionable as the warning was delivered too shortly before the actual flood (Steinmann, 2004). From this point, studies have been carried in association with the UCC Hydromet Research Group in order to develop more accurate forecasting tool to predict floods. A live flood warning website was created (www.irishfloodwarning.com) (Corcoran, 2004) and activated for the Munster Blackwater River. Even if the system appeared to be both effective and reliable, forecasting floods in the Munster Blackwater Valley is not considered to be solved as the Office

of Public Works, through the UCC Hydromet research group, is still undertaking analysis in order to develop a flood forecasting and warning system that will increase the warning periods.

## 1.3 Previous work

Different flow prediction methods have been studied within the UCC Hydromet Research Group. The Artificial Neural Networks (ANN) approach was used in order to develop the forecasting model used in www.irishfloodwarning.com. The ANN, a computing model uses only river stage and does not consider any of the catchment physical characteristics. This so called black-box model learns to recognise flow patterns so as to anticipate what a river flow will be considering a flow upstream. Results showed that the model, remarkably simple and efficient, was able to predict water levels ten hours before, with a good enough accuracy to be used in a warning scheme.

A physically-based rainfall-runoff model was also applied to the Munster Blackwater (Steinmann, 2005). The Real Time Integrated Basin Simulator (tRIBS), a really complex model using rainfall and flow measurements, hydrologic, topographic and soil characteristics, was used to simulate the hydrologic process taking place in the catchment. Even if its accuracy appeared to be lower than the one obtained with the former ANN model, mostly because of issues raised about calibration parameters, results were promising. This physically-based model did not replace the ANN approach used in the flood forecasting scheme.

## 1.4 Objectives

The main objective in this thesis was to gain a good understanding of rainfall-runoff processes involved in the valley, through a precise rainfall analysis and the application of a metric rainfall-runoff model. These objectives were carried out as follows:

- Explore the Munster Blackwater catchment physical and hydrological specificities
- Classify, collect and treat all the available data sets for both rainfall and river flows
- Run a precise rainfall analysis in order to have a good understanding of rainfall spatial and time variation above the catchment
- Apply a Unit Hydrograph based rainfall-runoff modelling to the studied area in order to determine flood hydrographs
- Evaluate results by comparing calculated and observed flow values at different locations on the river

## 1.5 Structure of the thesis

This thesis consists of 7 chapters, a list of references and some appendices. Following the general Introduction, Chapter 2 is a literature review presenting the rainfall-runoff processes and the state of art in rainfall-runoff modelling. The Munster Blackwater catchment is described in Chapter 3 in order to give its main characteristics, physical and hydrological. Chapters 4 and 5 are dedicated to rainfall and streamflow data sets, with general presentations, classification and analysis. A detailed rainfall analysis is contained in Chapter 4 and gives a better understanding of rainfall variation in term of both intensity and spatial variation. Particular attention is also given to 2006 and its drought. In Chapter 6, the Unit Hydrograph theory is applied to the studied catchment, with particular attention to three different Unit Hydrograph methods. The application of this metric rainfall-runoff model is assessed in different locations along the Blackwater river channel. Finally, Chapter 7 sums the conclusions and makes suggestions for further research.

# Chapter 2 Rainfall-Runoff modelling, a literature review

## 2.1 Introduction

One of the main reasons for modelling Rainfall-Runoff processes is the limitation of hydrological measurement techniques (Beven, 2001). This kind of modelling has a long history and even if it has evolved alongside with the development of more and more powerful computational tools, its aim has not changed over the years. The key aim is to understand the processes of rainfall-runoff and extend streamflow time series in both time and space (Wagener, 2004). They are now standard tools routinely designed for hydrological investigations, and are also used to suit many purposes beyond the scope of hydrology in both engineering and environmental science. These include catchment response to climatic events, calculations of design floods, management of water resources, estimation of the impact of land use change, and of course streamflow prediction and flood forecasting. This wide range of aims is reflected in the variety and complexity of hydrological models available. Given this variety, it is necessary to be able to identify as clearly as possible the purpose of the model the available data and the characteristics of the model itself (Wagener et al., 2000). When applied to river flow prediction and flood forecasting, the flood peak timing and the flood peak magnitude are the two key objectives.

As many different models have been developed over the years, it has become necessary to classify them according to their approaches and structures. Even if many distinctions in model types were made, the most commonly used classification was introduced by Wheater (1993) who distinguished four broad categories:

- Metric or empirical models (also called black-box models) which are derived from data (e.g. rainfall, river flow) observations with the aim of characterizing the response of the river system to these observations (Wheater et al., 1993).
- Conceptual or parametric models (also called grey-box models) whose structure is defined *a priori*, considering "the perception of the modeller", using mostly fluxes of water between various reservoirs.
- Physically based or mechanistic models (also called white-box models) based on the mathematical models of the underlying physical processes and discretised physical equations of motions.
- Hybrid metric-conceptual models which use both data observation and prior hypothesis about hydrological stores that could represent the catchment.

Another classification is based on the distinction between lumped and distributed models (Beven, 2001). Lumped models treat the catchment as a single unit, with state variables that represent averages over the catchment area (e.g. average storage in the saturated zone). Distributed models make predictions that are distributed in space, with state variables that represent local averages of storage. Parameter values must thus be specified for every element of the spatial distribution. After a general overview of the rainfall-runoff processes, more precise description of these four kinds of model will be given.

## 2.2 Rainfall-Runoff processes

The hydrological processes occurring in and above a catchment, from the formation of the precipitation to the streamflow leaving through a river, are many and complex. The most important of them are noted in figure 2.1. Considering the location of the studied area and its climatic characteristics, snow formation and snow melt will not be considered.

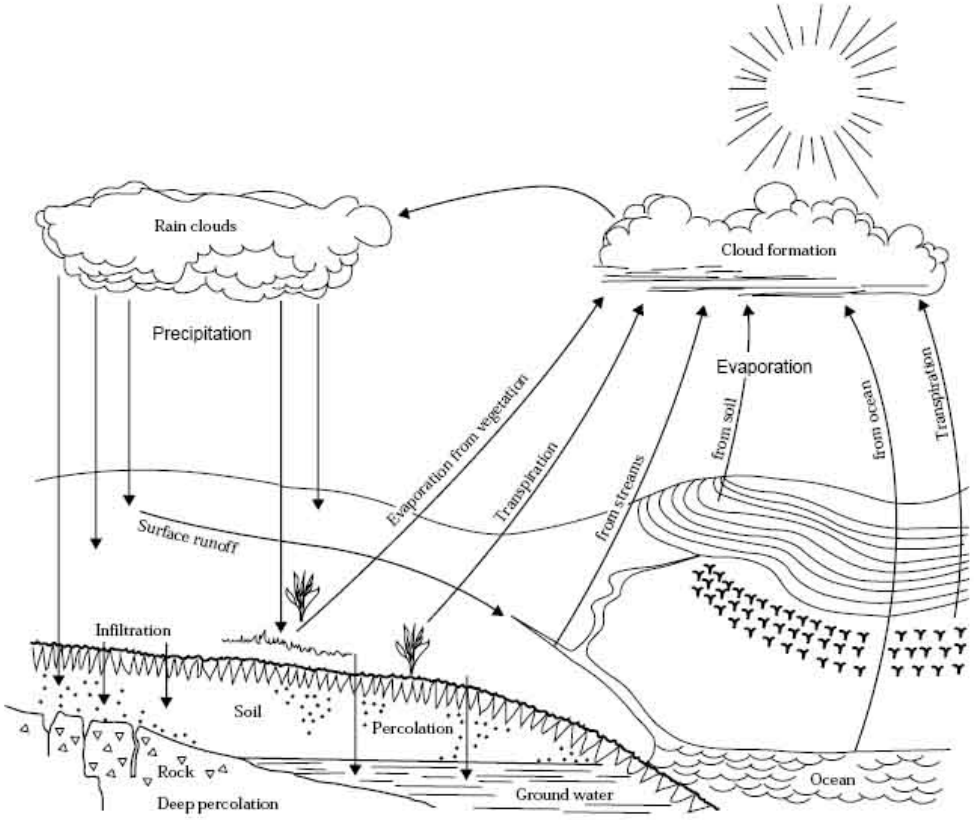


**Figure 2.1 Schematic presentation of hydrological processes**
**(Reproduced from the Natural Resources Conservation Service United States, 1993)**

Precipitation occurs when water vapour masses condense, driven by the cooling of air masses through upward movement. In mid-northern latitudes, precipitations are mostly frontal, i.e. warm moist air being lifted up by colder denser air moving underneath or convectional in which air masses are warmed by heat originating from the ground surface. In the following chapters, the total amount of precipitation will be referred as gross precipitation.

A small proportion of the precipitation, the channel precipitation, falls directly in the stream and river network and contributes immediately to runoff. Approximately 1 to 1.5 mm of any individual rainstorm is intercepted by the vegetation canopy (Wagener, 2004). The rest of the precipitation reaches the ground and is separated in losses, which infiltrates and percolates through the soils and net rainfall, which directly contributes to surface runoff.

Most of the intercepted precipitation and a part of the water that has reached the ground returns to the atmosphere through evapotranspiration (combination of evaporation of water in soil and transpiration by the vegetation), which involves a change of state from liquid water to water vapour, with an energy mainly provided by solar radiation.

Losses fill surface depressions and infiltrate the soils. Soil moisture content is then changed until saturation is reached, where all the water reaching the soil is directly converted in direct runoff. The subsurface is often divided into two overlying zones, a zone of aeration and a saturated zone. The first one can itself be divided into the soil zone and the intermediate zone. Percolation occurs through the three different zones and goes in the groundwater that lies below the saturation zone. The soil and rocks that contain the groundwater, called aquifers, are usually capable of transmission of significant quantities of water on a horizontal plan. The groundwater table is connected to the river channel through the river flanks.

Channel precipitation, direct surface runoff and groundwater then meet in the stream where their addition results in the stream discharge. The discharge is divided into its baseflow component, which is the part corresponding to the groundwater flow, and its storm runoff component which includes both channel precipitation and direct surface runoff.

## 2.3 Metric models

Metric models are strongly observation-oriented seeking to characterize the catchment system response by extracting information from the existing data (Kokkonen, 2001). Time series of rainfall and runoff are used to derive both the model structure and the corresponding parameters values as no prior knowledge about the catchment or flow processes are included in the structure, hence the name “black-box”. Metric models are usually spatially lumped, i.e. they treat the catchment as a single unit and are not suitable for ungauged catchments (Wagener,

2004). These methods are generally simple, easily understood, and have been widely and successfully used. On the other hand, this simplicity can be seen as a drawback considering the fact it may not account for several important factors such as antecedent catchment moisture conditions or other aspects of the catchment memory. Among the most currently popular examples of this type are Artificial Neural Networks and the Unit Hydrograph.

### 2.3.1 Artificial Neural Network

Artificial Neural Networks (ANN) were first introduced in the 1940s (McCulloch and Pitts, 1943) in an attempt to emulate the working of a biological nervous system, where information is transferred from neuron to node, and the human way of thinking and learning (see figure 2.2). The architecture of the model is determined trough a trial and error procedure. The model is then trained with different weight being adjusted until some criteria have been achieved. Their utilization became efficient in the 1980s with the advent of affordable microprocessors. Given sufficient data and complexity, ANN can be trained to model any relationship between a series of independent and dependant variables (Dawson et al, 2006), and are therefore considered to be a set of universal approximators and have been usefully applied to a wide variety of problems (e.g. finance, medicine, engineering). The particular application of ANN in hydrology and water resources started in the early 1990s and include very satisfactory rainfall-runoff modelling (Rajurkar et al, 2004; Kumar, 2004), hydrograph generation from hydro-meteorological data (Ahmad, 2005), flow forecasting (Sahoo et al, 2006; Leahy, 2006), and flow estimation at ungauged sites (Dawson et al., 2006). A complete state-of-the-art review of ANN applications in hydrology can be found in the ASCE task committee report (2000), which also gives a detailed overview on the theoretical aspect of ANN.

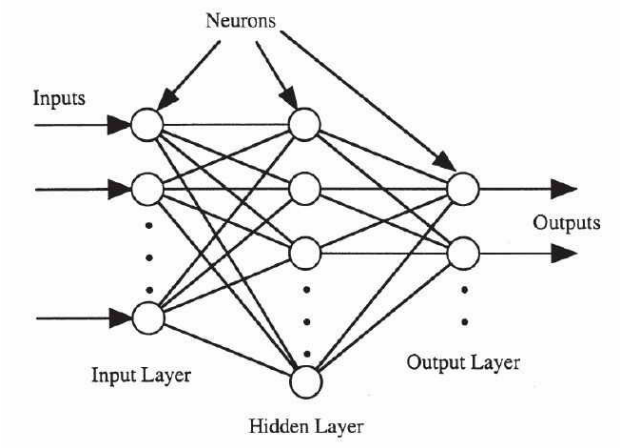


**Figure 2.2 Typical ANN structure (Dawson and Wilby, 2005)**

ANN modelling has already been applied to the Munster Blackwater catchment (Leahy 2006; Corcoran 2004) in order to predict flood levels ten hours ahead using a minimal set of input time series, namely river heights at three different locations (the flood point and two locations upstream). While an ANN using only the current stages at the three measurement locations (the three-input ANN) appeared to be not as good a predictor as a multiple linear regression (MLR) to the same input variables, results showed that ANNs with larger sets of inputs (e.g. six-input ANNs including the recent changes in levels as inputs and the nine-input ANNs which incorporate preceding levels) could produce better results than MLR to the same sets of inputs. It was concluded that ANNs could provide a viable method of flood forecasting for the Munster Blackwater catchment on condition that input values are carefully selected and presented to the network in a way in which the underlying patterns can be easily recognized.

### 2.3.2 The Unit Hydrograph

The Unit Hydrograph (UH) theory is also classified in the metric model category and has been widely and successfully used over the past decades. First introduced by Sherman (1932) as a basic tool that represents the hydrologic response of a watershed through which effective rainfall is transformed to direct runoff, the UH is the surface runoff hydrograph resulting from one unit of rainfall excess uniformly distributed spatially and temporally over the watershed for the entire specified duration. The UH theory is described in many reference books (Brutsaert, 2005; McCuen, 2004; Shaw, 1994; Wilson, 1990; Chow 1988, Linsley, 1988) which also give detailed utilization descriptions. Exploration and applications of the UH theory have lead to really satisfactory results over the years, this for a wide range of catchment type, and have been used in many flood forecasting and modelling schemes (Dooge, 1959; Nash, 1960; Pedruco, 2005). Many unit-hydrograph-based models such as IHACRES (Identification of unit Hydrograph And Component flows from Rainfall, Evaporation and Streamflow data) (Jakeman, 1990) or MESSARA (Croke, 2000) have been developed with a typical structure including a rainfall separation module followed by the conversion of effective rainfall into streamflow using a UH (Croke, 2006). Improvements to the UH were made with the introduction of the instantaneous unit hydrograph (IUH) (Nash, 1957; Raymond, 2003) which is defined as the UH obtained for a instantaneous effective rainfall burst and which main advantage on the UH is that it does not require uniform effective rainfall for a specific period of time. The geomorphological instantaneous unit hydrograph (GIUH) was as well introduced (Rodriguez-Iturbe, 1979; Gupta, 1980; Lee, 1997; Yen, 1997; Lee, 2005; Lopez, 2005; Agirre 2005) in order to incorporate the geomorphological properties of the watershed, using a hierarchic ordering of the channels within

the drainage network. UH modelling and its application to the Munster Blackwater, with special attention to IUH and GIUH are described in the Chapter 6.

## 2.4 Conceptual models

Conceptual models describe all of the component hydrological processes perceived to be of importance as simplified conceptualizations. This usually leads to a system of interconnected stores (also called buckets or reservoirs), which are recharged and depleted by appropriate component processes of the hydrological cycle (rainfall, infiltration, percolation and evapotranspiration, runoff, drainage, etc.). Conceptual models have a structure that is specified before their use, and defined by the modeller's understanding of the hydrological system (Wagener, 2004). Their parameters, which describe aspects such as the size of the reservoir or the distribution of flow between them, are derived using time series (mainly streamflow). Most of the conceptual models consider the catchment as a single homogeneous unit (lumped approach). Finally, a main objective of this kind of model is to balance model complexity and output accuracy.

Some advantages of the conceptual models are that they can incorporate non-linearity such as evapotranspiration processes and that they can be used in continuous time series as initial conditions are implicit to the model (Pedruco, 2005). On the other side, the main disadvantage lays in the fact that several parameter sets can produce similar optimal results. This may indeed lead to non-physical sets, which may not perform optimally once outside the calibration range (Beven, 2001).

One of the most known models of this category is TOPMODEL (Beven et al, 1979), a conceptual but spatially distributed model which implements an index of hydrological similarity known as the topographic index (Kirkby, 1975). It has been originally developed to simulate small catchments in the UK (Beven, et al, 1984), but has been applied to several different basins throughout the world (Lamb, 1997; Scanlon, 2000, 2004; Cameron, 2006; Gallart, 2006).

## 2.5 Physically-based models

Physically-based Rainfall-Runoff models provide a mathematically idealized representation of the catchment and all the different hydrological processes occurring during the transformation from rainfall to runoff, the mathematical representation being based on the conservation of mass, momentum and energy (Wagener, 2004). They use a spatial discretization

based on grids, hill slopes or some kind of hydrologic response unit. Most of their parameters have physical significance and are obtained from field measurements. They became practically usable in the 1980s, as a result of improvements in computer power. Their development was motivated by a will to obtain some models that could be run without any calibration step, i.e. which would be applicable to ungauged catchment or to catchment where available data is not enough to calibrate metric or conceptual models.

Unfortunately, mechanistic models suffer from extreme data demand, scale-related problems and over parameterization (Beven, 1989) and still require to go through a calibration phase in order to determine some key parameters (Wagener, 2004). They are then applied in a way that is similar to lumped conceptual models, without necessarily getting more accurate results than simpler approaches. Furthermore, the high complexity of physical models generally requires large amounts of computing time, which make them for example, unsuitable for live flood forecasting. Finally, some of the physical parameters (especially subsurfaces processes) are commonly derived in small scale laboratory experiments and are then extrapolated catchment scale, which often leads to incorrect values and loss of the heterogeneity of the catchment (Wheater, 2002).

The TIN-based real-time interactive basin simulator (tRIBS) model (Ivanov et al, 2004) is a fully-distributed, triangulated irregular network (TIN) mechanistic model updated from the real-time interactive basin simulator (RIBS) (Garrotte, 1993). First developed for its application to Illinois River at Watts where it showed good results, it was also applied to the Munster Blackwater catchment (Steinmann, 2004). Really demanding in term of input, tRIBS needs a lot of input parameters (9 parameters concerning the vegetation properties, e.g. canopy capacity or optical transmission coefficient; 11 parameters for the soil hydraulic and thermal properties, e.g. saturated hydraulic conductivity or saturation soil moisture content; 5 parameters for channel and hillslope routing parameters, e.g. channel roughness coefficient or hillslope velocity coefficient), an elaborated TIN, soil and land use information, the groundwater spatial distribution, rainfall input (either radar-rainfall of raingauge data) and some meteorological data inputs (e.g. atmospheric pressure, relative humidity). Such a complexity leads to complex data collection and transformation, and to high calculation times. After calibrating and testing the model on 5 floods between January 2002 and January 2005, it was concluded that even if the results were promising, the model's accuracy was lower than the one obtained with the much simpler ANN metric model (Corcoran, 2004; Leahy, 2006).

## 2.6 Hybrid metric-conceptual models

These types of model are driven by observational data, and are used to investigate hypothesis regarding the hydrological processes and storages of a system (Wheater et al, 1993). It uses statistical investigation of the data to determine the structure of the model. The resulting structure and parameters are then used to investigate the structure of the hydrological system. It is usual for these models to be run on a continuous basis and incorporating initial conditions directly into the model (Pedruco, 2005). Model's inputs (usually rain and potential evapotranspiration) are linearly combined to produce output (stream discharge). The main drawbacks of this category is that it took its metric model parent characteristic of being seen as a "black-box" model (Tilford, 2003) and that the assumption of linearity may not be justified for the entire range of flows.

The Rainfall-Runoff Modelling Toolbox (RRMT) (Wagener et al, 2001) provides its user with different hybrid lumped models and was used to simulate phosphorus transfer in the River Enborne (UK) (Smith, 2005). Two different hybrid metric-conceptual models were evaluated, both driven by readily available rainfall, potential evaporation and land use data, in order to generate daily estimates of flow and in-stream P concentrations.

# Chapter 3 Catchment description

## *3.1 Ireland*

### 3.1.1 Introduction

Before describing the Blackwater catchment, a brief introduction to Ireland with respect to hydrology is given. The location, topography, rivers, geology, soils and land uses characteristics are given in order to highlight different aspects of Irish hydrology. Climatic impacts, which is a major factor in all hydrology is also described.

### 3.1.2 Location

Ireland, which is the third biggest island in Europe, is located on the far western end of the European continent, surrounded by waters of the Atlantic Ocean on its West and the Irish Sea on its East. The total area of the "Emerald Isle" is 84,000 $km^2$ with 69 000 $km^2$ being the Republic of Ireland.

### 3.1.3 Topography

With only a few peaks, Ireland has a relatively low elevation (the majority of the island is less than 150 meters above sea level). Only 5% of the total area has an elevation between 300 and 600 m a.s.l and only 0.2% at a height of greater than 600 m a.s.l (Rohan, 1975). Most of the highest peaks are located in the South-West of the country (Mt Carrauntoohil, the highest at 1041m a.s.l) (Rohan, 1975). The topography features a hilly, central lowland surrounded by a broken border of coastal mountains. The mountain ranges vary greatly in geological structure. Ireland has often been described as saucer or bowl shaped.

### 3.1.4 Geology and soils

Ireland is largely composed of palaeozoic and precambrian rocks (Holland, 2001) with the Precambrian outcrops of schist, gneiss and quartzite mostly in the North West and palaeozoic sandstone, limestone and shale over on the rest of the country.

The soils of the centre of Ireland are dominated by luvisols being developed from the underlying Limestone parent material. These soils are porous and well aerated and have a high moisture capacity (Food and Agriculture Organisation,2001). Intermixed with these luvisol soils are histosols which are associated with peat bogs having a high organic content and often being water logged (Food and Agriculture Organisation, 2001).

Surrounding this interior are gleysol soils. The cambisols of the east coast are usually found in alluvial planes and are freely draining with excellent agricultural properties. The older podzolic soils are typically found in conjunction with the precambrian and older palaeozoic rocks. These aged soils are usually of a sandy composition with the upper horizons being leached due to heavy rainfall. A common occurrence in this type of soil is mineral precipitation at the bottom of the A horizon where an impermeable crust forms known as an iron pan. These soils are not known for their water holding capacity nor their agricultural properties (Food and Agriculture Organisation, 2001).

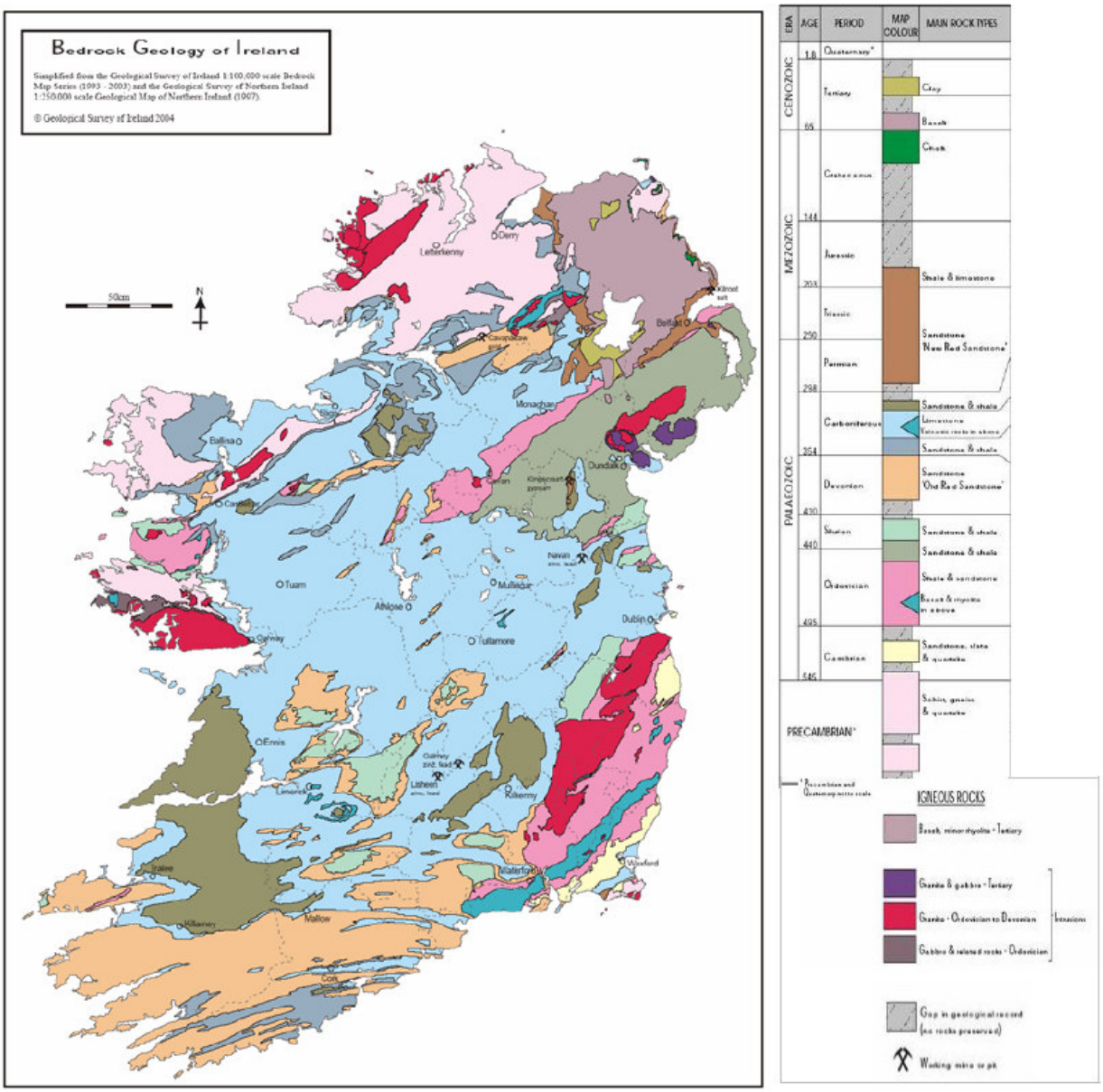


**Figure 3.1** **Geology of Ireland (Geological Survey of Ireland)**

### 3.1.5 Climate

The dominant influence on Ireland's climate is the Atlantic Ocean. Consequently, Ireland does not suffer from the extremes of temperature experienced by many other countries at similar latitude. The other important factor impacting on Ireland's climate is the westerly atmospheric circulation of the mid latitudes (Rohan, 1975; Hargy, 1997; Keane & Sheridan, 2004). This association gives the Irish climate a distinct maritime character which is moderated by the influence of Gulf Stream.

The average annual temperature of Ireland is about 9 °C. In the middle and east of the country temperatures tend to be somewhat more extreme than in other parts of the country. For example, summer mean daily maximum is about 19 °C and winter mean daily minimum is about 2.5 °C in these areas.

Most of the eastern half of the country has between 750 and 1000 mms of annual rainfall. Rainfall in the west generally averages between 1000 and 1250 mm. In many mountainous districts, it exceeds 2000mm per year. The wettest months, almost everywhere are December and January. Hail and snow contribute relatively little to the precipitation measured. During late summer or early spring depression or anticyclonic conditions may dominate bringing wide spread rain. This is generally replaced by westerlies through October and November which are relatively warm and lead to frontal rain (Rohan, 1975). Typically rainfall does not occur in heavy showers rather as drizzle or rain. Irish rainfall tends to be low intensity over long periods (Rohan, 1975) or archetypal frontal rainfall which is dominated by the west to east flow of air across Ireland.

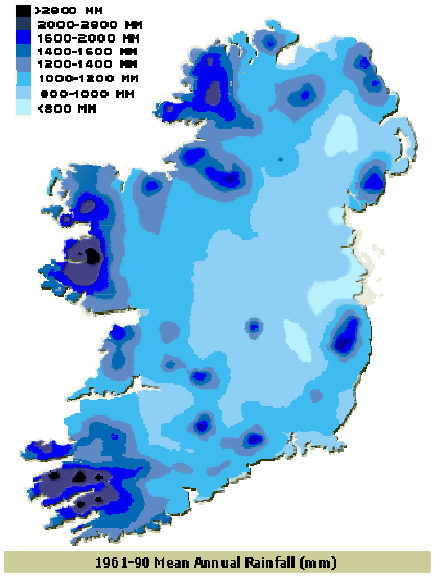


**Figure 3.2 Mean Annual Rainfall over Ireland (Met Éireann)**

Figure 3.2 shows the long term mean annual rainfall over the country. A gradient of precipitation can be seen from West to East, with some higher amounts associated with the high topography.

## 3.2 Blackwater catchment

### 3.2.1 Location

The Munster Blackwater catchment is located in the southwest of Ireland (see figure 3.3). The catchment is primarily within North West County Cork, Mid Cork and East Cork. The total area of the catchment is 3324km$^2$ which is almost 4% of the total land area of Ireland (Doheny, J. 1997). The Munster Blackwater catchment drains most of the Northern Division of County Cork and a large part of east County Waterford.

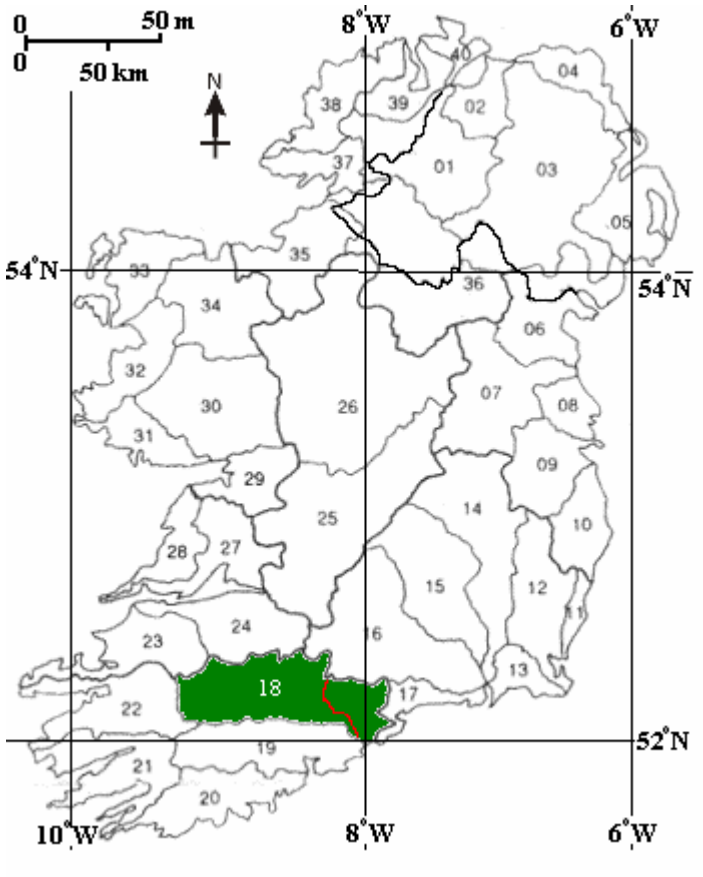


**Figure 3.3 Munster Blackwater catchment location is shown shaded (Office of Public Work)**

### 3.2.2 Topography and river path

The Munster Blackwater catchment is a broad valley surrounded by mountains on its North (Mullaghareirk Mountains, Seefin Mountains, Galty Mountains and Knockmealdown Mountains) and its South (Caherbarnagh Moutains, Derrynasaggart Mountains and the Boggeragh Mountains). The highest point of the catchment is located in the Galty Mountains at an altitude of 892m a.s.l, while the lowest part of the catchment is at sea level (Youghal). The full length of the Blackwater from its rising point near Ballydesmond to the sea at Youghal is 134 km.

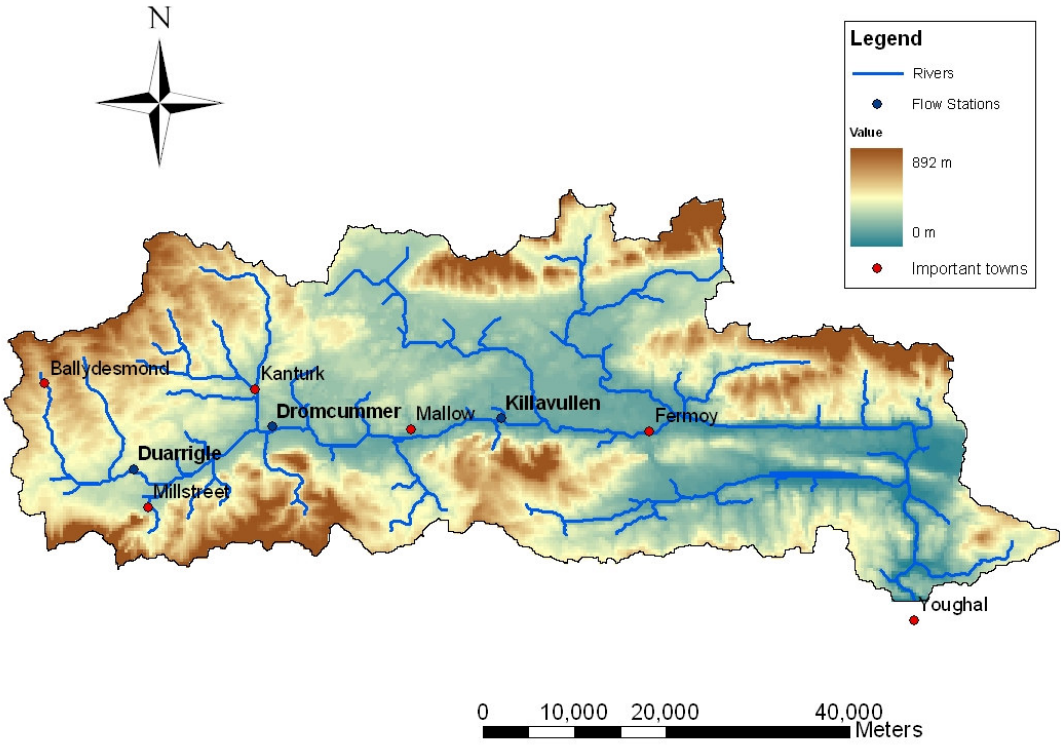


**Figure 3.4 Munster Blackwater catchment topography**

The river rises in the foothills of the Mullaghareirk Mountains at Knockanefune (near Ballydesmond) in County Kerry. The river flows due south to Rathmore along the Cork and Kerry border. At Rathmore the river turns and flows due east passing near Millstreet and Kanturk and then through Mallow and Fermoy into County Waterford. At Cappoquin the river turns to flow due south and enters the sea at Youghal. There are 29 tributaries running into the Blackwater (Hydrological Data, EPA) the main ones being the Bride, close to Cappoquin, the Awbeg, between Fermoy and Mallow, the Allow, which is close to Kanturk, and the Owentaraglin which is close to Millstreet. It is tidal for a distance of approximately 20km upstream to Cappoquin.

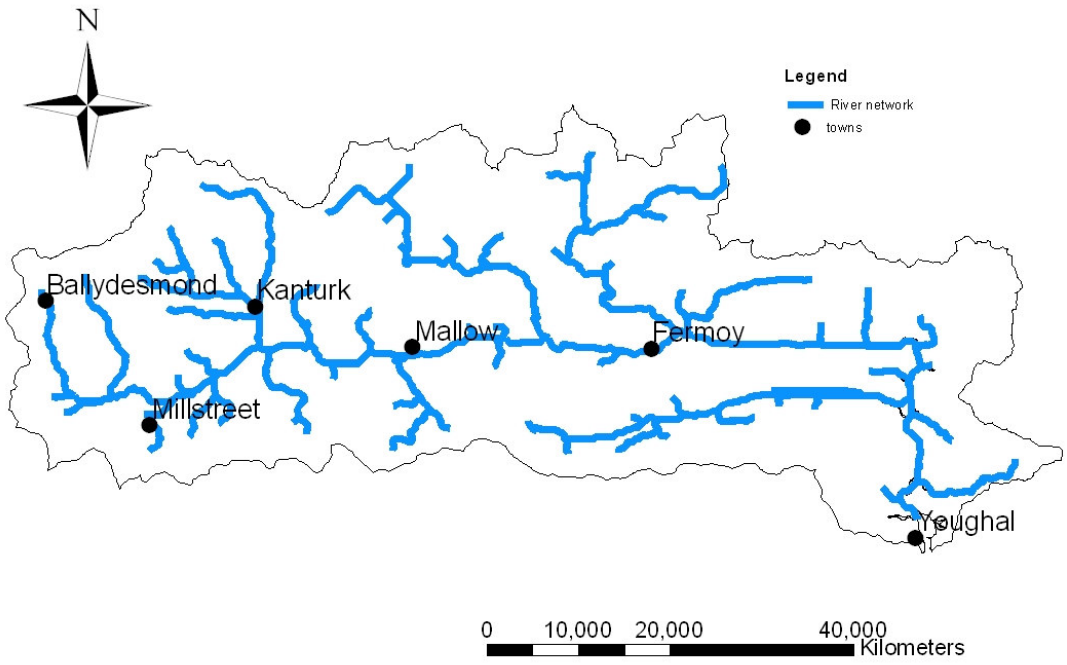


**Figure 3.5 Munster Blackwater river network**

### 3.2.3 Soils and geology

#### 3.2.3.1 Soils

An important soil database is being built by the Environmental Protection Agency (EPA) which is currently undertaking a Soil Survey for Ireland. Most of the catchment is covered by the survey except for a small area in the north (see figure 3.6). Soils are classified according to the Irish Forest Soils (IFS) classification which at level 1 is: deep well drained minerals, shallow well drained minerals, deep poorly drained minerals, poorly drained minerals with peaty topsoils, alluvium, peats and miscellaneous.

As can be seen on figure 3.6, most of the Blackwater catchment is covered with deep well drained minerals. Shallow well drained minerals represent the second proportion and appear in patches all over the catchment. Poorly drained mineral soils are concentrated in the north-eastern part of the catchment and the greatest proportions of peats can be found in the western end. As alluviums cover the main river beds, its location identifies the floodplains.

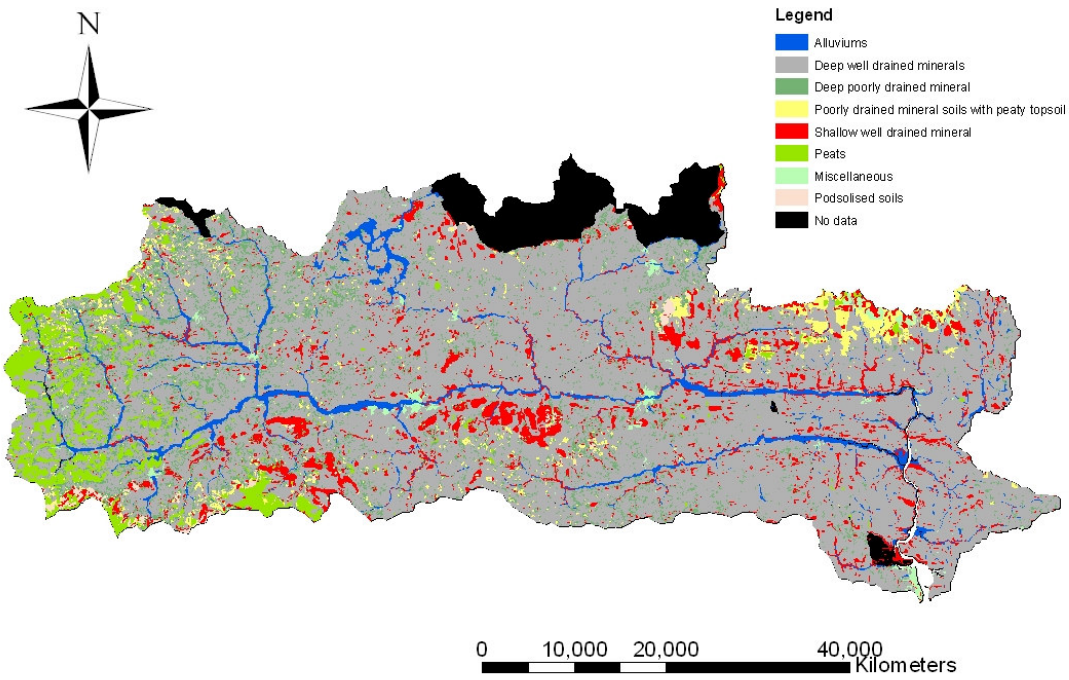


**Figure 3.6 Munster Blackwater catchment soil types**

The EPA has also funded a Subsoil Survey which, like the Soil Survey, covers almost all the catchment (see figure 3.7). Most of the valley is covered with materials originated from tills (TDSs, TLs and TNSSs). Peats can also be found on the western end and bedrock is found at the surface (Rck) as patches all over the catchment.

Tills are diamicton (nonlithified, nonsorted or poorly sorted sediments that contain a wide range of particle sizes) deposited by or from glacier ice. They correspond to the well drained and poorly drained mineral soils. The association of soils and subsoils allows reference to the general soil map classification and thus give more details about the nature of the soil. Indeed acidic well drained minerals from tills can be associated, in that area with Brown Podzolics which are gravelly loams. In the same way acidic poorly drained minerals from tills mostly refer to Gleys which are clay loams, and acidic shallow well drained minerals to Lithosols which are sandy loans.

Peat is a post-glacial deposit, consisting mostly of vegetation which has only partially decomposed. Alluvium is a post-glacial deposit and may consist of gravel, sand, silt or clay in a variety of mixes and usually consists of a fairly high percentage of organic carbon (10%-30%). Rocks close to the surface are often associated with shallow well drained areas.

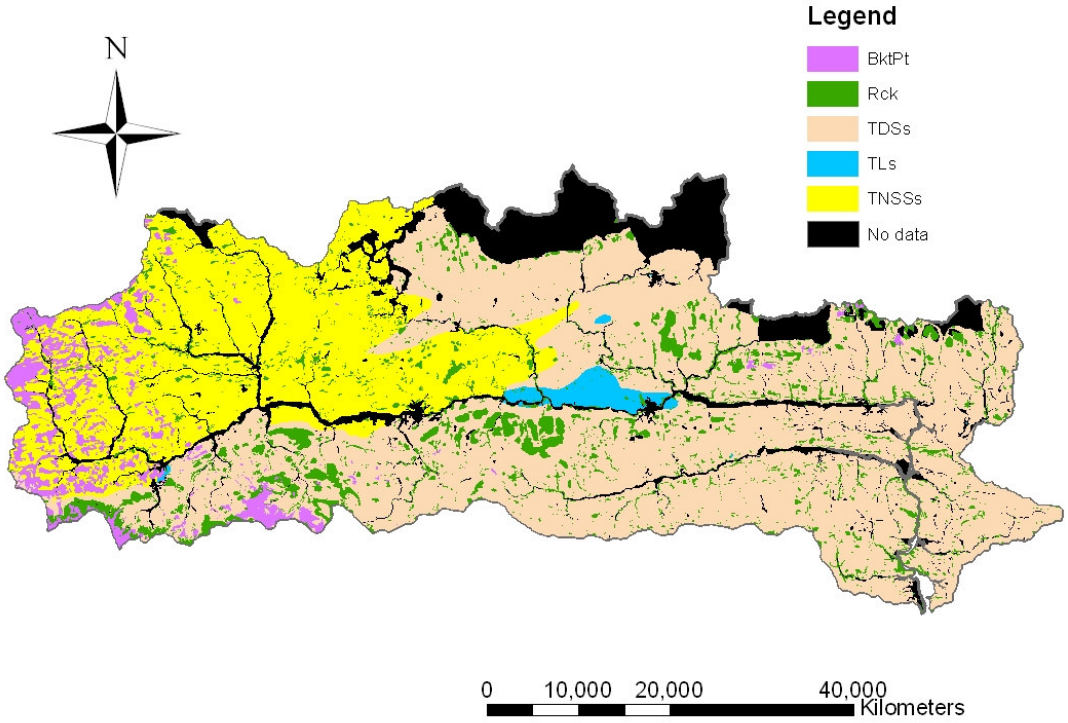


**Figure 3.7 Munster Blackwater catchment sub-soils types**

### 3.2.3.2 Geology

There are two main rock types in the Munster Blackwater catchment: Devonian Sandstone is the principal rock type to the South and Dinantian Limestone is the dominant rock type north of the river (Geological Survey of Ireland, 2004).

.

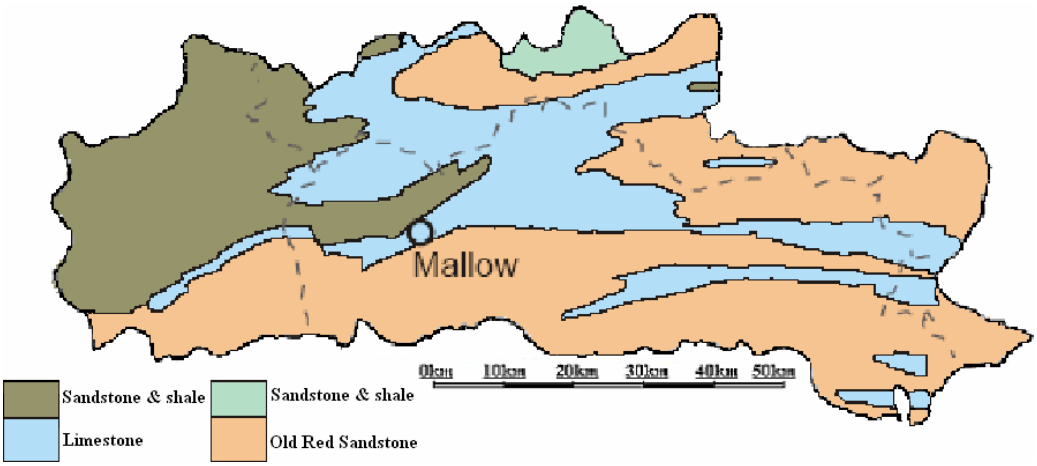


**Figure 3.8 Munster Blackwater catchment bed rock geology (Corcoran, 2004)**

### 3.2.4 Land uses

Land use information and spatial distribution is available trough the CORINE (Co-Ordination of Information on the Environment) Land Cover database elaborated by the EPA. The survey covers the whole catchment and classifies the different land uses using three different levels. Figure 3.9 shows a graphical repartition of the different land uses, according to the 1st level of CORINE nomenclature.

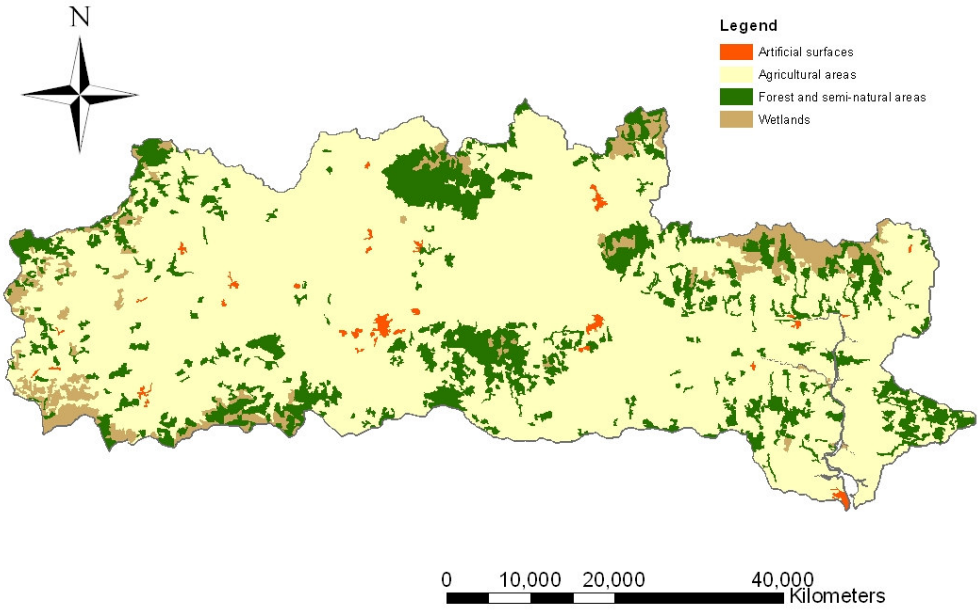


**Figure 3.9 Munster Blackwater catchment land uses**

Agriculture is dominant with more than 90% of it being grassland. Forest and semi-natural areas come second with a much lower proportion. The artificial surface over the catchment represents a really small amount of the total area, which mainly reflects the low urbanization level of the catchment. The main artificial surfaces area (orange colour on figure 2.4) being the town areas of Kanturk, Millstreet, Mallow, Fermoy, Mitchelston and Youghal.

### 3.2.5 Climate

Precipitation over the catchment is the most important climatic factor for hydrological response. Precipitation can be considered as being the rainfall only considering the really low occurrence of snow and hail. The catchment has a 1200 mm annual average rainfall and a 300-400 mm evapotranspiration (Corcoran, 2004). The rainfall occurs during the whole year with

amounts from October to March. Evapotranspiration losses are considered significant only during the summer months (May to September). Precipitation amounts are higher on the western edge of the catchment and around the highest hills and peaks. The rainfall regime is characterized by long duration events of low hourly intensity. Short duration events of high intensity are more seldom and mostly occur in summer. A more precise study of the catchment rainfall is reported Chapter 4.

Considering the catchment latitude, the daily air temperatures over the course of the year have a small range of variation, mainly because of the influence of the warn Gulf Stream. Temperatures go from a maximum of ~20ºC to a minimum of ~0ºC, with an average of 15ºC in summer and 5ºC in winter (Jaksic, 2004).

The UCC Hydromet research group runs a meteorological station in Dounoughmore, 5km south of the catchment. Data recorded there are considered to be representative of the meterological conditions within the studied catchment. Figure 3.10 shows two annual wind roses recorded in Dounoughmore. It can be seen that the prevailing wind direction is from the southwest.

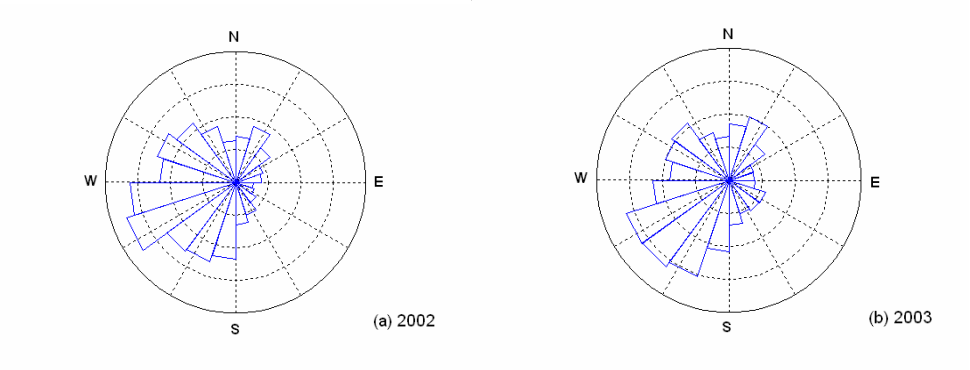


**Figure 3.10 Wind roses (a) for 2002 and (b) for 2003 (Jaksic, 2003)**

The general pattern of river flow in the Munster Blackwater is a temperature oceanic river regime (Corcoran, 2004).

### 3.2.6 Subcatchments

Some particular subcatchments will be considered in the following chapters. Those have been chosen considering the availability and the quality of their data. Three main Subcatchments were considered, Duarrigle, Dromcummer and Killavullen. Table 2.6 gives the area, the river length to the outlet and the S-1085 slope.

**Table 3-1 Nested sub-catchments**

| Catchment | Area (km2) | Length (km) | Slope – S1085 |
|---|---|---|---|
| **Duarrigle** | 245 | 21 | 3.9 |
| **Dromcummer** | 861 | 39 | 2.7 |
| **Killavullen** | 1292 | 68 | 2 |

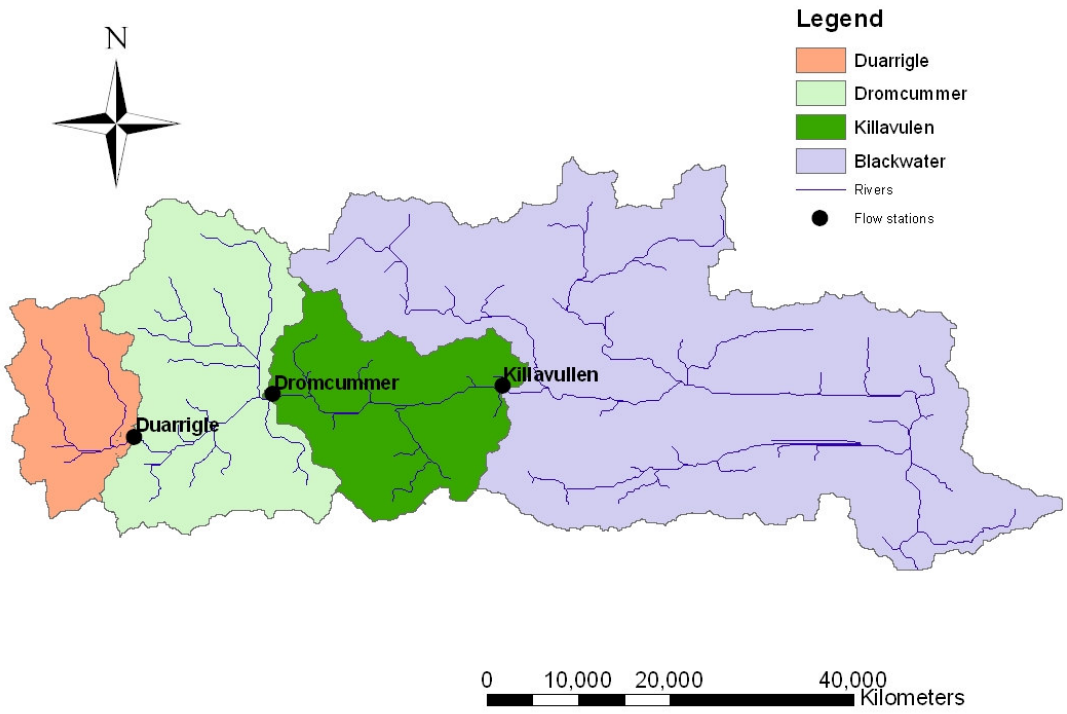


**Figure 3.11 Duarrigle, Dromcummer and Killavulen nested sub-catchments**

# Chapter 4 Rainfall Analysis

## 4.1 Introduction

Precipitation data is the most important hydrologic parameter in the hydrological study of the Blackwater. Obtaining reliable data over time and space was an essential step before modelling the rainfall-runoff. Irish rainfall is being recorded at many places by the Meteorological Office. The time step of the records is either hourly or daily. A lot of effort was put in obtaining as much rainfall data as possible covering the catchment. In the following chapter, the different sources of rainfall data are discussed and trends of rainfall over the catchment are analysed.

## 4.2 Meteorological Office data

The Irish Meteorological Office monitoring network has 14 synoptic stations around Ireland providing hourly reading of temperature, precipitation, wind speed and direction, sunshine, cloud cover, pressure, humidity, soil and grass temperature, with evapotranspiration and solar radiation being measured at some of these stations (Sweeney *et al.*, 2002). Daily temperature and precipitation are measured at over 100 climatological stations and sunshine, soil and earth temperatures being recorded at some (Keane, 1986). Additionally there are a further 1850 stations which measure daily rainfall (Sweeney *et al.,* 2002). All are data collected and quality controlled by Met Éireann. Unfortunately, none of the 14 synoptic stations is located in the Blackwater catchment. Thus, daily rainfall data was provided by the Meteorological Office with some hourly data from their sites with non digitised paper autographic records.

### 4.2.1 Automatic raingauges

Some of Met Éireann stations are still operating with automatic gauges. An automatic driven pencil directly plots the rainfall intensity on a 24-hours chart that has to be changed every day. When well operated, this kind of raingauge can provide a good 1-hour step dataset. Unfortunately, changing the chart every day represents a heavy constraint that often causes the rainfall of different days to be recorded on the same chart. Those charts are generally not digitised by Met Éireann but retained for further analysis if required. Figure 4.1 gives an example of a 24-hours recording chart.

Some of the data requested from the Met Service for Millstreet, Freemount and Mallow (for the period 1988 to 2000) were only available in hard copies stored in the Meteorological Office Headquarter in Dublin. Digitising of those were expensive as it was necessary to go to

Dublin and spend a lot of time translating the hard copy charts into Excel files that were then usable.

Nowadays, at a time when automatic digital recording raingauges are easy to use and are affordable, such a method of recording and storing the information is obsolete. Furthermore, as the data is not digitised nor used afterwards, it seems that putting efforts in this data collection scheme is expensive on time and money. Replacing these gauges by automatic gauges with integrated digital data loggers would provide a good quality rainfall dataset, and would require less work as this kind of modern loggers can be downloaded every few months and the obtained data directly available as usable digital tables.

Each time the 24-hours chart is not changed, rainfall for consecutive days are superimposed which makes it difficult to extract the data corresponding to each day. When confronted with this situation, the different curves were compared to those corresponding to the same days in a station nearby, that allowed us to recognise the rainfall variation over time and then choose the appropriate values. Figure 4.1 shows an example of two superposed daily plots.

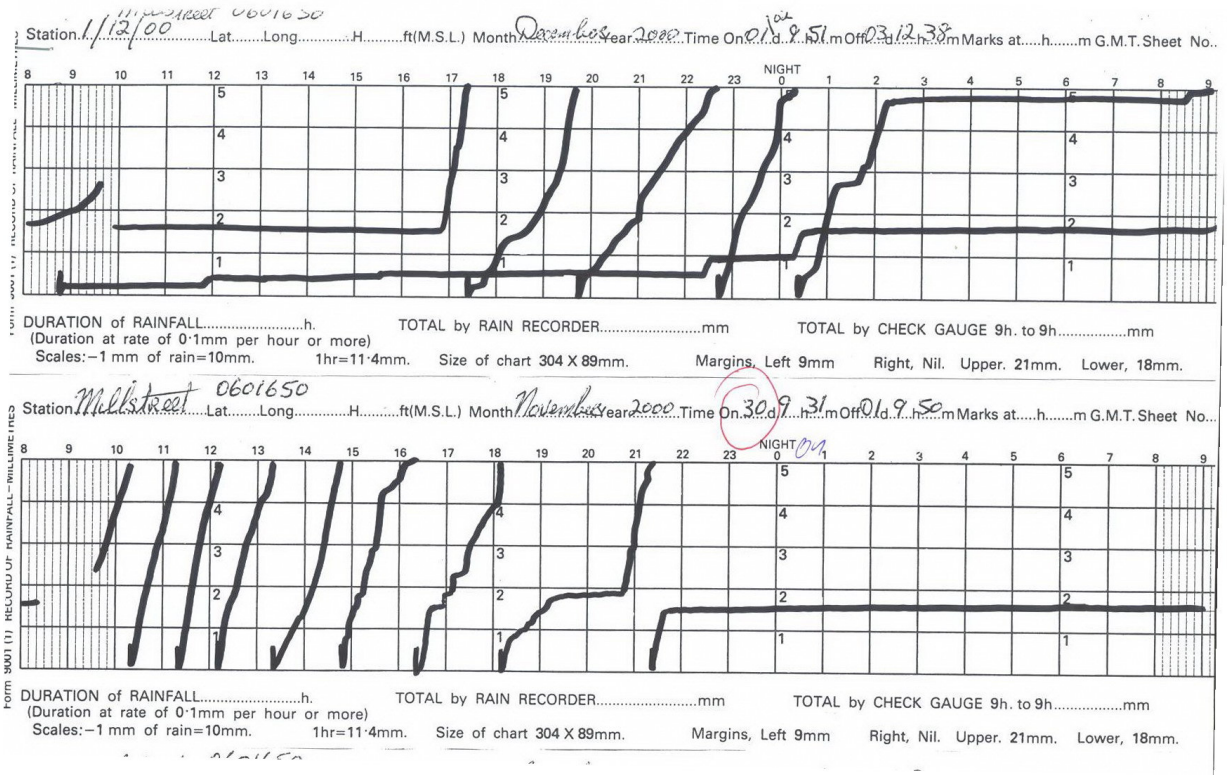


**Figure 4.1 Example of an automatic raingauge chart (Met Service)**

### 4.2.2 Daily rainfall

The Meteorological Office has built a large daily rainfall data set over Ireland. Figure 4.2 shows all the available raingauges within the Blackwater catchment. All the still operating stations, their coordinates and their opening dates are listed in table 4.2.

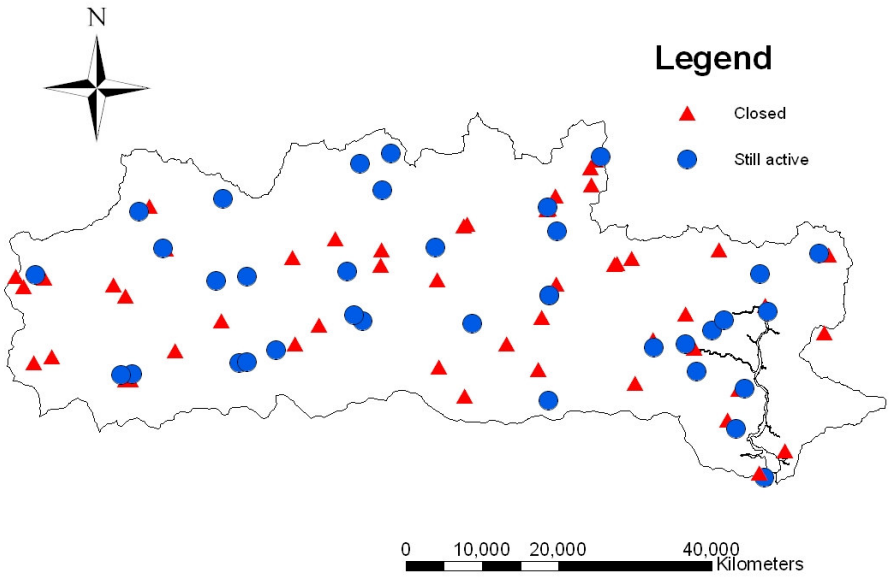


**Figure 4.2 Met Service daily raingauges network**

Data was requested for all the still operating stations. Mr Niall Brooks (Climatological Division, Met Éireann) forwarded data to us as tables indicating the date, the rainfall depth and an indicator code. This indicator code identifies the quality of the data and their description is given in Table 4.1.

**Table 4-1 Raingauge data indicator code description**

| Code | Description |
|---|---|
| 0 | Satisfactory |
| 1 | Estimated |
| 2 | Cumulative, no reading |
| 3 | Estimated cumulative total |
| 4 | Trace |
| 5 | Estimated trace |
| 6 | Cumulative trace |
| 7 | Estimated cumulative trace |
| 8 | Not available |
| 9 | Cumulative total |

As suggested by the indicator code table, all stations show gaps in their data (due to equipment failure or operator absence) and periods where rainfall depth is measured over a cumulative period of a few days. These cumulative values are not considered as a problem when dealing with weekly, monthly or yearly data, but have to be avoided when using daily data.

**Table 4-2 Still operating daily raingauges in the Blackwater catchment**

| ID | Station Number | Name | X | Y | Open |
|---|---|---|---|---|---|
| **1** | 706 | MALLOW (HAZELWOOD) | 155596 | 104416 | 1941 |
| **2** | 1106 | CAPPOQUIN (MT.MELLERAY) | 209549 | 104071 | 1944 |
| **3** | 1406 | KANTURK (VOC.SCH.) | 138481 | 103207 | 1944 |
| **4** | 3606 | FERMOY (MOORE PARK) | 181991 | 101313 | 1961 |
| **5** | 3706 | RATHLUIRC (FOR.STN.) | 157331 | 118466 | 1962 |
| **6** | 4006 | KNOCKANORE | 207577 | 89076 | 1964 |
| **7** | 4106 | YOUGHAL (GLENDINE W.W.) | 206440 | 83820 | 1982 |
| **8** | 5206 | NEWMARKET BALLINATONA P.H. | 128406 | 112246 | 1982 |
| **9** | 5306 | MOUNT RUSSELL | 161321 | 119793 | 1984 |
| **10** | 3806 | YOUGHAL (ST.RAPHAEL'S HOSP.) | 210173 | 77490 | 1963 |
| **11** | 5506 | BALLINAMULT (DOON) | 217253 | 106719 | 1984 |
| **12** | 6206 | LOMBARDSTOWN (DROMPEACH) | 146327 | 94120 | 1985 |
| **13** | 6306 | BANTEER LYRE | 141566 | 92443 | 1985 |
| **14** | 5406 | GALTEE MOUNTAINS SKEHEENARINKY | 188724 | 119407 | 1984 |
| **15** | 6406 | TALLOW KILMORE | 201288 | 91265 | 1986 |
| **16** | 6506 | MILLSTREET SEWAGE WORKS | 127507 | 90927 | 1986 |
| **17** | 6606 | MALLOW (SEWAGE TREATMENT) | 157592 | 97937 | 1988 |
| **18** | 6906 | MILLSTREET (COOMLOGANE) | 126039 | 90856 | 1991 |
| **19** | 7006 | BARTLEMY | 181903 | 87558 | 1992 |
| **20** | 7306 | NEWMARKET (NEW STREET) | 131603 | 107471 | 1993 |
| **21** | 7406 | MALLOW (SPA HOUSE) | 156572 | 98688 | 1996 |
| **22** | 7506 | BANTEER (GLENSOUTH) | 142539 | 92586 | 1997 |
| **23** | 7706 | TALLOWBRIDGE | 199860 | 94882 | 2000 |
| **24** | 7806 | MITCHELSTOWMN (CORK STREET) | 181768 | 112751 | 2000 |
| **25** | 7906 | BALLYHOOLY (CASTLEBLAGH) | 171990 | 97526 | 2001 |
| **26** | 8006 | GLENCAIRN (TOURTANE HOUSE) | 203341 | 96676 | 2001 |
| **27** | 8106 | CAPPOQUIN (STATION HOUSE) | 210623 | 99159 | 2002 |
| **28** | 8206 | MITCHELSTOWN (GLENATLUCKEY) | 183066 | 109655 | 2001 |
| **29** | 8306 | SHANBALLYMORE | 167205 | 107509 | 2002 |
| **30** | 8406 | CONNA (CASTLEVIEW) | 195672 | 94482 | 2003 |
| **31** | 8506 | LISMORE | 204862 | 97975 | 2003 |
| **32** | 5706 | CASTLEMAGNER | 142535 | 103746 | 1985 |
| **33** | 5806 | FREEMOUNT PUMPING STATION | 139372 | 113862 | 1984 |
| **34** | 906 | RATHMORE G.S. | 117026 | 93163 | 1941 |

## 4.3 The Office of Public Works data

### 4.3.1 Project

The Office of Pubic Works is currently undertaking a Flood Studies Update (FSU) over several Irish catchments, one of them being the Munster Blackwater River. UCC Flood Studies Group has been hired to provide the preliminaries of the project, which include different tasks: management of a raingauges network, data collection, data analysis and flood event analysis.

### 4.3.2 Recording network description

32 raingauges were installed in order to determine the spatial variation of rainfall over the catchment. These were installed between August and October 2005 and the data set is in service since November 2005.

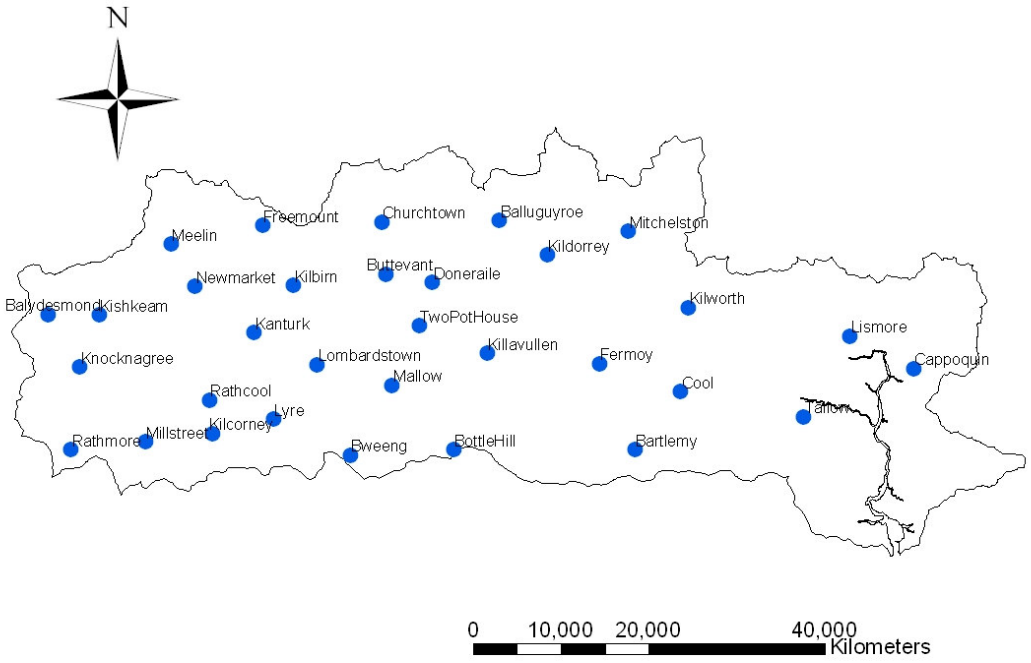


**Figure 4.3 OPW 32 raingauges network**

As can be seen on the figure 4.3, all the catchment, except from a small area in the south-east (around the Youghal estuary) is covered with this dense network. The longest distance between one raingauge and its furthest neighbour being 19 km (between BottleHill and Bartlemy).

The 32 units were installed in different locations owned by Cork County Council (mostly wastewater treatment plants, reservoirs, water intake plants and landfills) in order to facilitate their access and improve their security.

**Table 4-3 OPW raingauges network in the Blackwater catchment**

| Name | Four letters name | Irish National Grid | Elevation (meters a.s.l.) |
|---|---|---|---|
| Bottle Hill - Pump House | Bott | W610884 | 210 |
| Bweeng - Pump House | Bwee | W493878 | 220 |
| Lyre - Reservoir | Lyre | W405919 | 280 |
| Kilcorney - Reservoir | Kilc | W337903 | 220 |
| Millstreet - Reservoir | Mill | W260893 | 200 |
| Buttervant - Pump House | Butt | R533084 | 105 |
| Ballyhoura Way - Water intake works | Chur | R528143 | 95 |
| Freemount - Waste water treatment plant | Free | R394139 | 140 |
| Meelin - Water treatment plant | Balt | R290118 | 200 |
| Newmarket - Reservoir | Newm | R316070 | 180 |
| Ballydesmond - Pump house | Bald | R150038 | 215 |
| Knocknagree - Old pump house | Knoc | W185978 | 170 |
| Duhallow Way - Reservoir | Ratm | W176885 | 290 |
| Kanturk - Waste water treatment plant | Kant | R384017 | 80 |
| Mallow - Pump house | Mall | W541957 | 60 |
| Kishkeam - Waste water treatment | Kish | R207038 | 200 |
| Rathcoole - Waste water treatment plant | Ratc | W334941 | 100 |
| Pallas - Old pump house | Lomb | W455981 | 105 |
| Doneraile - Pumphouse | Done | R586075 | 80 |
| Kilbrin - Resevoir | Kilb | R429071 | 190 |
| Two Pot House - Resevoir | Twop | R571025 | 120 |
| Ballygugroe - Landfill | Balg | R662145 | 220 |
| Kildorrey - Sewage Works | Kild | R717106 | 75 |
| Mitchelstown - Water Treatment Plant | Mitc | R809133 | 90 |
| Castlecooke - Pumphouse | Kilw | R877046 | 110 |
| Bartlemy - Pumphouse | Bart | W817885 | 130 |
| Fermoy - Pumphouse | Ferm | W776982 | 40 |
| Coole - Pumphouse | Cool | W868950 | 80 |
| Tallow - Resovoir/Pumphouse | Tall | W008922 | 80 |
| Lismore - Resevoir/Pumphouse | Lism | S061014 | 175 |
| Cappoquin - Cappoquin | Capp | X133977 | 18 |
| Killavullen - Water Treatment Plant | Kill | W648994 | 50 |

### 4.3.3 Instrumentation and site management

Each site is provided with a raingauge, linked to an external data logger which is stored in a plastic security box near the gauge.

#### 4.3.3.1 Raingages

Casella CEL provided the Tipping Bucket Rain Gauge (Casella, 2002) (see figure 4.4).


**Figure 4.4Tipping Bucket Rain Gauge (Casella, 2002)**

The body and funnel are made from aluminium alloy with a machined septum ring at the top giving a receiving surface of 400 $cm^2$. The tipping bucket mechanism is mounted inside the body on a cast aluminium-alloy base, incorporating a built-in spirit level to ease correct positioning. The rain gauge comprises a divided bucket assembly, which is pivoted at the centre. Rain collects in one side of the bucket, which then tips when 0.2mm of water has been collected. The tipping action discharges the collected water and repositions the opposite side of the bucket under the discharge nozzle ready for filling. In order to obtain an accurate measurement of rainfall, the raingauges were installed in location where interception (by vegetation or constructions) would be as low as possible. No major problems were encountered after using the device for almost 1 year.


**Figure 4.5 To avoid interception, the gauge is installed on the roof of a reservoir in Knocknagree**

### 4.3.3.2 Data loggers

Casella was also selected to provide the logging equipment. Casella Sensus Logger (Casella, 2002) (see figure 4.6) is an external multi channel data acquisition module and can thus be used for many measurements devices in the same time (rainfall, temperature, wind speed, wind direction, etc.). The OPW decided to use this complex device, obviously capable of a lot more than raingauge logging with the idea of implementing other measurement devices in the future.


**Figure 4.6 Sensus Logger (Casella, 2002)**

Logging could originally be set at different time interval (from 1 minute to one day) and information could be stored in the internal memory for a long period of time. The Sensus was originally powered by a 12v d.c. 7Ah Lead Acid battery that was supposed to have a 2 months life time if logging every 5 minutes. Data can be downloaded via a RS232 port to laptop or palmtop devices, and directly saved as friendly format files. Communications between the user and the logger are made through the Online Pro Software (Casella CEL, 2002) which allows uploading and downloading settings to and from the logger, to download the recorded data and to display the information. The Sensus is kept in a hermetic plastic shelter (30 x 30 x 18 cm) within a meter or two of the gauge (see figure 4.7).


**Figure 4.7 The raingauge and its data logger in Bweeng**

### 4.3.3.3 Troubleshooting

The first months showed different problems associated with the use of the loggers. Contrary to what was expected, battery life could not exceed 15 days if the logging time was set to 5 minutes, which made the data collection work a heavy task. Three days were required to drive to and collect data from the 32 raingauges network (more than 400km).

Enhancements were thus made on the logging system. Casella was asked to provide an upgraded software version that could modify the logger configuration so it could log only when precipitation actually occurred and return in sleep mode 1 minute later. Table 4.4 gives a comparison between the old and the new logging system for July 2006 in Ballyguyroe. This modification increased noticeably the battery life as it required a considerably lower number of logging steps. The system was also improved by using 12Ah batteries instead of 7Ah batteries.

**Table 4-4 Number of logging data entry values (rows)**

| | **Old system** | **New system** |
|---|---|---|
| **Number of logging** | 8640 | 146 |

With these improvements, it appeared that the Casella CEL Sensus is not perfect for outdoor conditions powered by small batteries. It would have been wiser to use some other devices such as the Onset Hobo Logger (Onset, 2001), much cheaper and easily usable than the complex and expensive Casella CEL Sensus.

The UCC Hydromet research group uses the Onset Hobo Logger to record precipitation in a few locations. This logger, small enough to be incorporated inside the gauge's body has a battery that can last more than 1 year without being changed. This battery is similar to that in a digital watch.

**Table 4-5 Comparison of two data loggers**

| | **Casella Sensus Logger** | **Onset Hobo Logger** |
|---|---|---|
| **Type of battery** | 7Ah Lead Acid | CR-2032 Lithium |
| **Battery's life** | 1 month | 1 year |
| **Battery's size** | 15 x 6 x 9 cm | Ø 2cm |
| **Logger size** | 22 x 13 x 4 cm | 7 x 8 x 1 cm |

Choosing to use the Casella Sensus Logger instead of some Onset Hobo like logger was a mistake that lead to significant loss of time and energy. The choice of the appropriate

instrumentations is a really important task when installing a scientific survey scheme and should always be advised by actual scientists working in the field more than by traders.

## 4.4 UCC Hydromet data

The UCC Hydromet research group also ran 5 raingauges in the Mallow subcatchment for the full year 2005. Rainfall was recorded on an hour basis using the previously presented Onset Hobo Logger. The five recording locations are listed in table 4.6.

**Table 4-6 Location of Ucc Hydromet gauges**

| Name | X | Y | Irish National Grid |
|---|---|---|---|
| **Banteer** | 141500 | 92500 | W415250 |
| **Millstreet** | 127400 | 90600 | W274060 |
| **Ballydesmond** | 114900 | 104000 | R149040 |
| **Newmarket** | 128300 | 112300 | R283123 |
| **Castlemagner** | 142500 | 103800 | R425038 |

## 4.5 Raingauges contributing areas

When a basin has more than one raingauge in the area considered, these raingauges inevitably record different amounts of precipitations whether it is for a single rainstorm or over a specified period of time. In this chapter, contributing areas of each raingauges are defined using the Thiessen polygon associated with each station. The Thiessen polygon of a gauge is the region in which any point at random is closer to this particular gauge than to any other gauge in the recording network. The precipitation is assumed to be constant and equal to the gage value throughout the whole region. It should be noted that

Here, a gauge represents a sub area $A_i$ which denotes the area of influence of each gauge which is obtained by constructing polygons determined by drawing perpendicular bisectors to lines connecting the gauges. The bisectors are the boundaries of the effective area for each gauge, each enclosed are can be measured using GIS tools. The spatial average is calculated by weighting the individual stations with their respective area given by:

$$\langle P \rangle = \frac{1}{A} \sum_{i=1}^{n} A_i P_i \tag{4.1}$$

where $n$ is the number of raingauges in the area, and $A_i$ is the surface area of the catchment, that is the sum of the sub areas, or $A = \sum_{i=1}^{n} A_i$ .

It should be noted that even if the Thiessen polygons method is the most widely used, it does not take into account the elevation factor and that the denser the recording network is, the more reliable the Thiessen method will be.

In the following chapters of this thesis, rainfall-runoff modelling is applied to 3 sub-catchments within the Blackwater catchment (Duarrigle, Dromcummer and Killavulen). Thiessen polygons were therefore constructed regarding to these areas (see figures 4.8 to 4.11). The construction has to be made for all the different recording networks used for the corresponding dates (see table 4.7). Average rainfall data over each sub-catchment can be determined as a weighted average (regarding to the surface areas) of its Thiessen polygons.

**Table 4-7 Recording step and period of availability for the different recording network**

| Data source | Recording step | Period of availability |
|---|---|---|
| **Met Service daily gauges** | 1 day | 1941 to now (depending on the gauge) |
| **Met Service Automatic Gauges** | 1 hour | 1988 to 2004 |
| **UCC Hydromet** | 5 minutes | 2005 |
| **OPW** | 5 minutes | November 2005 to now |

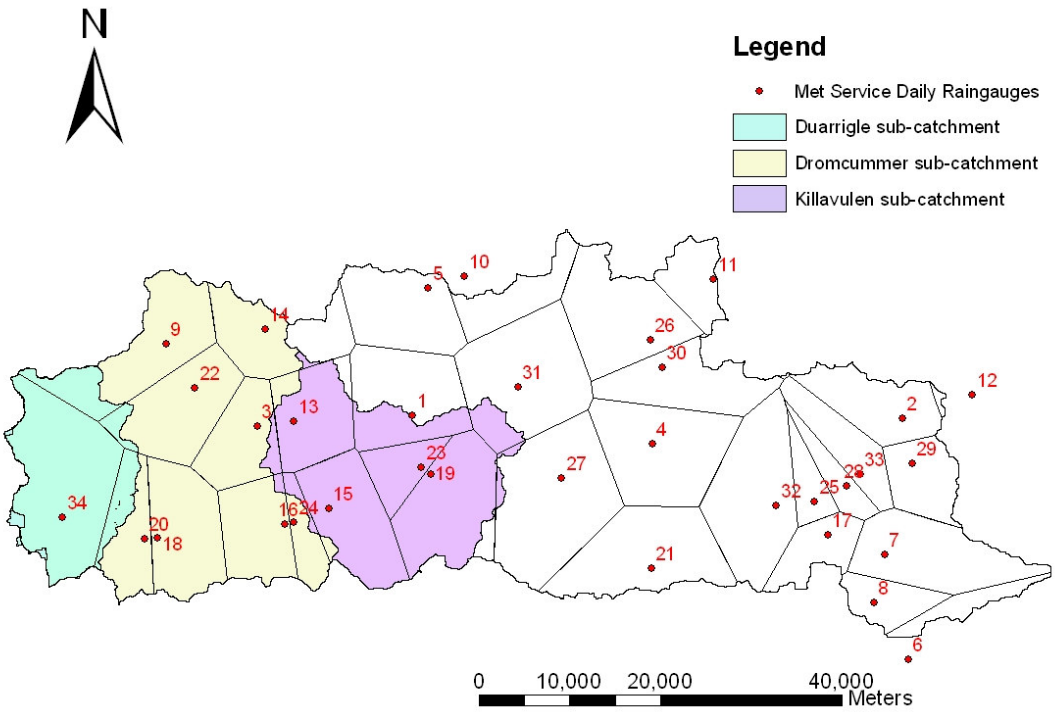


**Figure 4.8 Thiessen polygons - Met Service Daily raingauges**

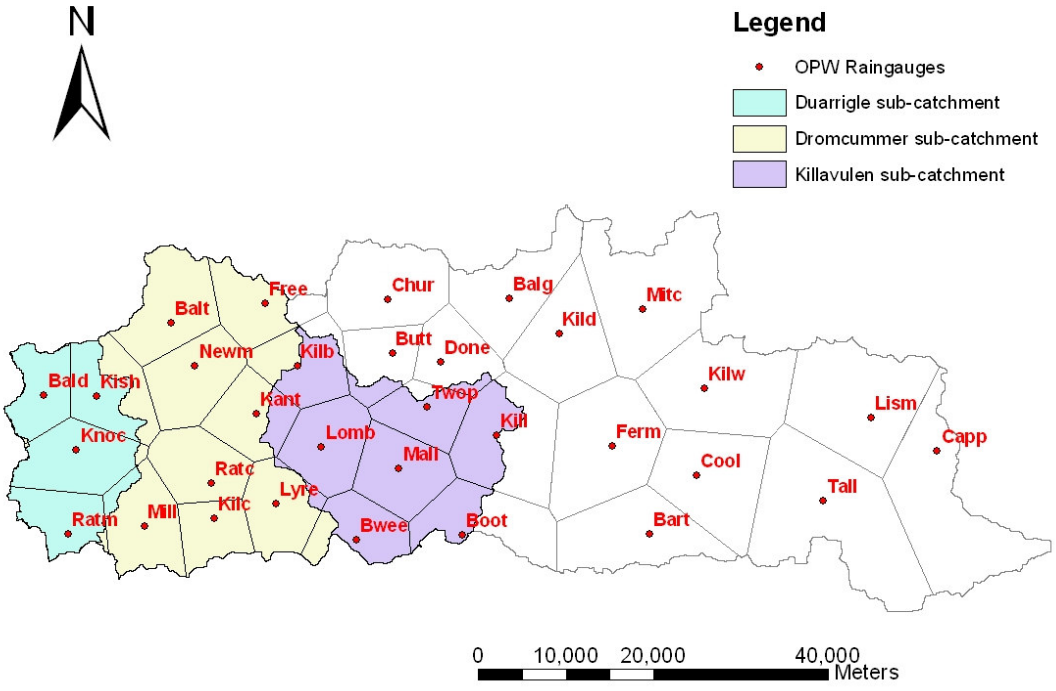


**Figure 4.9 Thiessen polygons - OPW raingauges**

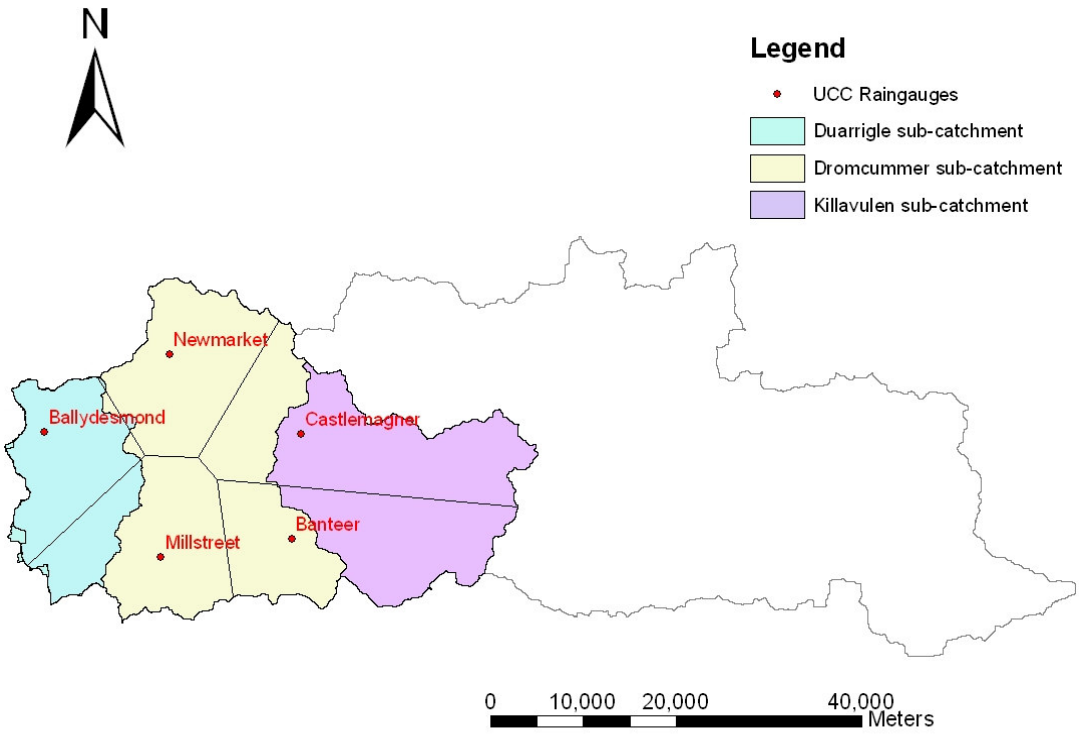


**Figure 4.10 Thiessen polygons - UCC raingauges**

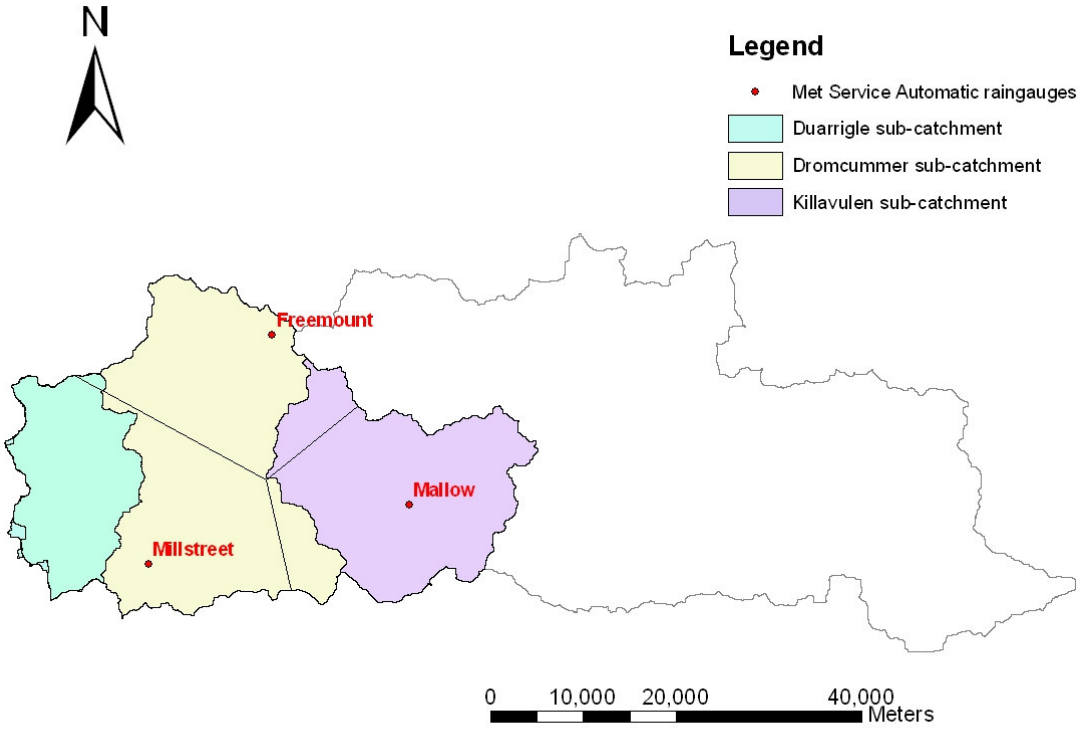


**Figure 4.11 Thiessen polygons - Met Service Automatic raingauges**

## 4.6 Analysis

### 4.6.1 Comparison between the different sources

The daily Met Éireann data and the 5-minutes step OPW data cover a mutual period of record (from the 1st of November 2005 to the 1st of August 2006). Data was compared in locations where both Met Éireann and OPW gauges could be found. In order to be representative of the spatial variation, three locations were particularly analysed: Millstreet in the West, Mallow in the catchment centre and Tallow in the East.

**Table 4-8 Comparison between Met Eirean daily raingauges and new OPW gauges**

| | Millstreet | Mallow | Tallow |
|---|---|---|---|
| **Met Éireann (mms)** | 661 | 419 | 416 |
| **OPW (mms)** | 734 | 486 | 485 |
| **OPW/Met** | 1.11 | 1.16 | 1.16 |

For each of the three locations, a strong linear relationship is observed between the two sources of data (see figure 4.13), but the depths recorded by the Met Éireann appear to be lower, with an approximate linear coefficient of 15% (this underestimation was noticed in the whole recording network). A one day scale comparison tells more about the difference in depths. Figure 4.12 gives an example of a two weeks observation period in Mallow.

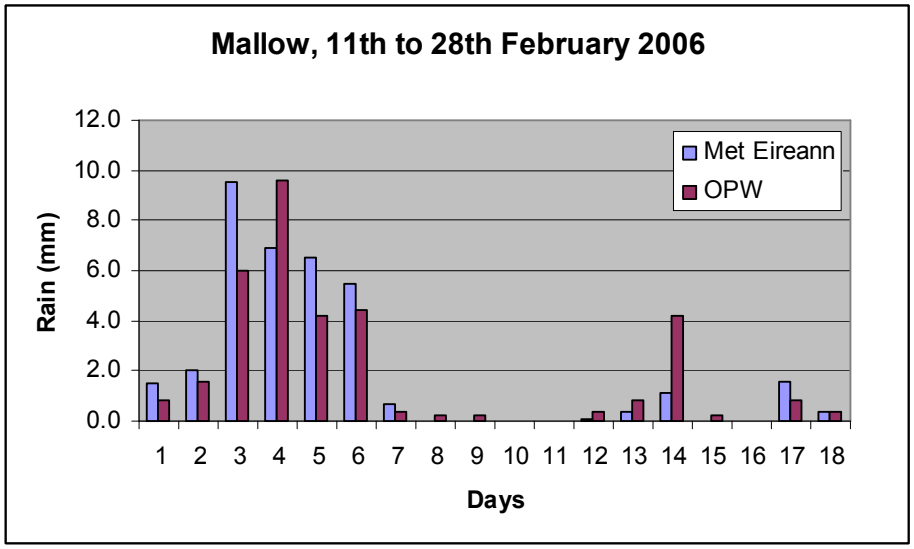


**Figure 4.12 One day scale comparison between Met Éireann and OPW data**

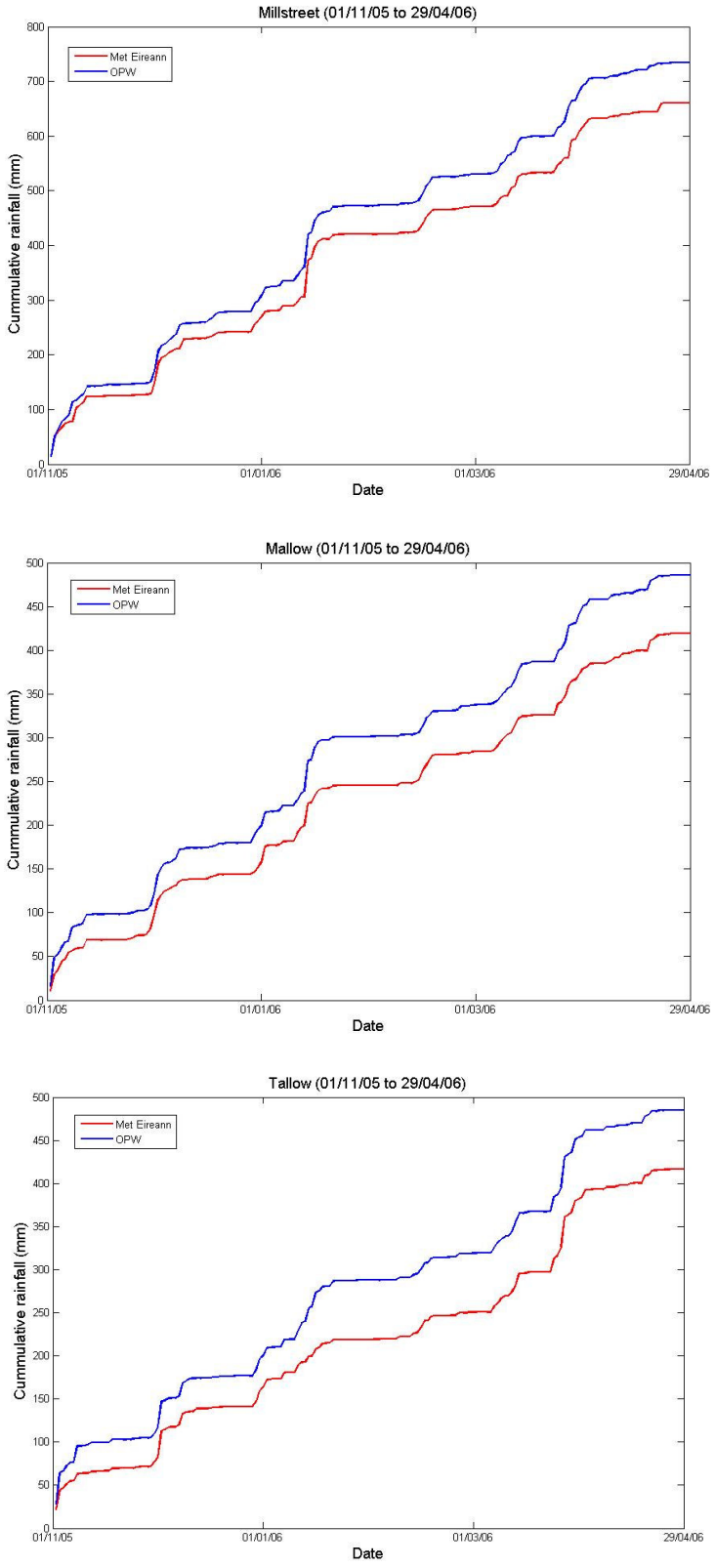


**Figure 4.13 Comparison between Met Éireann raingauges and new OPW gauges**

At this scale, the constant underestimating is not observed. We can see that the OPW depths are sometime lower than the ones observed by Met Éireann. This apparent absence of linear relationship between the two dataset may be explained by the data collection operating mode. Most of Met Éireann gauges are manually checked on a daily basis. As data are given for 9am to 9am day, late reading in the morning will imply an erroneous value, especially on a day when it is actually raining around the reading time. Furthermore, every fault in reading the gauge will imply a 2 days cumulative value for the next day. This issue is reflected in the Data Indicator Description given with each value by Met Éireann (see table 4.1).

Considering the high correlation observed for the 6 months cumulative rain comparison, Met Éireann data was considered accurate enough to be used. Nevertheless, the OPW data, with its very precise 5 minutes-step dataset, was preferred as soon as available. Considering this point, all the rainfall studies carried in the following chapter were made using OPW data coming from the 32 raingauges network of the Munster Blackwater Catchment, for the 9 months of data available at the time of the writing (November 2005 to July 2006).

### 4.6.2 9 months data

#### 4.6.2.1 Daily and monthly analysis

The wettest day in the 9 months was recorded on the 12th January 2006 (Julian day 377), when 41.4 mms were recorded in Rathmore (see figure 4.14). Most of the stations (14) had their wettest day on the 21st May 2006 (Julian day 506), when a maximum of 36.4 mms was recorded in Kishkeam and a minimum of 19.8 mms in Kildorrey.

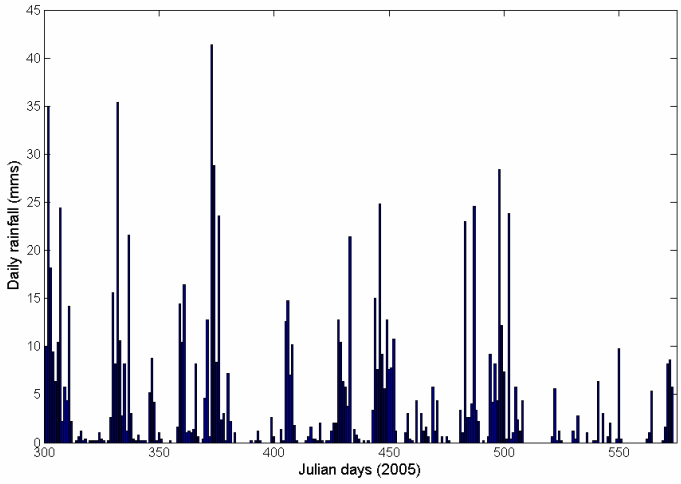


**Figure 4.14 Daily Rainfall in Rathmore (9 months data)**

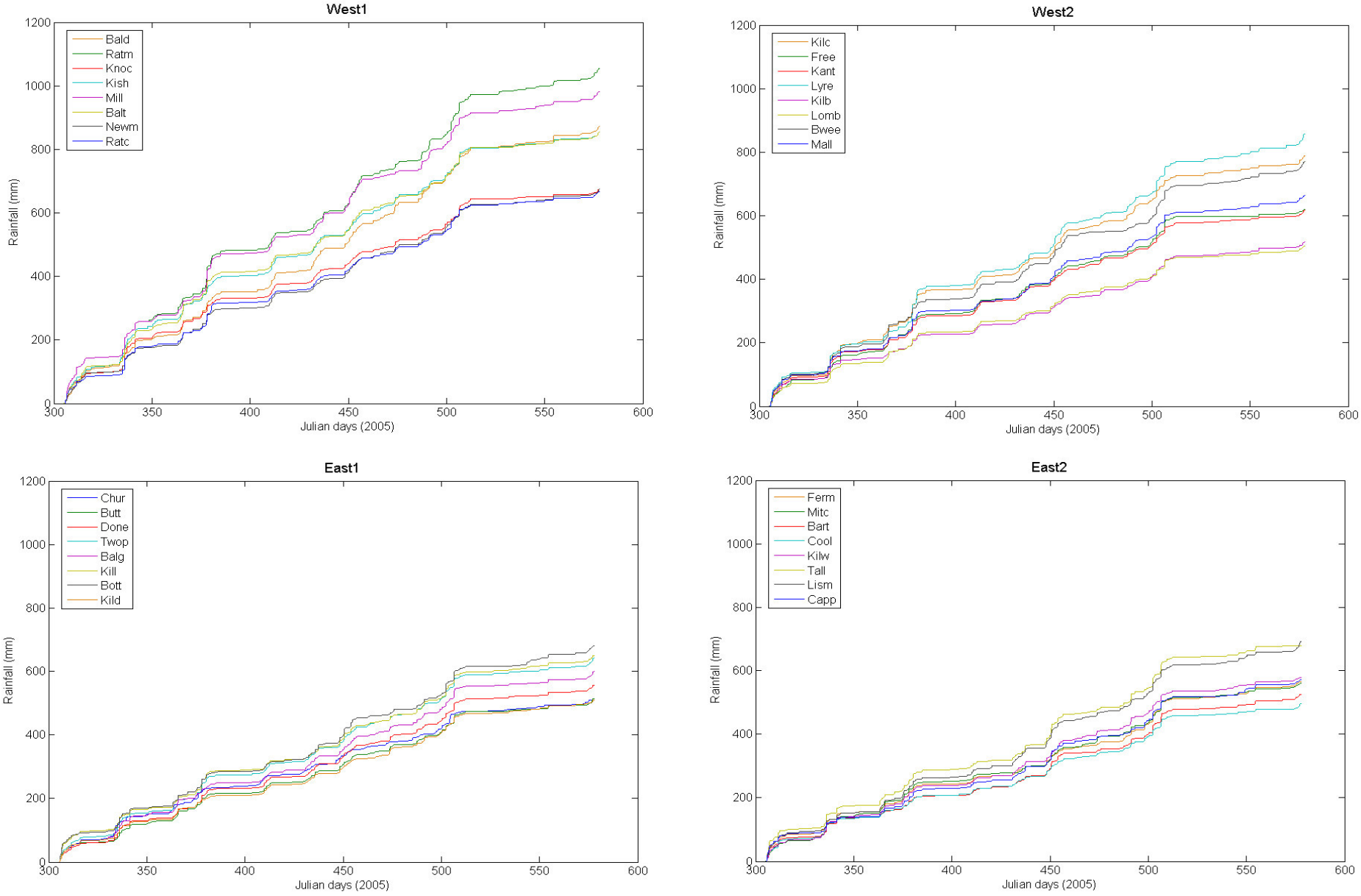


**Figure 4.15Cumulative rainfall for the 32 stations, November 2005 to July 2006.**

Cumulative rainfall depths over the 9 months period (see figure 4.15) show a high linearity between each curve, which highlights the homogeneity of the catchment in term of rain events timing. Higher cumulative depths are found in the western part of the catchment, where the highest record (1054 mms in Rathmore) is more than twice the lowest (495mms in Conna). 9 months is a short period to observe such a difference in cumulative rainfall between two stations separated by only 70 kilometres. This important spatial variability will therefore be studied in the next paragraph.

A comparison between average monthly depths calculated with the 9 months data and data recorded for 22 years (1983-2004) shows that rainfall depths in the analysed period are significantly lower than the previous years (table 4.9). March and May 2006 are the only exceptions. With only 42 mms of rainfall (less than half the average value), February 2006 was a particularly dry winter month. The same difference can be observed in April 2006 when only 43 mms were recorded. June and July 2006 were also particularly dry, even for summer months. Monthly depths were higher than the average in March and May, but these precipitations were not sufficient to balance the drought observed during the other months. As a result, cumulative depth over the 9 months is 25% lower than the corresponding long term average value.

**Table 4-9 Monthly rainfall depths in the Blackwater Catchment (mms)**

| | Nov | Dec | Jan | Feb | Mar | Apr | May | Jun | Jul | Cumulative |
|---|---|---|---|---|---|---|---|---|---|---|
| **Min** | 72.6 | 66.6 | 47.2 | 26.2 | 76 | 20 | 83.6 | 0 | 21.2 | 495.6 |
| **Max** | 161.8 | 173.2 | 150.6 | 64.8 | 163.2 | 86.6 | 205.2 | 25 | 61.2 | 1054.8 |
| **Mean (9 months)** | 106.6 | 106.5 | 81.0 | 41.7 | 108.3 | 43.1 | 127.9 | 13.7 | 36.6 | 665.4 |
| **Mean (1983-2004)** | 116.5 | 129.0 | 133.0 | 103.1 | 91.7 | 82.7 | 71.2 | 72.1 | 61.5 | 860.7 |

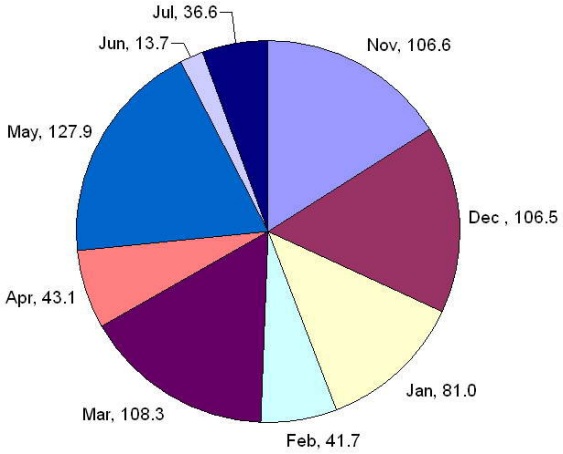


**Figure 4.16 Pie chart of monthly variation of rainfall in mms (9 months data)**

As can be seen in figure 4.17, the range of monthly records between the different stations depends with the period of the year. The three wettest months (December, March and May) have the more spread ranges.

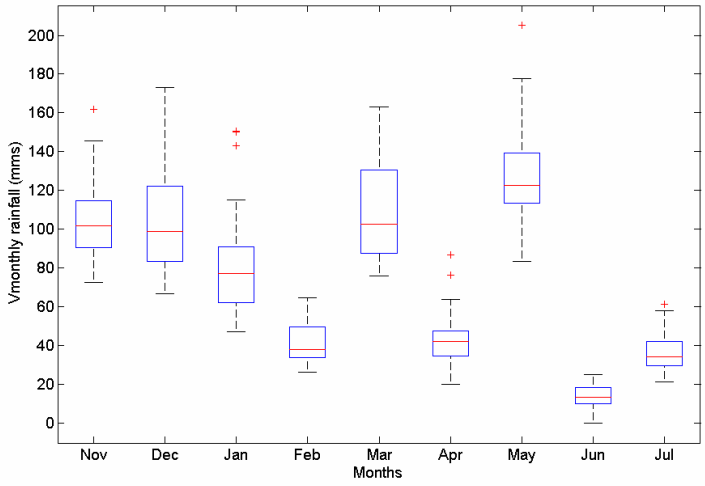


**Figure 4.17 Monthly box plots (9 months data)**

### 4.6.2.2 Drought assessment

A long flat part from the end of May to end of the records (about 80 days, i.e. approximately 30% of the data length) can be observed in each of the 32 raingauges (see figure 4.15). Such a long period without significant rain events is not common in Ireland and does not reflect the monthly average values usually recorder in this catchment. In order to judge the importance of this dry period, daily rainfall records were compared with data from the summer 1976, when the more important ever recorded drought in Ireland was observed (McCartaigh, 1996).

Periods of little or no rain are described using the terms introduced by Met Éireann, that are more useful than the World Meteorological Organisation (WMO) definition, and more quantifiable for the conditions pertaining in Ireland. An absolute drought is a period of 15 or more consecutive days, on none of which 0.2 mm or more of rain fell. A partial drought is a period of at least 29 consecutive days, the mean daily rainfall of which does not exceed 0.2 mm. Finally, a dry spell is a period of 15 or more consecutive days, on none of which 1.0 mm or more of rain fell.

Table 4.10 gives the number of days that meet the requirements for absolute droughts, partial droughts and dry spells.

**Table 4-10 Number of days fulfilling the requirements for the different drought indicators**

| Station | Absolute drought Requirements (needs to be >15) | Partial drought Requirements (needs to be >29) | Dry spell Requirements (needs to be >15) |
|---|---|---|---|
| **Bottle Hill** | **22** | **31** | **22** |
| **Bweeng** | 13 | 14 | 13 |
| **Lyre** | 13 | 14 | 14 |
| **Kilcorney** | 13 | 14 | 14 |
| **Millstreet** | 13 | 14 | 14 |
| **Buttevant** | 13 | 24 | 14 |
| **Churchtown** | 11 | 20 | **22** |
| **Freemount** | 14 | 23 | **22** |
| **Balinatona** | 14 | 23 | 14 |
| **Newmarket** | 14 | 22 | 14 |
| **Ballydesmond** | 13 | 14 | 14 |
| **Knocknagree** | 13 | 24 | **22** |
| **Rathmore** | 14 | 14 | 14 |
| **Kanturk** | 13 | 22 | 14 |
| **Mallow** | 13 | 14 | 14 |
| **Kishkeam** | 14 | 22 | 15 |
| **Rathcoole** | 13 | 19 | 14 |
| **Lombardstown** | 13 | 22 | **16** |
| **Doneraile** | 13 | 22 | 14 |
| **Kilbirn** | 13 | 22 | 13 |
| **Two Pot House** | 13 | 22 | 13 |
| **Ballyguyroe** | 12 | 20 | **23** |
| **Kildorrey** | 13 | 22 | **22** |
| **Mitchelston** | 13 | 22 | 14 |
| **Kilworth** | 13 | 24 | **22** |
| **Bartlemy** | 13 | 14 | 13 |
| **Fermoy** | 13 | 14 | 14 |
| **Cool** | 14 | 28 | 14 |
| **Tallow** | 13 | 28 | 14 |
| **Lismore** | 14 | 24 | 14 |
| **Cappoquin** | 13 | 28 | **24** |
| **Killavulen** | 13 | 14 | 14 |

Among the 32 stations, only one absolute drought was recorded, in Bottle Hill, where no rainfall was recorded for a total period of 21 days (from 27$^{th}$ May to 17$^{th}$ June 2006). Most of the stations located in the Western part of the catchment saw at least 12 days (from 27$^{th}$ May to 10$^{th}$ June 2006) without any rainfall, while the total absence of rainfall lasted 13 days (from 27$^{th}$ May to 11$^{th}$ June 2006) in most of the Eastern locations. It should be noted that such a long period without any rainfall at all was not observed in 1976, where no absolute drought occurred (MacCarthaigh, 1996).

The partial drought analysis also showed that Bottle Hill was the only station to meet the requirements, with a 31-days period from the 27th May to the 26th June. Three other Eastern stations (Fermoy, Coole and Lismore) recorded 28 consecutive days the mean daily rainfall of which did not exceed 0.2 mm, and where therefore just below the threshold of 29 days. In 1976, a 33 days long period of partial drought was observed in Fermoy Moorepark. The longest dry spell was observed in Cappoquin from the 27th May to the 20th June 2006 (24 days). Dry spells were also observed in 8 other stations from the 27th May (Bottle Hill, Churchtown, Freemount, Knocknagree, Lombardstown, Ballyguyroe, Kildorrey and Kilworth). It should also be noted that dry spells, unlike absolute and partial droughts, occurred at other different time in the year (after the 13th November 2005, the 21st January and the 28th May) for a majority of the 32 recording stations. In 1976, the longest dry spell lasted only 22 days in Fermoy Moorepark. A small amount of rainfall, falling at the end of a drought, may break the formal definition of an absolute/partial drought but may not be sufficient to cause surface runoff or may cause a small amount of surface runoff. In the latter case, the river levels will return very quickly to the pattern which pertained prior to the rainfall because the groundwater component has not increased. For this reason, MacCarthaigh defines a term called “periods of insignificant rainfall” which have regard to the runoff effects of small rainfall amounts in drought periods, and is used to asses the severity of droughts in conjunction with river flow records. A period of insignificant rainfall (PIR) starts with a period of no rainfall and ends when the corresponding river flow stops to decrease. Unlike the absolute drought, partial drought and dry spell, the definition of a PIR is subjective. The length of the period is decided from the observation of both rainfall and river flow data.

Figure 4.18 shows daily river flows in 1976 and 2006, from the 1st of January to the 30th of September. It should be noted that due to missing data in Killavulen river station, the 2006 plot was taken from Duarrigle data. The only observed factor being the hydrograph shape (in order to know if the flow is following a recession), flow values are neglected, and the fact that general trend was the same in both Killavulen and Duarrigle allow us to compare the two plots. As shown in figure X, a long period of flow recession ant therefore a PIR is observed from the 27th May to the 1st September 2006, i.e. 95 days. According to MacCarthaigh, the longest PIR ever recorded in the Blackwater was 66 days (15th July to 18th September 1976). Another PIR was observed from the 17th May to 5th July 1976.

Taking into account only the longest absolute droughts, partial droughts, dry spells and PIRs would lead to consider the 2006 drought as being more important than the one observed in 1976. Figure 4.18 is nonetheless showing longest periods of flow recessions in 1976 than in 2006, physical sign of a dryer period.

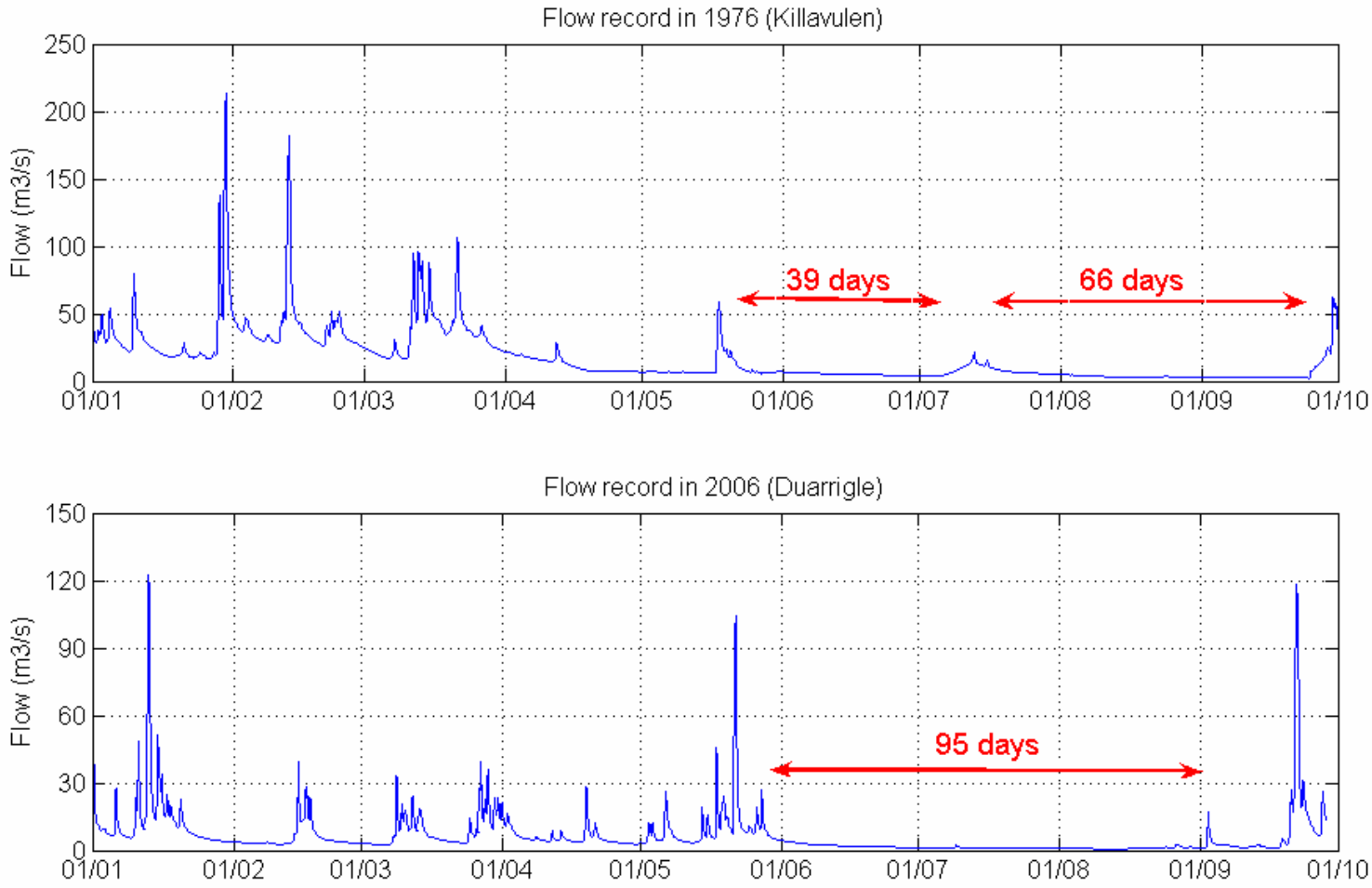


**Figure 4.18 Comparison of river flows, 1976 and 2006**

### 4.6.3 Spatial variation

Rainfall depths recording at different points in the catchment show a high spatial variability. Coupling the precise OPW dataset and the long term Met Éireann daily dataset provides a good understanding of this variation.

An effective way to visualize the rainfall spatial variation is to examine rainfall contours, which display lines where rainfall amounts are constant. Such visualization highlights the different peaks, slopes and low intensity areas. As can be seen on figure 4.19, rainfall contours constructed from the 9 months cumulative rainfall show that the wettest areas are located on the western edge of the catchment and the rainfall seems to decrease with the longitude (from West to East), with a reduction in the increase at the eastern edge. This tendency is also noticeable in figures 4.15 (9 months cumulative rainfall) where cumulative depths appear to be greater in the West. As outlined in chapter 2, the main wind direction is from South West. Winds that blow over the catchment come from the Atlantic Ocean where it is loaded with moisture. Once reaching the boundary between ocean and land, the moisture is lifted above and condensed in clouds that would cause precipitation when going over the land. This meteorological phenomenon explains the precipitation gradient that can be found in South West Ireland in general, and in the Munster Blackwater catchment in particular with the very important precipitation difference between the Western and the Eastern parts of the catchment. This can also serve to explain the flow variation in the Blackwater with much higher flow rates per $km^2$ in the West than in the East (see Chapter 5).

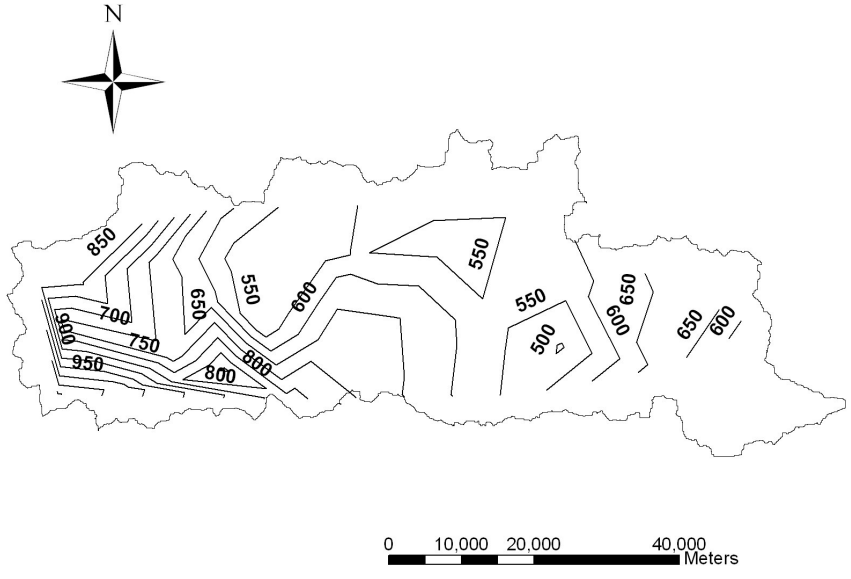


**Figure 4.19 Rainfall contours in the Blackwater catchment - 9 months rainfall**

As can be seen in figure 4.20, a strong linear relationship is noted between the gauge location longitude and its rainfall depth. The linear regression was applied to 29 of the 32 OPW raingauges. The three points shown in red on the plot (Tallow, Lismore and Cappoquin) which represent the eastern edge of the catchment, did obviously not fit this regression and where therefore excluded.

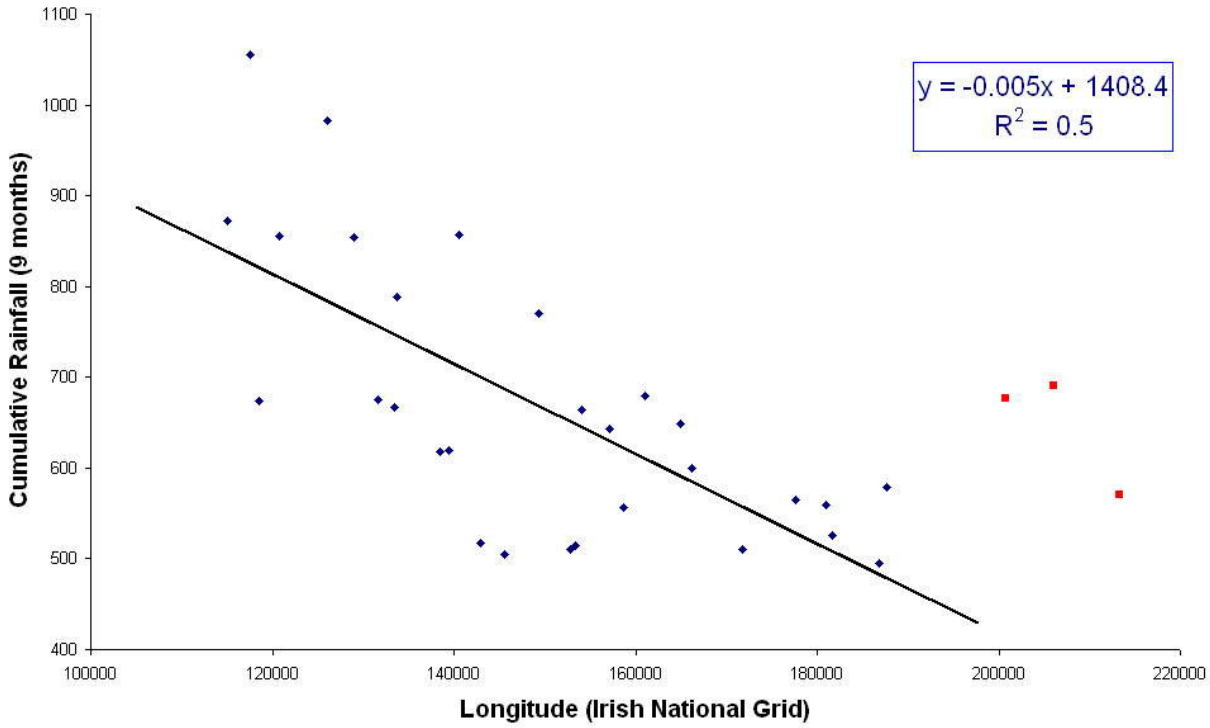


**Figure 4.20 Linear regression between rainfall depth and longitude (OPW 9 months dataset)**

It was also found that the topography and thus the elevation had a significant impact on spatial variation. As can be seen in figure 4.21, high elevations (areas in brown on the map) are associated with important rainfall depths while gauges installed in the valley (areas in green on the map) receive less precipitation. This trend is also noticeable in figure 4.22, in which a relation between the gauge's elevation and the cumulative rainfall is highlighted.

As shown by the two regressions, both longitude and elevation are significantly factors impacting the rainfall spatial variation. Fixing one of the two parameters allows us to observe more clearly the impact of the other one. For example, if fixing the longitude between 115000 and 120000 (a 5 km wide stripe which includes Ballydesmond, Rathmore, Knocknagree and Kishkeam), the influence of the elevation appears to be clearer (see table 4.11).

**Table 4-11 Elevation and cumulative depth for 4 locations on the same longitude**

| | Elevation (m a.s.l.) | Cumulative depth over 9 months(mms) |
|---|---|---|
| **Knocknagree** | 170 | 674 |
| **Kishkeam** | 200 | 856 |
| **Ballydesmond** | 215 | 872 |
| **Rathmore** | 290 | 1054 |

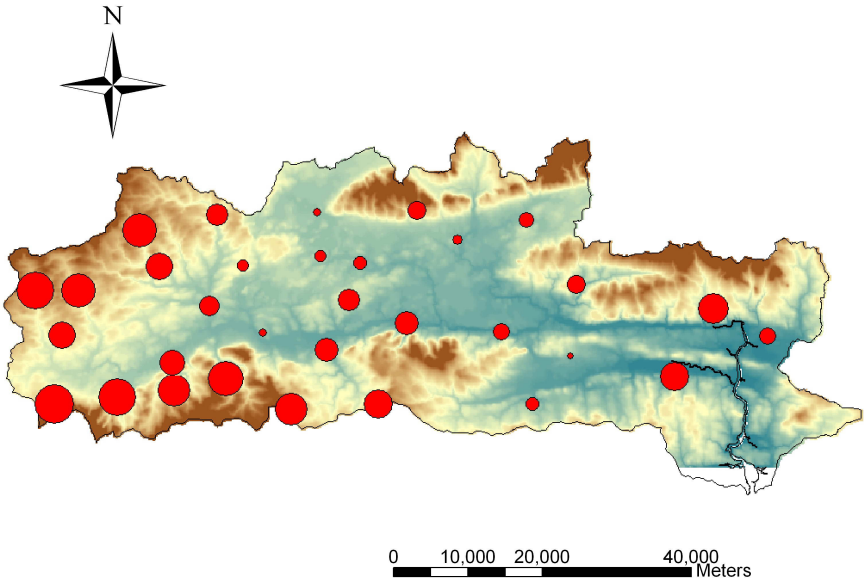


**Figure 4.21 Rainfall intensity (in red) regarding the elevation**

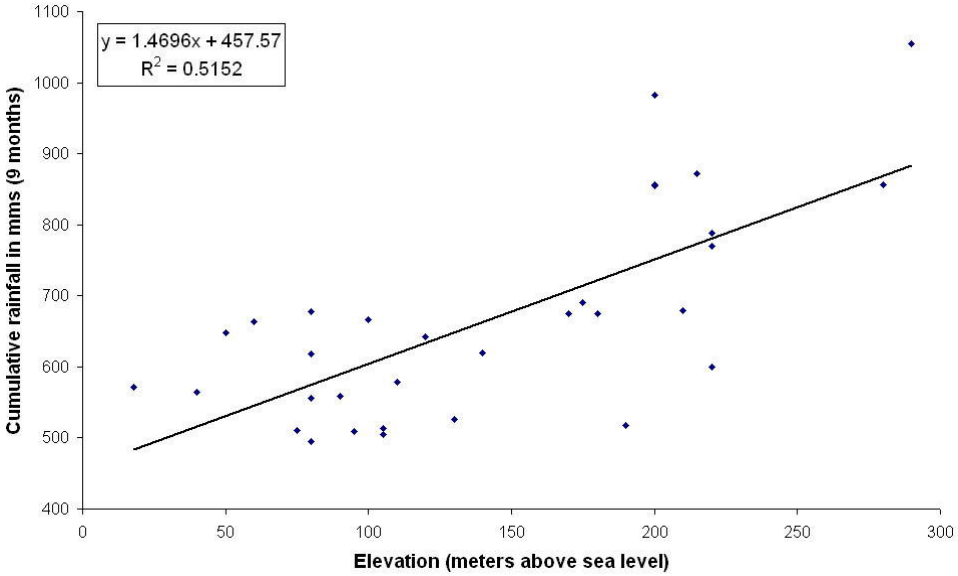


**Figure 4.22 Linear regression between rainfall depth and elevation (OPW 9 months data)**

A particular attention was given to the three gauges that were excluded from the first regression (see Figure 4.20). They receive a high volume of rainfall when their locations are at the far eastern side of the valley, just below the Knockmealdown Mountains, and are therefore not following the West-East variation observed above. It should also be noted that the elevation factor is not enough to explain the high recorded depths. Lismore, even if it is located on the hillside (175 m a.s.l.) received 690 mms which is more precipitation than other gauges with equivalent elevations and smaller longitudes (517 mms in Kilbirn, 190 m a.s.l; 675 mms in Newmarket, 180 m a.s.l. and 674 mms in Knocknagree, 170 m a.s.l.). Tallow also receives an important cumulative depths (677.2 mms) when it is only located at 80 m a.s.l. Finally, while almost at sea level (18 m a.s.l) Cappoquin receives 570 mms, being therefore the 11$^{th}$ highest wettest location in the catchment.

A possible explanation for this particularity is an association of the elevation factor with a specific topographic feature. The Blackwater catchment is indeed surrounded by high range mountains on both its North and South, for almost its whole length. This topographic barrier is nevertheless absent on the far south-eastern side of the catchment, from Fermoy to the Youghal estuary (see figure 4.21). Because of this topographic specificity, winds can penetrate more easily here than in the rest of the valley. High intensities recorded in Tallow, Lismore and Cappoquin could therefore be explained by the manifestation of the orographic effect. When air is confronted to a topographic barrier, it is lifted up and sees its temperature dropping as it rises. As air cools to its saturation point, the water vapour condenses and clouds form, ready, to turn into rain. In the particular case of the Eastern Blackwater catchment, Knockmealdown Mountains are the topographic barrier and block the air loaded in moisture coming from the South-West (prevailing wind direction in the catchment). Important clouds are thus forming on the leeside of the mountain and are the cause of the high precipitation recorded in the valley on its South (see figure 4.23).

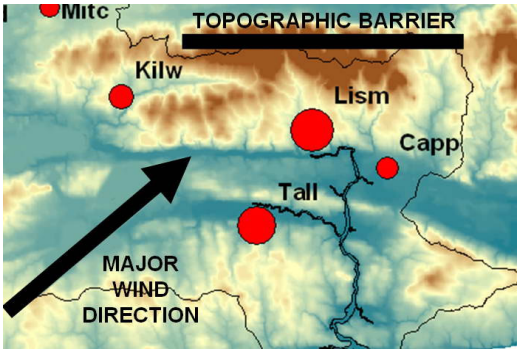


**Figure 4.23 Manifestation of the orographic effect in the Blackwater Valley**

### 4.6.4 Summary statistics

It was decided to statistically analyze the general characteristics of the catchment rainfall in order to have a better understanding of its rainfall patterns. To do so, yearly, monthly, daily and hourly statistics were computed. In order to take into account the spatial variation, three different locations were considered: Newmarket on the West, Mallow in the centre and Fermoy on the East using Met Éireann data.

#### 4.6.4.1 Yearly precipitation

The following table gives the summary statistics of yearly precipitation in the three sites, for the years 1973 to 2005 (23 years).

**Table 4-12 Summary statistics of yearly precipitation, in mms**

| | Newmarket | Mallow | Fermoy |
|---|---|---|---|
| **Mean** | 1460.6 | 1116.9 | 1018.2 |
| **Median** | 1451.1 | 1123.0 | 1032.6 |
| **Standard Deviation** | 171.9 | 121.9 | 103.0 |
| **Range** | 609.2 | 444.0 | 339.3 |
| **Minimum** | 1145.1 | 919.6 | 860.4 |
| **Maximum** | 1754.3 | 1363.6 | 1199.7 |

The mean precipitation is everywhere greater than 1 meter (1460 mms for Newmarket, 1117 mms for Mallow and 1018 mms for Fermoy) and decreases going from West to East. This decrease is also true for the three statistics indicators: the median, the standard deviation and the range between minimum and maximum values. It reflects the fact that the yearly precipitations are more steady form one year to another on the eastern part of the catchment.

As can be seen on figure 4.24, which is a plot of annual rainfall depth versus years, differences between Mallow and Fermoy records are less important than those between Newmarket and the two other locations. The general tendency is the same for the whole studied period: Newmarket always has the greatest depth, followed by Mallow and then Fermoy.

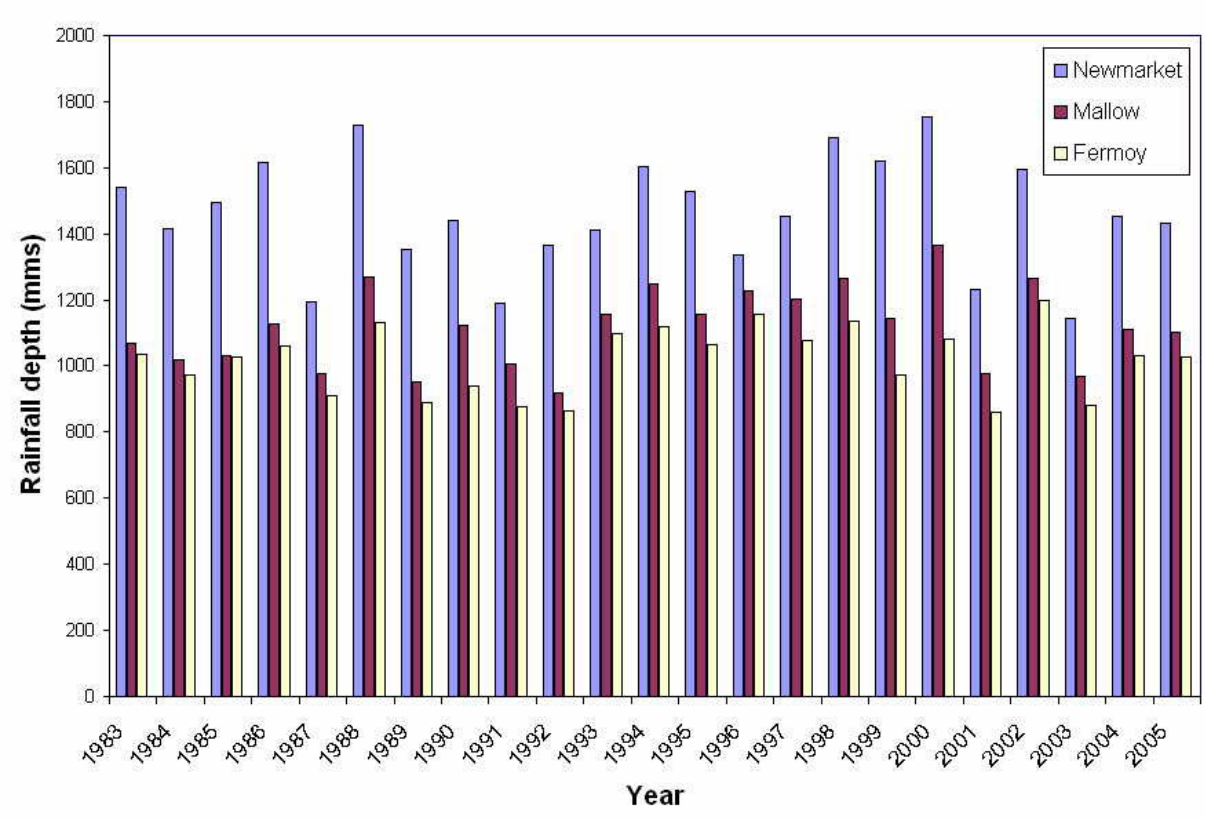


**Figure 4.24 Yearly precipitation in Newmarket, Mallow and Fermoy**

### 4.6.4.2 Monthly precipitation

The following table gives the summary statistics of the monthly precipitation for the 275 months observed (1983 to 2005).

**Table 4-13 Summary statistics of monthly precipitation, in mms**

| | Newmarket | Mallow | Fermoy |
|---|---|---|---|
| **Mean** | 121.5 | 93.1 | 84.9 |
| **Median** | 110.8 | 89.76 | 79.2 |
| **Standard Deviation** | 66.4 | 49.4 | 46.1 |
| **Range** | 360.1 | 240.8 | 228.5 |
| **Minimum** | 0 | 2.9 | 2 |
| **Maximum** | 360.1 | 243.8 | 230.5 |

It can be seen from table 4.13 that relative ranges (ranges compared to the mean values) are more important than those obtained for the yearly analysis. The intensity gradient from West to East is also noticeable at the month scale.

Monthly precipitations were ranked into classes of 10mms in order to plot the rainfall depth versus its density (see histograms in figure 4.25). Even if the plotted histograms are not perfectly smooth, they can be fitted with "gamma-shaped" distribution. When depth densities in Mallow and Fermoy show good agreement with Gamma function distributions, data in Newmarket could not be fitted with such a probability distribution because of the too high density corresponding to the 0-10 mms events. A logistic distribution showed better results. The Gamma ($G$) and Logistic ($L$) distributions are respectively defined as follow:

$$G(x,a,b) = \frac{x^{a-1}e^{x/b}}{b^a \Gamma(a)} \tag{4.1}$$

$$L(x,a,b) = \frac{1}{1+e^{-(x-a)/b}} \tag{4.2}$$

**Table 4-14 Monthly depth curve fitting and their parameters**

| Gauge location | Probability distribution | a | b |
|---|---|---|---|
| Newmarket | Logistic | 116.8 | 37.2 |
| Mallow | Gamma | 2.97 | 28.46 |
| Fermoy | Gamma | 2.82 | 30.05 |

Monthly variations in depth in the mean were also studied (see figure 4.26). Good agreement in standard deviation show that the general trend observed in figure 4.26 is a good representation of monthly variation through a complete year. As highlighted in many rainfall studies in Ireland (Dufour, 1995), the Irish weather exhibits few striking differences between summer and winter time, but still have a generally observed trend, with important depths from October to February and a lowest intensity period in between.

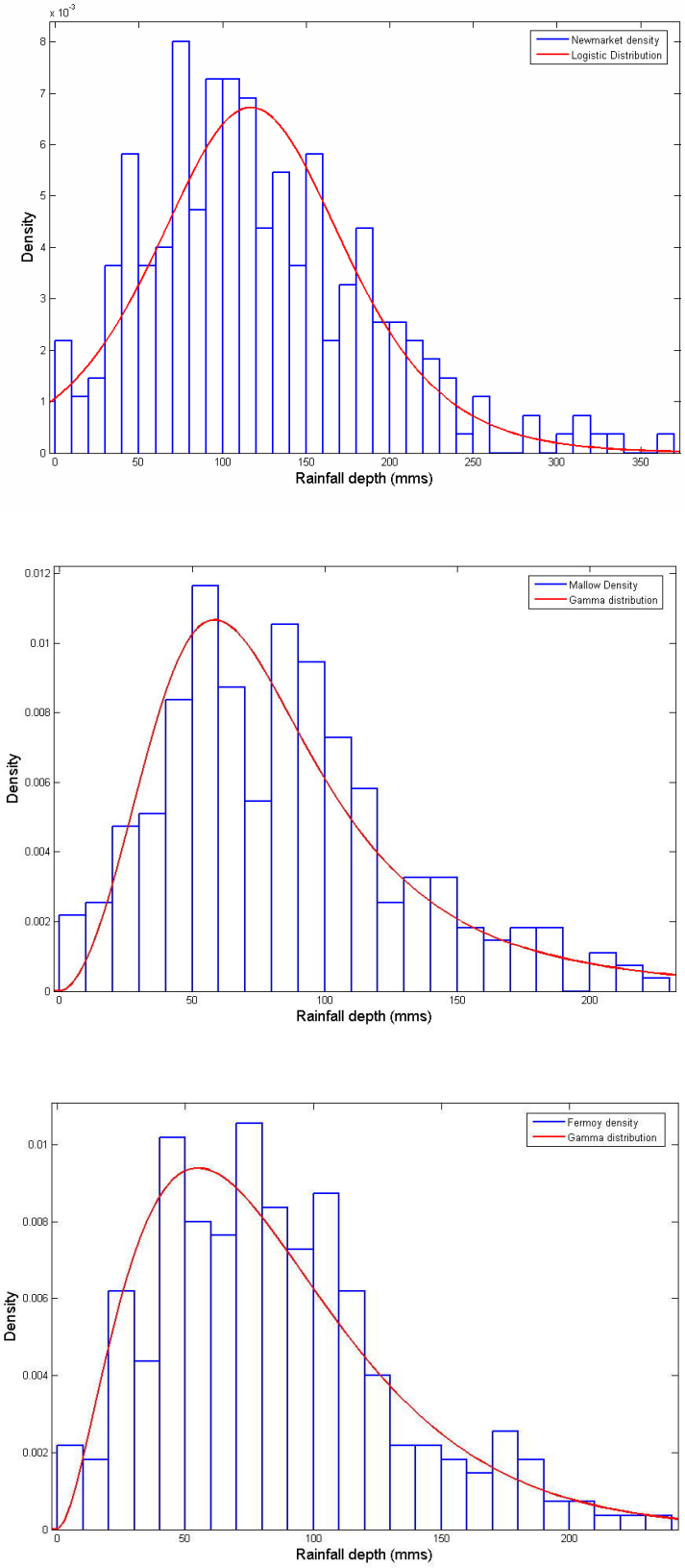


**Figure 4.25 Histograms of monthly precipitation with fitted "gamma-shaped" distribution**

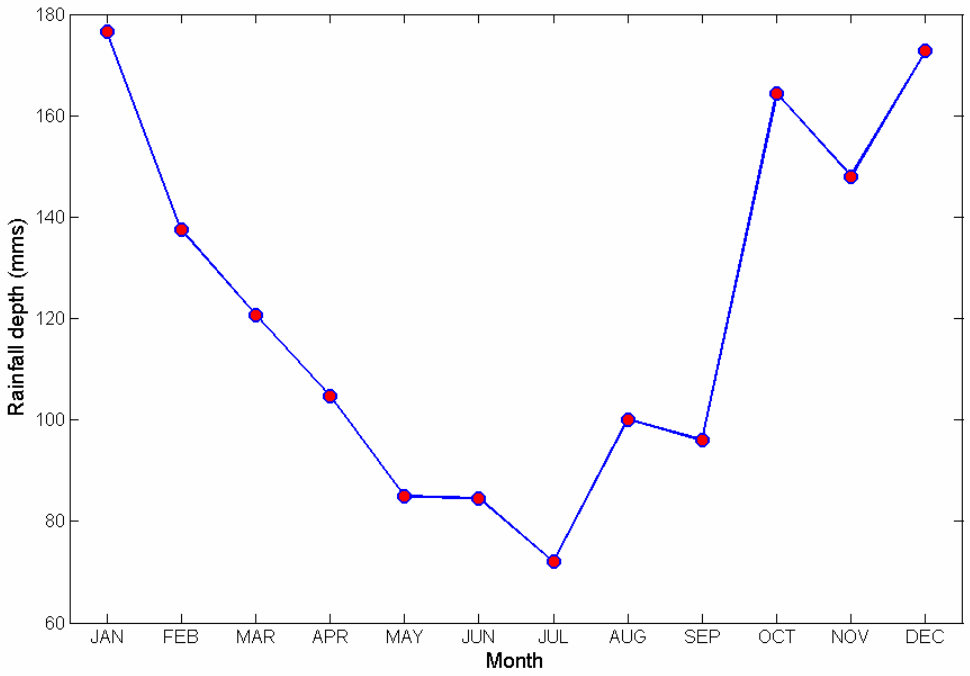


**Figure 4.26 Monthly variations in mean depth (Newmarket)**

### 4.6.4.3 Daily precipitation

Before analysing the daily data, a choice had to be made in order to define the recording depth below which the day is said to be without rain. It is indeed known than when using tipping bucket raingauges (ground sources), small values can be recorded without actual rain. This mainly happens when morning condensation is important enough to reach a volume that will make the bucket tipping. Table 4.15 gives the proportion of small recorded values for the three stations and shows a high occurrence of 0.1 mms recording (~10% of the total number of recorded values) for both Newmarket and Mallow. It was therefore decided to neglect the 0.1 mms values and calculate the 0.2 mms tipping occurrence (see table 4.16).

**Table 4-15 Occurrence of small recording values (0.1 and 0.2 mms)**

| | **0.1 mms** | | **0.2 mms** | |
|---|---|---|---|---|
| | Number of records | Percentage | Number of records | Percentage |
| **Newmarket** | 705 | 11.4 | 957 | 15.5 |
| **Mallow** | 479 | 8.6 | 818 | 14.6 |
| **Fermoy** | 265 | 5.5 | 497 | 10.2 |

**Table 4-16 Occurrence of 0.2mms events after neglection of 0.1mms events**

| | Number of records | Percentage |
|---|---|---|
| **Newmarket** | 252 | 4.6 |
| **Mallow** | 339 | 6.6 |
| **Fermoy** | 232 | 5.1 |

With approximately 5% of occurrence, the 0.2 mms records were considered to be representative of actual precipitation. The following statistics are therefore calculated with the smallest record possible being 0.2mms per day.

The following table gives the summary statistics of the daily precipitation for the 8400 days observed (1983 to 2005). Statistics were calculated using daily data from the Met Service, calculated from 9am to 9am the following day.

**Table 4-17 Summary statistics of daily precipitation**

| | Newmarket | Mallow | Fermoy |
|---|---|---|---|
| **Number of days without rain** | 2219 | 2816 | 3540 |
| **Percentage** | 26% | 33% | 42% |
| **Mean (mms)** | 5.43 | 4.60 | 4.82 |
| **Median (mms)** | 3.00 | 2.31 | 2.60 |
| **Skewness (mms)** | 2.10 | 2.73 | 2.78 |
| **Standard Deviation (mms)** | 6.58 | 6.08 | 6.27 |
| **Range (mms)** | 58.20 | 60.28 | 63.80 |
| **Minimum (mms)** | 0.10 | 0.10 | 0.10 |
| **Maximum (mms)** | 58.30 | 60.40 | 63.90 |
| **Number of days with rain** | 6182 | 5585 | 4861 |

The minimum of non-rain days is found in Newmarket (26%) on the western part of the catchment, and decreases when moving towards East. This spatial relationship is not true for the mean daily depth as it can be seen that this value is higher in Fermoy than in Mallow. On the other hand, the percentage of non-rain days is much higher in Fermoy than in Mallow (42% and 33%). Daily rain events are occurring less often in the first location, but are stronger.

Skewness is a measure of the asymmetry of the probability distribution of a real-valued random variable. Roughly speaking, a distribution has positive skew (right-skewed) if the right tail is longer. Calculated values in three sites are high and suggest that the rainfall depth density could be approached by a “gamma-shaped” probability distribution.

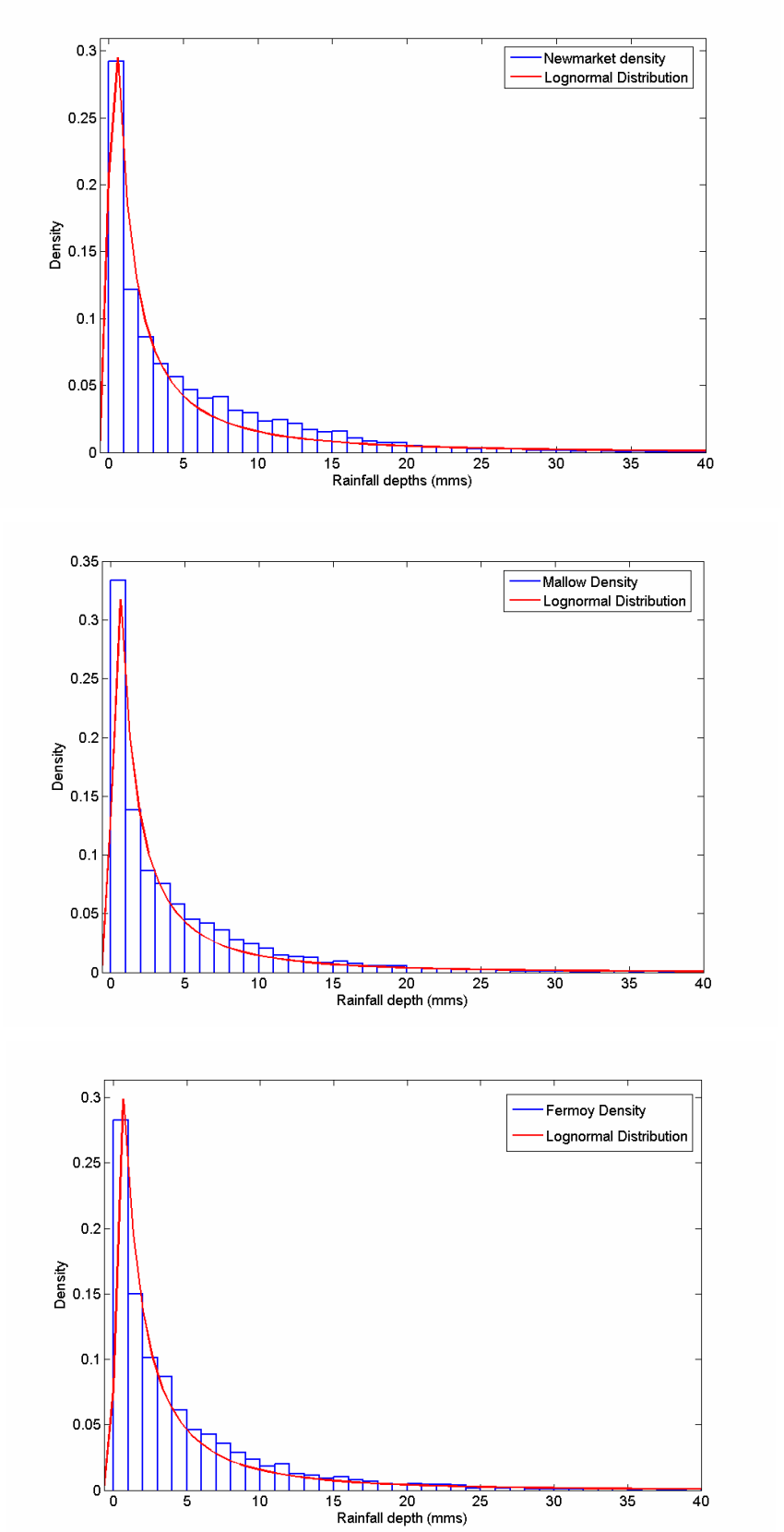


**Figure 4.27 Histogram of daily precipitation with fitted distributions**

For the three locations, gamma and lognormal distributions were the best candidates to fit the depth density. In the three cases, gamma distributions were producing too important densities for the first few depths (0-2 mms). Lognormal distributions (see equation 4.3) showed better results even if the fitting curve produced low values for rainfall depths between 5 and 20 mms (see figure 4.27).

$$LN(x,a,b) = \frac{e^{-(\ln x - a)^2 / 2b^2}}{xb\sqrt{2\pi}} \tag{4.3}$$

**Table 4-18 Parameters for daily depth lognormal fitting**

| Gauge location | a | b |
|---|---|---|
| Newmarket | 0.74 | 1.64 |
| Mallow | 0.63 | 4.51 |
| Fermoy | 0.74 | 1.45 |

### 4.6.4.4 Hourly precipitation

The following hourly precipitation analysis was undertaken using the 9-months OPW dataset, which represents 6552 hourly recorded time intervals. Table 4.19 gives the summary statistics of the three studied stations.

**Table 4-19 Summary statistics of hourly precipitation**

| | Newmarket | Mallow | Fermoy |
|---|---|---|---|
| **Number of hours without rain** | 5552 | 5635 | 5726 |
| **Percentage** | 84% | 86% | 87% |
| **Mean (mms)** | 0.68 | 0.70 | 0.68 |
| **Median (mms)** | 0.40 | 0.40 | 0.40 |
| **Standard Deviation (mms)** | 0.75 | 0.89 | 0.85 |
| **Skewness (mms)** | 2.87 | 2.97 | 3.46 |
| **Range (mms)** | 6.00 | 6.80 | 7.20 |
| **Minimum (mms)** | 0.20 | 0.20 | 0.20 |
| **Maximum (mms)** | 6.20 | 7.00 | 7.40 |
| **Number of hours with rain** | 1000 | 917 | 826 |

As can be seen in table 4.19, the mean hourly depth values are similar in the three stations, approximately equal to 0.7 mm/hour. Considering the gradient (from West to East) already observed in the yearly and monthly rainfall depths, and this similarity in hourly intensities, it can be concluded that these differences amongst global cumulative depth between West and East are due to the duration of the rainfall events more than its intensity. It was therefore decided to run a statistic study of wet events duration from 1-hour data. Event duration is defined as the length of a sequence of wet hours bound by either side by at least one dry hour.

**Table 4-20 Summary statistics of event duration, calculated from hourly data**

| | Newmarket | Mallow | Fermoy |
|---|---|---|---|
| **Mean (hrs)** | 2.49 | 2.36 | 2.35 |
| **Standard Deviation (hrs)** | 2.39 | 2.50 | 2.43 |
| **Skewness (hrs)** | 2.16 | 2.86 | 3.27 |
| **Range (hrs)** | 13 | 16 | 21 |
| **Minimum (hrs)** | 1 | 1 | 1 |
| **Maximum (hrs)** | 14 | 17 | 22 |
| **Number of events** | 401 | 388 | 351 |

As predicted, the mean value for event durations is higher in Newmarket (2.5 h hours) than in Mallow and Fermoy (approximately 2.35 hours). This small difference (6%) is enough to explain the higher cumulative rainfall depths recorded in the western part of the catchment. Rainfall intensity does not significantly vary but longer event durations on the West lead to higher cumulative depths.

With only 14 hours, the maximum event duration in Newmarket is low. Mallow and Fermoy values are higher (respectively 17 and 22 hours) but are still lower than for example the 42 hours value calculated for Cork Airport (see Dufour, 1995). With only 9 months of analysed data, these values can not be considered as representative as some yearly averages, but are still some good sign that the studied period (November 2005 to August 2006) was a particularly dry one.

From figure 4.28, it can be seen that short wet events are much more frequent than longer ones. An exponential decrease of the frequency of occurrence can be noticed. The one-hour duration events account for nearly 60% of the total number of wet events.

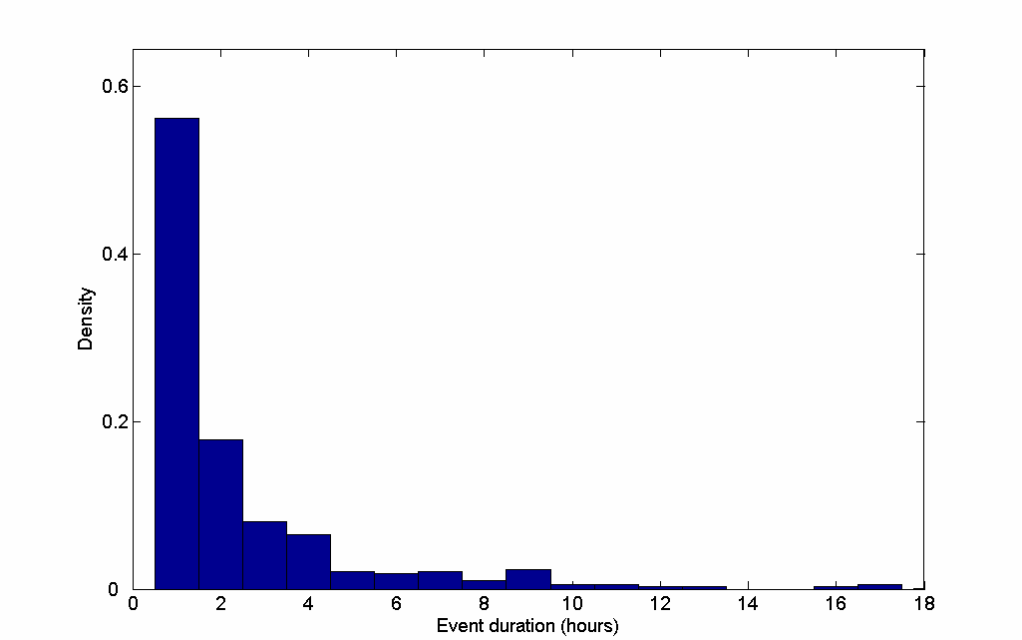


**Figure 4.28 Histogram of event durations - Mallow station**

## 4.7 Discussion

In the first part of this chapter, a precise description of the different recording raingauges network was made in order to list all the different data sets, its quality, availability and the precision of the coverage. With three different sources of information (the Met Service, the OPW and the UCC Hydromet research group), and particularly with the newly installed OPW hourly dataset, the Blackwater catchment precipitations are well recorded in both time and space. The long records of daily rainfall available from the Met Service are also a powerful tool to monitor long term trends within the catchment.

In the second part, the data previously described was used to produce a precise rainfall analysis of the catchment, in term of both intensity and spatial variation.

Observation of the 9 months period recorded by the OPW recording network (November 2005 to July 2006) showed the particularly low rainfall values recorded in this period. The year 2006 has so far been really dry, with precipitation values much lower than those usually observed in Ireland and in the Blackwater catchment. This drought was compared to the one that occurred all over Ireland during the summer 1976. Assessing a drought severity appeared to be a subjective and difficult task. Depending on the chosen drought indicators, one of the two studied drought period can be considered as being more severe than the other one. From all the studied indicators (absolute drought, partial drought, dry spell, period of insignificant rainfall and river flow observation), it is concluded that the 1976 and 2006 droughts are comparable. Like records from

1976, rainfall data from 2006 is likely to become a standard against which to compare the severity of future droughts.

An investigation of the spatial variation of rainfall depth, with both Met Service and OPW data showed a really neat intensity gradient between the western and eastern parts of the catchments, with depths twice as important in the West as in the East. The relationship between rainfall depths, longitude and elevation were clearly identified and give a good understanding of rainfall repartition among the different part of the catchment. A particular meteorological phenomenon, called the orographic effect was also identified as potentially responsible for a particularly wet area in the extreme East of the catchment.

Finally, a precise statistical analysis was run with yearly, monthly, daily and hourly rainfall depths, in three different locations in the catchment (Newmarket in the West, Mallow in the centre and Fermoy in the East). Extracted information confirmed the West-East gradient as highlighted before. For all different time period, depth densities were approached with "Gamma-shaped" probability distribution, with good fitting results. Occurrence of rainfall depths appeared to follow regular trends, with a systematic high peak for low depths, and longer tails in the high depths direction. Good accordance between observed depths and probability distribution let us believe that using the Blackwater rainfall data as an input of rainfall prediction model would be an interesting further work. A one-hour rain event analysis showed that hourly intensities were not generally more important in the West than in the East. The difference in cumulative depths recorded between the two parts of the catchment is therefore explained by longer event durations in the West.

# Chapter 5 Flow data

## 5.1 Available data

River flows are obtained from river heights data that is being measured at many different points along the river path and are part of different survey schemes. The different sources of the data are Cork County Council (through the Environment Protection Agency) and the Office of Public Works.

### 5.1.1 Measurement sites

Table 5.1 shows the five main flows measurement stations along the Blackwater River, with their responsible bodies, catchment area and the date when the record started. In each of the different stations, flow is being measured at a time interval of 15 minutes.

**Table 5-1 River flow stations in the Blackwater catchment**

| Station ID | Name | X | Y | Responsible body | Area (km2) | First record |
|---|---|---|---|---|---|---|
| **18048** | Dromcummer | 140000 | 99100 | Cork Co Co | 861 | 1981 |
| **18050** | Duarrigle | 124900 | 94470 | Cork Co Co | 245 | 1981 |
| **18006** | Mallow Sugar Fact | 151800 | 98000 | Greencore | 1040 | 1977 |
| **90701** | Mallow Rail Bridge | 155600 | 98150 | OPW | 1180 | 2001 |
| **18003** | Killavullen | 165000 | 100000 | Cork Co Co | 1252 | 1955 |

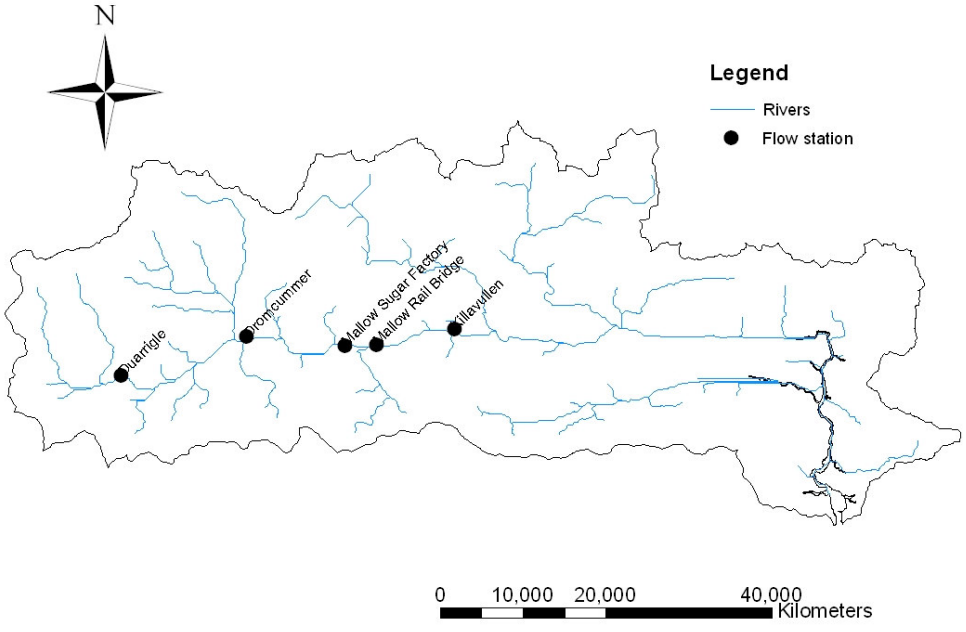


**Figure 5.1 Flow stations in the Blackwater catchment**

In the following chapter of this thesis, rainfall-runoff modeling is applied to only 3 sub-catchments: Duarrigle, Dromcummer and Killavulen. As a consequence, flow in Mallow was not further analysed.

### 5.1.2 Instrumentations

Sophisticated instrumentations were installed in Duarrigle and Dromcummer in 2003, in order to provide good data for a flood forecasting scheme in Mallow (Corcoran, 2004). Two water level recording sensors were installed in each site in order to provide a back up system in case one of them was to fail. Both sensors were provided by Ott-Hydrometry: the Ott-Hydrometry Thalimedes Shaft Encoder (see figure 5.2) (Ott-Hydrometry, 2002) and the Ott-Hydrometry Kalesto Radar Sensor (see figure 5.3) (Ott-Hydrometry, 2002).

The float-operated Thalimedes Shaft Encoder with integral data logger is designed for continuous, unattended monitoring of water level in ground and surface waters. In the case of changing water level, the smooth running float pulley is put into motion via the float and the float cable, a potentiometer inside the pulley records the change and represents the change as a change in the height on the LCD display. The change is also recorded by the inbuilt data logger.

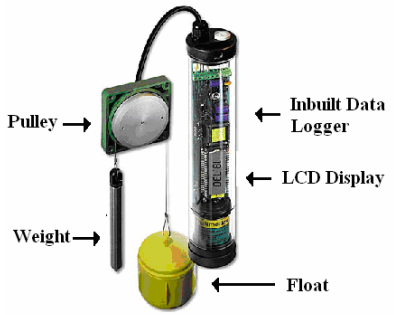


**Figure 5.2 Thalimedes shaft encoder (Ott-Hydrometry, 2004)**

The Kalesto Radar Sensor is designed for continuous unattended monitoring of surface water level. Compared with conventional level measuring systems (pressure probes, float operated or ultrasonic systems) the installation and handling of a Radar Sensor is cost and time effective. The Kalesto sends radar waves (microwaves) perpendicular to the water surface. These waves are then mixed with the signals reflected on the surface. The distance travelled is then calculated within the Kalesto and sent to the data logger.


**Figure 5.3 Kalesto Radar Sensor (Ott-Hydrometry, 2004)**

In both case, recorded water level are stored in an Ott-Hydrometry Hydrosens Multi-Channel data logger, which can then be downloaded using a laptops, palmtops, Infra Red devices or modem connexion.

In Duarrigle and Dromcummer, data is directly sent via telephone line and modem to two different work stations (in UCC Hydromet Research Station, Cork and the EPA Office in Dublin) so that the data was directly available to be used in the Mallow flood forecasting scheme (Corcoran, 2004). The Hydras3 Pro software is used to receive the data, save it and alert the user in case of a faulty sensor. No modem transfer system was installed in Killavullen. Data is saved in the on-site data logger, and is collected at given time intervals.

### 5.1.3 Rating curves

In Duarrigle and Dromcummer data was only available in river height (meters). The river flow can then be calculated from these values using a Rating Curve equation:

$$Q = a\,h^{b} \tag{5.1}$$

$Q$ being the river flow in $m^3 \cdot s^{-1}$, $h$ the water level in meters, $a$ and $b$ being dimensionless.

The EPA and the OPW have elaborated rating curves for their respective flow stations. The coefficient $a$ and $b$ are obtained by extrapolation of the measured data, by plotting $Q$ against $h$ (see figure 5.4). As the Rating Curve is calculated for a specific location in the river channel, the coefficients $a$ and $b$ can vary very quickly from one place to another. It is then imperative to determine a different equation for each of the 3 different stations.

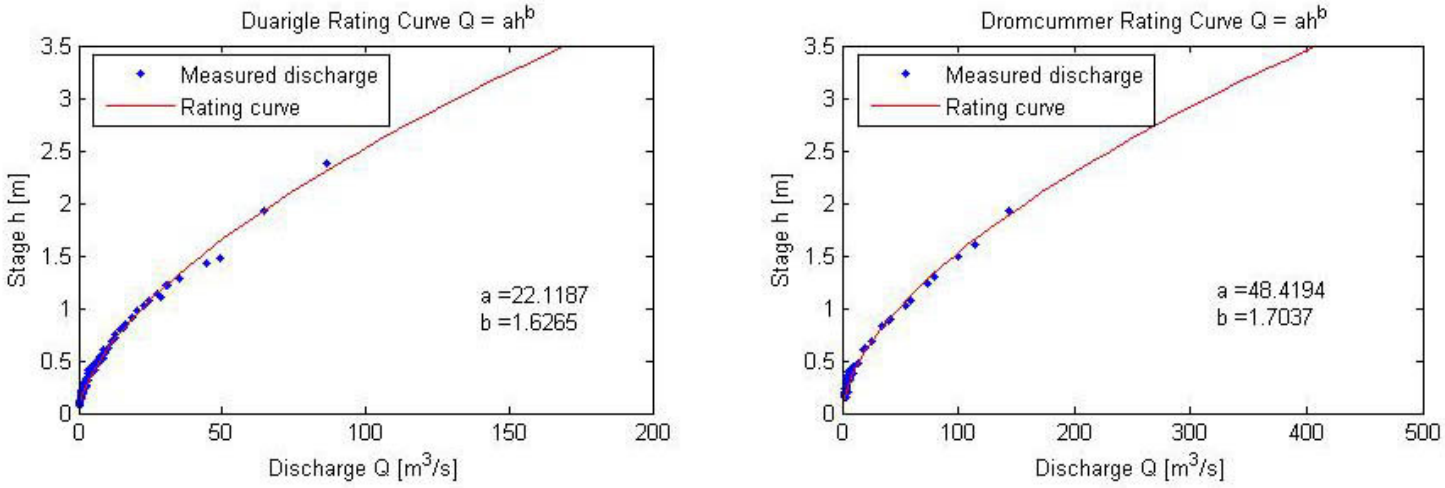


**Figure 5.4 Rating curves in Duarrigle and Dromcummer (Steinmann, 2005)**

As all the points plotted on the curve are obtained by measuring the actual flow and water level at different times, rating curves are usually plotted for low flow and normal flow conditions. Indeed, high flow conditions (corresponding to flood flows) make measurements more difficult and rarely happen. Low flow points are plotted and extrapolated to obtain the rating curve equation that will be applied to a wider range of flow. The rating curves are consequently considered less accurate for high flows than for low flow. *a* and *b* are considered reliable for the all range of flow encountered by the river.

As the data from Killavullen flow station was directly available in cubic meters, a rating curve was not used for this location.

### 5.1.4 Period of availability

Flows in Killavullen were measured since 1955 and represents consequently a very strong database. The recording periods in Duarrigle and Dromcummer, even if starting only in 1982 provides enough data for the further modelling.

**Table 5-2 Period of availability of the three flow stations**

| | **Killavullen** | **Duarrigle** | **Dromcummer** |
|---|---|---|---|
| **Opening Date** | October 1955 | January 1982 | January 1982 |

Missing data, even if infrequent in all the three stations, were encountered and replaced with linear interpolation. Flow interpolation is an easy task to run and gives reliable results. Flow missing data is therefore less problematic than rainfall missing values.

Two major gaps were found in both Duarrigle and Dromcummer in the year 1987, but appeared in times of low river height. Since the undertaken modelling is based on flood events, these omissions were not considered as being important.

## *5.2 Analysis*

### 5.2.1 River flow range in the three stations

For the 1982-2006 period, the minimum recorded flow of the River Blackwater at Duarrigle was 0.250 $m^3/s$ on the 10th of October 2000. The maximum recorded flow is 195.4 $m^3/s$ on the 21st of October 1988. As can be seen in figure 5.5, which displays 20 years of recorded river flow in Duarrigle, flow uncommonly exceeds 150 $m^3/s$ (8 events in total) and reaches 100 $m^3/s$ less than 40 times in 25 years. The mean of 8.5 $m^3/s$ illustrates a low baseflow.

For the 1982-2006 period, the minimum recorded flow of the River Blackwater at Dromcummer was 1.36 $m^3/s$ on the 14th of May 1982. The maximum recorded flow is 319.7 $m^3/s$ on the 7th of January 1982. As can be seen in figure 5.5, flow uncommonly exceeds 250 $m^3/s$ (9 events in total) but reaches 150 $m^3/s$ quite often. The flow range of 318.4 $m^3/s$ is more important than in Duarrigle and the highest flow is more than 200 hundred times the lowest value.

For the 1955-2006 period, the minimum recorded flow of the River Blackwater at Killavulen was 1.6 $m^3/s$ on the 16th of September 2003. The maximum recorded flow is 602.7 $m^3/s$ on the 2nd of November 1980. As can be seen in figure 5.5, flow uncommonly exceeds 300 $m^3/s$ (10 events in total) but easily reaches 250 $m^3/s$. The flow range of 601.1 $m^3/s$ can be considered as being very important, and forebodes major issues when floods occur.

**Table 5-3 Summary statistics of river flows (m3/s)**

| | Duarrigle | Dromcummer | Killavullen |
|---|---|---|---|
| **Min** | 0.25 | 1.36 | 1.6 |
| **Max** | 195.5 | 319.7 | 602.7 |
| **Mean** | 8.56 | 28.74 | 34.1 |
| **Median** | 4.88 | 17.26 | 22.9 |
| **Standard Deviation** | 11.38 | 33.95 | 35.85 |
| **Range** | 195.25 | 318.4 | 601.1 |

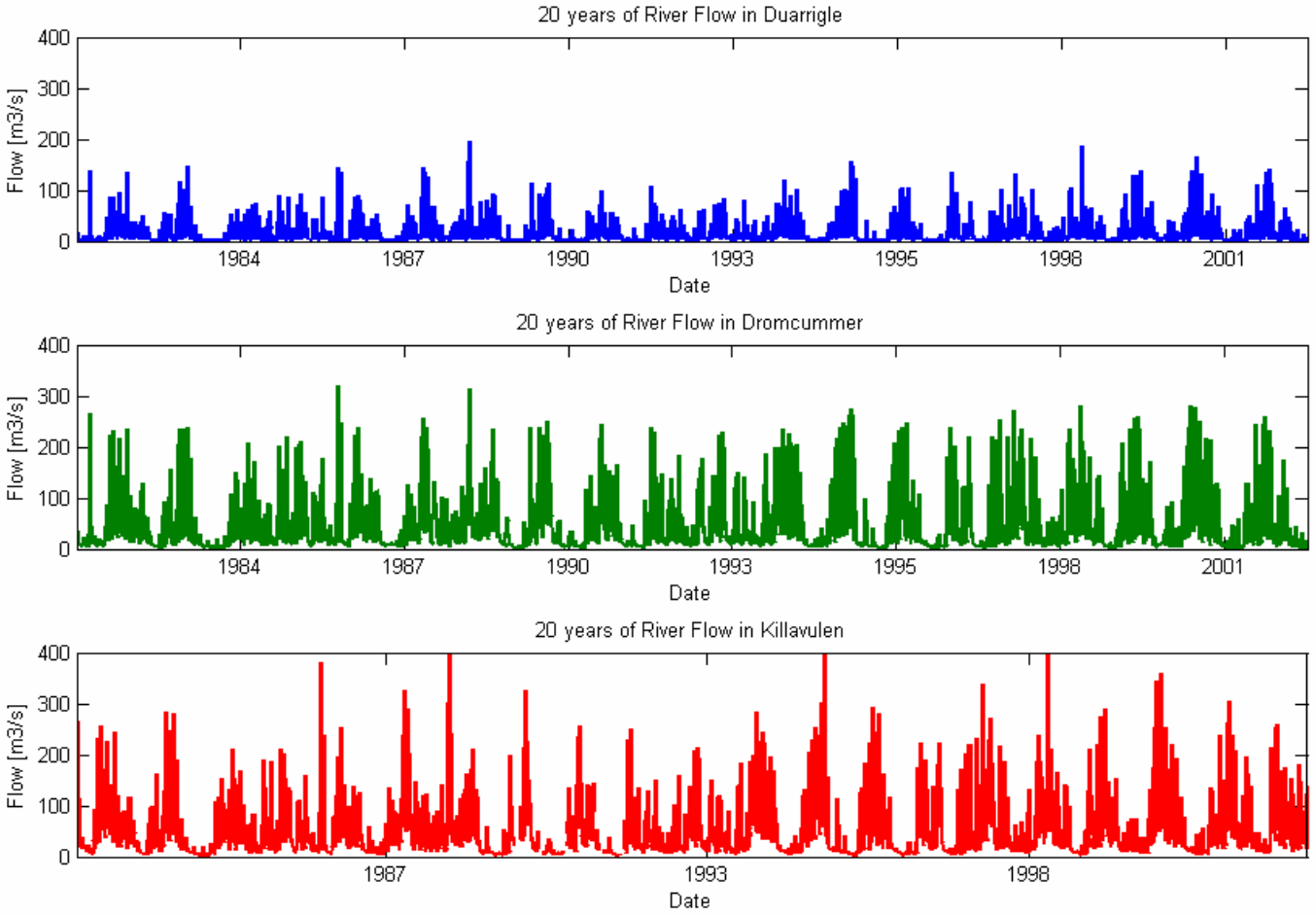


**Figure 5.5 Samples of continous flow from 1980 to present at the three river flows stations**

## 5.2.2 Data comparison

### 5.2.2.1 Lag time

As the River Blackwater flows from West to East, flows increase in the following order: Duarrigle, Dromcummer and Killavulen. As can be seen in figure 5.6, this difference in flows is observable for both baseflow and stormflow. Baseflow, which roughly is the river flow when no surface runoff of water table recharge is occurring, is a function of the river geometry at each site. Stormflows (which occur after high precipitation) are much higher in Dromcummer and Killavulen than in Duarrigle.

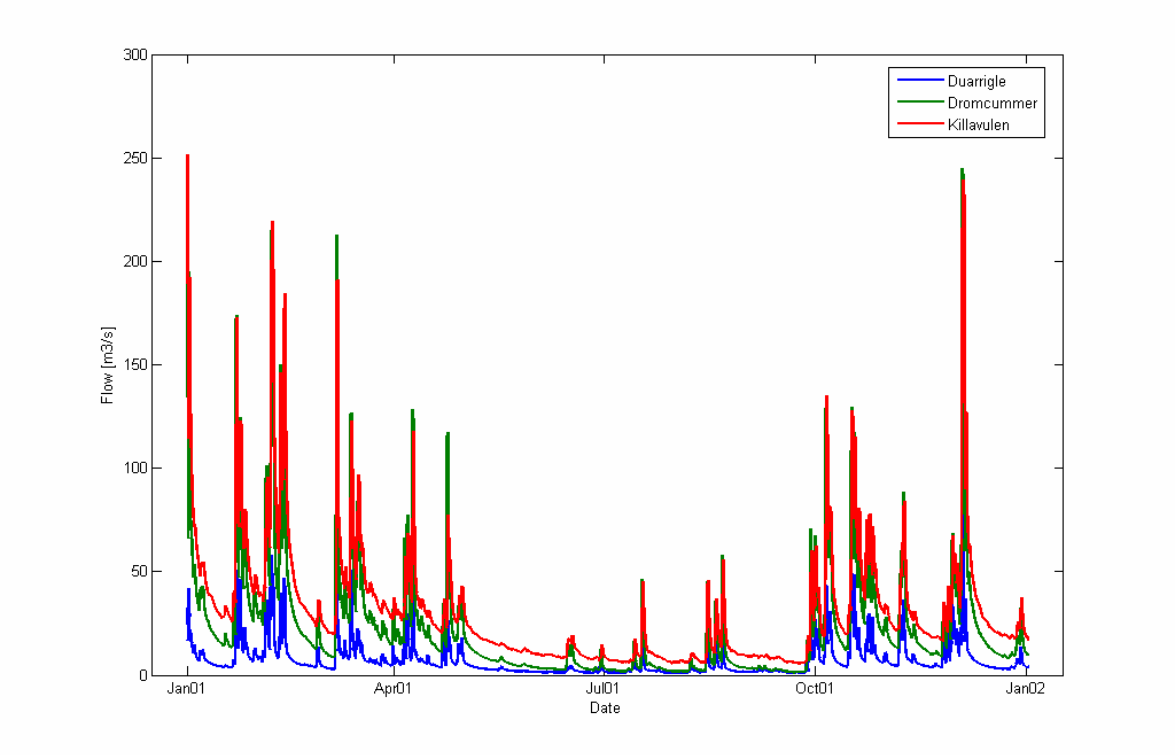


**Figure 5.6 Samples of continuous flow for one year (2001) at the three river flow stations**

When looking at a finer scale, a lag time is observable between the three stations. River flow first reaches its peak in Duarrigle, then in Dromcummer and finally in Killavulen. Figure 5.7 compares the flood event that occurred on the 27th May 1995 at the three sites. It can be seen that the peak occurs first in Duarrigle (~40 $m^3 \cdot s^{-1}$), then 2 hours later in Dromcummer (~95 $m^3 \cdot s^{-1}$) and after another 5 hours in Killavulen (~115 $m^3 \cdot s^{-1}$). It is also clear that the hydrograph peak in Duarrigle is much narrower than in Dromcummer, which also is narrower than in Killavulen.

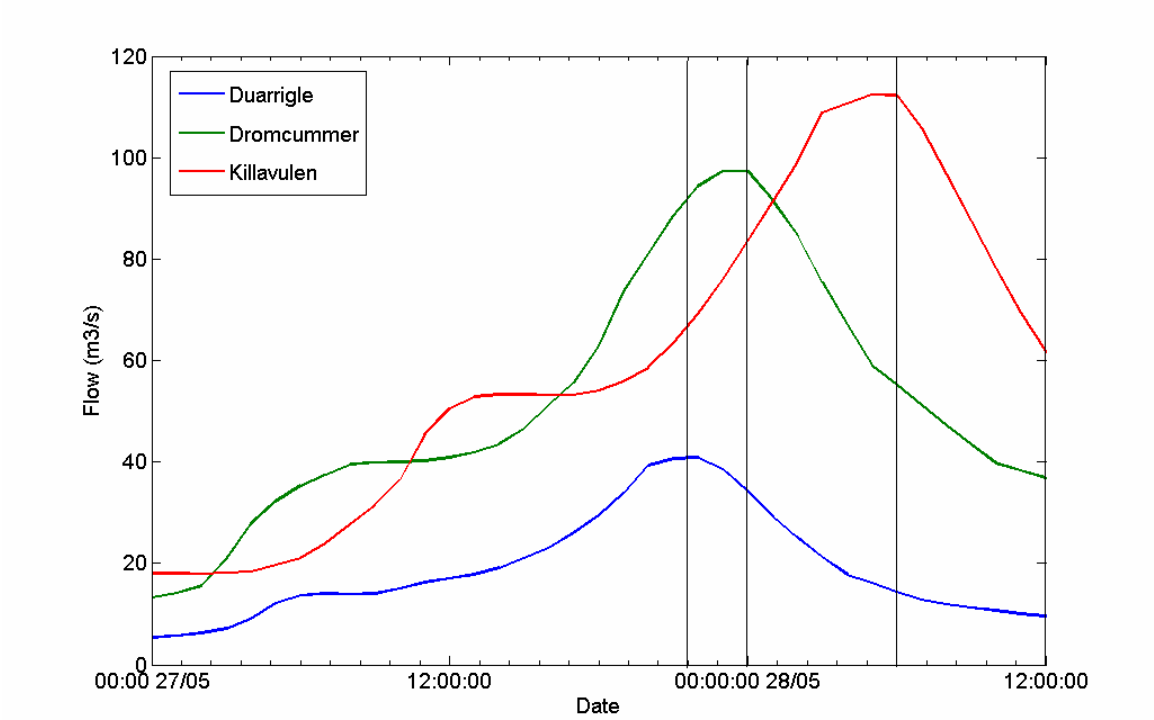


**Figure 5.7 Rising flow in the three stations (27th May 2000)**

The lag-time underlined above is a dynamic parameter which varies from one event to the other. It depends on both rainfall intensity and its spatial variation. It can indeed be seen from figure 5.1 that several tributaries enter the Blackwater during the different river stations. The timing of the flood wave from these tributaries determines the flood wave size downstream at Dromcummer and in particular at Killavulen. If the tributaries flood waves "synchronize" (depending on how the rainfall occurs above each tributary's sub-catchment), significant flood waves can occur downstream. When the flood waves of the tributaries are out of synchronisation, then rather modest flood waves tend to occur at Killavulen, due to flood wave attenuation in the long and wide Blackwater Valley (Fenton, 2006).

### 5.2.2.2 Average river flows

As can be seen in table 5.4, the average river flow is the smallest in Duarrigle, followed by Dromcummer and Killavulen is the highest (34.58 $m^3.s^{-1}$). Average flows per unit of area ($m^3.s^{-1}.km^{-2}$) are obtained by dividing the average flows by the corresponding sub-catchment area. These values are also listed in table 5.4, and show that Duarrigle has the highest flow per unit of area (0.035 $m^3.s^{-1}$ per square kilometre), followed by Dromcummer and finally Killavulen. This trend

tends to illustrate the fact that the western parts of the catchment drain more runoff to the river network than in the East. This observation is linked with the previous highlighted gradient of rainfall intensities from West to East (see chapter 4).

**Table 5-4 Average flows in the three stations**

| | **Average river flow ($m^3.s^{-1)}$** | **Sub-catchment area (km2)** | **River flow per unit of area ($m^3.s^{-1}.km^{-2}$)** |
|---|---|---|---|
| **Duarrigle** | 8.58 | 245 | 0.035 |
| **Dromcummer** | 27.11 | 861 | 0.031 |
| **Killavulen** | 34.58 | 1252 | 0.027 |

# Chapter 6 Unit Hydrograph based Rainfall-Runoff Modelling

## 6.1 General description of an hydrograph

Before beginning to analyse a streamflow hydrograph, which describes the time history of the changing rate of flow from a catchment due to a rainfall event rather than just the peakflow, it is an essential step to appreciate some of the hydrograph's main components (Shaw, 1994). The discharge hydrograph is obtained from continuously recorded river stages and the rating curve relationship appropriate to the specified river station (see Chapter 5). Figure 6.1 shows an example of a flood hydrograph and its rain event.

The hydrograph (plotting of the discharge against the time) has two main components: the area under the hump, called direct response runoff (or surface runoff), and the horizontal-like line near the time axis representing the baseflow, i.e. the part of the flow contributed from groundwater.

At the beginning of the rain event, the flow is only composed of the baseflow part. A period of time elapses before the flow begins to rise (period when the rainfall is intercepted by the vegetation, fills the soil surface cavities and makes up the soil-moisture deficits). Once the surfaces and soils are saturated, the effective rainfall starts to contribute to flow as surface runoff: this part of the hydrograph is called the *rising limb*. The *peak*, at the top of the hydrograph occurs when the effective rainfall contribution is cancelled. The *recession curve* is the part of the curve that joins the inflection point to the baseflow line at the *inflection point*. Even if there are many different methods to determine the *lag time*, i.e. the catchment response time, the most commonly used is to measure the difference between the centroids of the net rainfall hyetograph and the hydrograph. The *time of concentration* can de defined as the difference in time between the end of the net rainfall hyetograph and the end of the recession curve.

## 6.2 The Unit Hydrograph general theory

### 6.2.1 Definition

First introduced by Sherman (1932), the Unit Hydrograph (UH) is the hydrograph that results from 1 unit depth of rainfall excess generated uniformly over the watershed at a uniform rate during a specified period of time. The UH theory relies on three basic assumptions (Shaw, 1994):

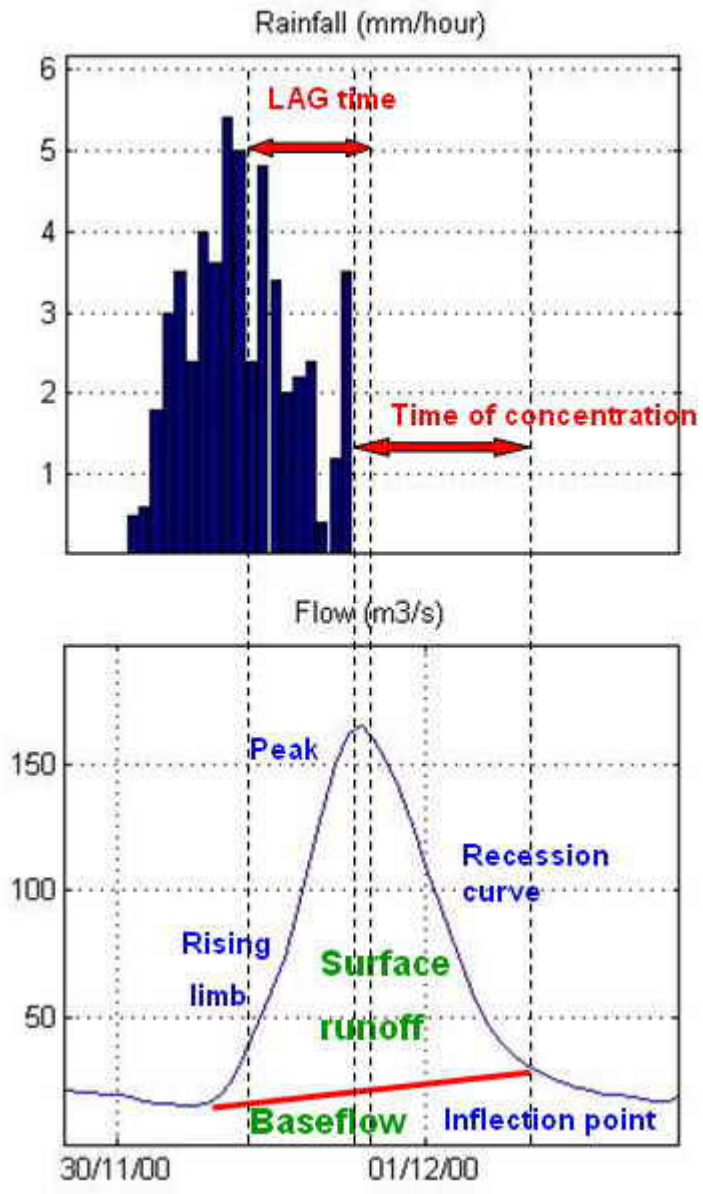


**Figure 6.1 Rainfall hyetograph and hydrograph, 30th November 2000, Duarrigle**

- Linearity: there is a direct proportional relationship between the effective rainfall and the surface runoff.
- Invariance: the relationship mentioned above does not change with time
- Superposition: runoff hydrographs derived for successive rain events can be summed to obtain the total runoff hydrograph.

### 6.2.2 Convolution

Once the UH is available for a given catchment, using these three principles of linearity, invariance and superposition, once the UH is available for a given catchment, it is possible to derive the surface runoff hydrograph for any rainfall event. The process by which the effective rainfall is transformed into direct runoff is called the *convolution*. Analytically speaking, convolution is referred to as the theory of linear superposition (McCuen, 2004) and conceptually, it is a process of multiplication, translation with time and addition. It can be used for processes with either a discrete or continuous distribution function. In discrete form, which is the form used in hydrology, the convolution equation is:

$$y(t) = \sum_{i=0}^{t} x(i).U(t-i) \tag{6.1}$$

where $x$ is the net rainfall distribution, $y$ the direct runoff and $U$ the UH.

The first burst of net rainfall of duration D is multiplied by the ordinates of the UH. The UH is then translated for a time length of D, and the next burst of net rainfall is multiplied by the UH. After the UH has been translated for all bursts of net rainfall of duration D, the total surface runoff hydrograph is obtained by summing the results of all the multiplications.

### 6.2.3 The S-Hydrograph method

As a UH is determined for a given net rainfall duration, it is important to have a method that transforms a *d1*-UH into a *d2*-UH (where *d1* and *d2* are different durations): the *S-Hydrograph* method can be used for this. An S-Hydrograph is the total hydrograph resulting from a series of continuous uniform-intensity storms delivering 1 mm in *dt* on the catchment. It is obtained by summing an infinity of *dt*-UH, all of them separated by *dt* in time. A *dt2*-UH can be obtained from a *dt1*-S-Hydrograph by subtracting the *dt1*-S-Hydrograph *dt2* shifted S-Hydrograph, and multiply the result by *dt1/dt2*. For more details, refer to Engineering Hydrology (Wilson, 1990, pp 160).

### 6.2.4 Catchment average UH

Each particular rain event results in a unique hydrograph, which shape can vary even if the duration of effective rainfall is similar It is necessary to build an average catchment unit hydrograph that can be used to forecast the discharge flow for any given rainfall hyetograph. Average UHs were obtained in this thesis using the Aligned Peaks Method (Boorman, 1981) in which the highest values of each rain event's UH are aligned before the averaging.

Even if catchment average UH gives less accurate predictions of time to peak and peak flow rates than an UH that was developed with an intensity that was close to the average intensity of the test event (Kilgore, 1997), the averaging process is a necessary step that has to be carried in order to obtain an UH that may be applicable to the widest range of rainfall events and antecedent soil moisture conditions.

## *6.3 Four different approach to the unit hydrograph*

### 6.3.1 The Rainfall-Excess Reciprocal method

The first and simplest Unit Hydrograph approach is the Rainfall-Excess Reciprocal (RRR) method (McCuen, 2004), is to be used only with simple storm event, in which the storm hydrograph has a smooth shape. The T-hour UH is computed by multiplying each ordinate of the direct-runoff hydrograph by the reciprocal of the depth of rainfall excess, which equals the depth of direct runoff (McCuen, 2004). Since the UH must have a depth of 1mm and the direct-runoff hydrograph has a volume equivalent to the depth of rainfall excess, the reciprocal of the depth of rainfall excess can be used as a proportionality constant to convert direct-runoff hydrograph to a UH.

This basic determination method should only be used as a first step in modelling to give an idea of the UH application.

### 6.3.2 The ordinate least-squares regression method

The least-squares regression procedure is a well known mathematical tool used in many fields, and even if it has some limitations, its application to the UH determination has been proved to be very convenient (Boorman, 1981). The underlying criterion in this method consists of the minimization of the sum of the squares of the difference between the measured data and the calculated values (Brutsaert, 2005). These differences are called the *residuals* and are noted $\varepsilon_i$ .

The usual way of deriving the least-squares solution *U* is to express the linear convolution equation that links excess rainfall, UH ordinates and direct runoff response as some matrix equations.

$yi = \sum_{k=1}^{i} x_{i-k+1}.u_k$ is then rewritten as $Y = X\,.\,U$ where X, U and Y are respectively the excess rainfall matrix, the UH ordinates and the direct runoff response. If the excess rainfall input is

composed with $p$ bursts, the direct runoff response with m ordinates, the size of the UH is $n = m - p + 1$ and the matrixes *X*, *U* and *Y* are constructed as follows:

$$X = \begin{bmatrix} x_1 & 0 & 0 & 0 & 0 \\ x_2 & x_1 & 0 & 0 & 0 \\ . & x_2 & . & 0 & 0 \\ . & . & . & . & 0 \\ x_{p-1} & . & . & . & x_1 \\ x_p & x_{p-1} & . & . & x_2 \\ 0 & x_p & . & . & . \\ 0 & 0 & . & . & . \\ 0 & 0 & 0 & . & x_{p-1} \\ 0 & 0 & 0 & 0 & x_p \end{bmatrix} \quad , \quad U = \begin{bmatrix} u_1 \\ u_2 \\ . \\ . \\ u_{n-1} \\ u_n \end{bmatrix} \quad \text{and} \quad Y = \begin{bmatrix} y_1 \\ y_2 \\ . \\ . \\ y_{m-1} \\ y_m \end{bmatrix} \qquad (6.2\text{-}4)$$

The matrix *X* having a strictly positive rank, it is reversible and the matrix $X^{-1}$ therefore exists.

When *X* and *Y* are known, the solution *U* is obtained by writing $U = (X^t.X)^{-1}.{}^tX.Y$ .

This UH derivation is applicable to a wide range of rain events and can be written in a Matlab (Mathworks, date) code in order to make the calculations easier. Finally, application of the least-squares method to derive a UH from an observed event often produces an unrealistic solution (UH showing oscillation or negative values) and therefore has to be smoothed in order to provided an acceptable shape. The smoothing process is done by temporarily fixing the UH extremities to null values, and by running a neighbour to neighbour averaging coupled with a shifting operator. Figure 6.2 shows an example of a smoothed UH.

In the remainder of this chapter, the ordinate least-squares regression method is referred as the ordinates method.

### 6.3.3 Nash Instantaneous Unit Hydrograph

The formulation of Nash's Instantaneous Unit Hydrograph (IUH) (Nash, 1957) was obtained under the assumption that the catchment processes from instantaneous rainfall are equivalent to a succession of routings through linear storages (see figure 6.3). This form of IUH has been widely applied (Raymond, 2003) due to its simplicity and efficiency.

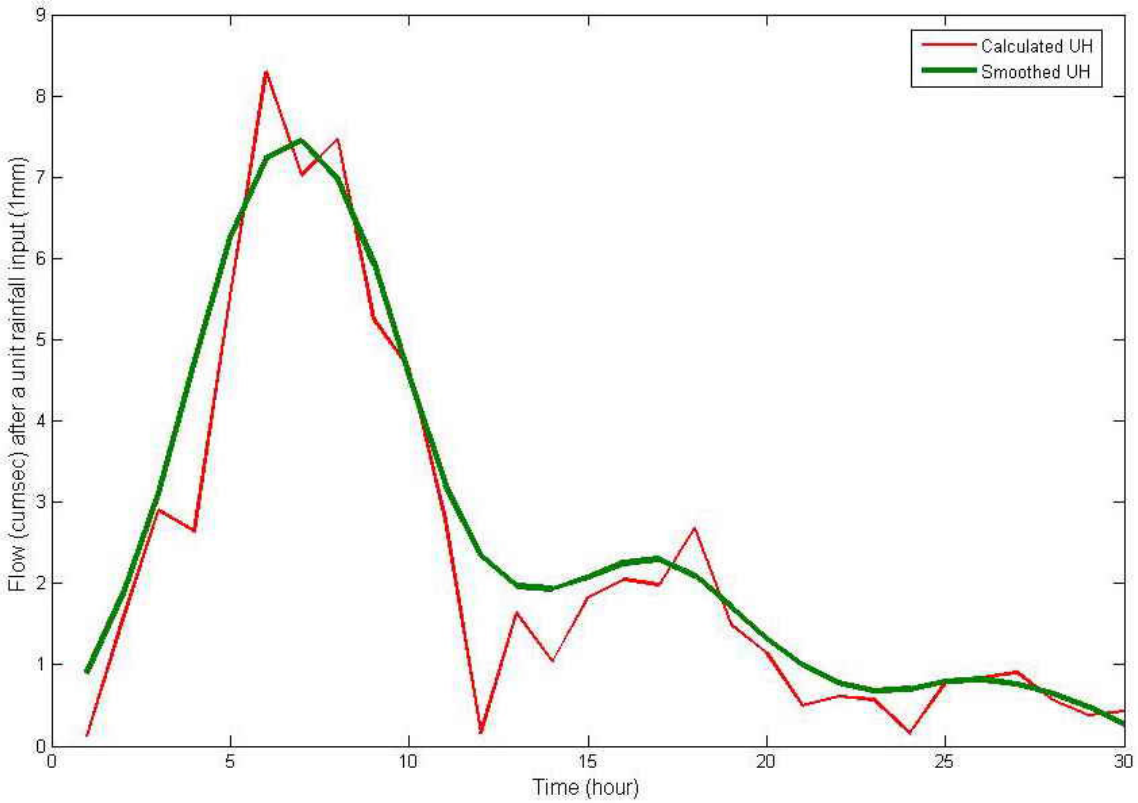


**Figure 6.2 Calculated Vs Smoothed Unit Hydrograph (Duarrigle, 5th February 2005)**

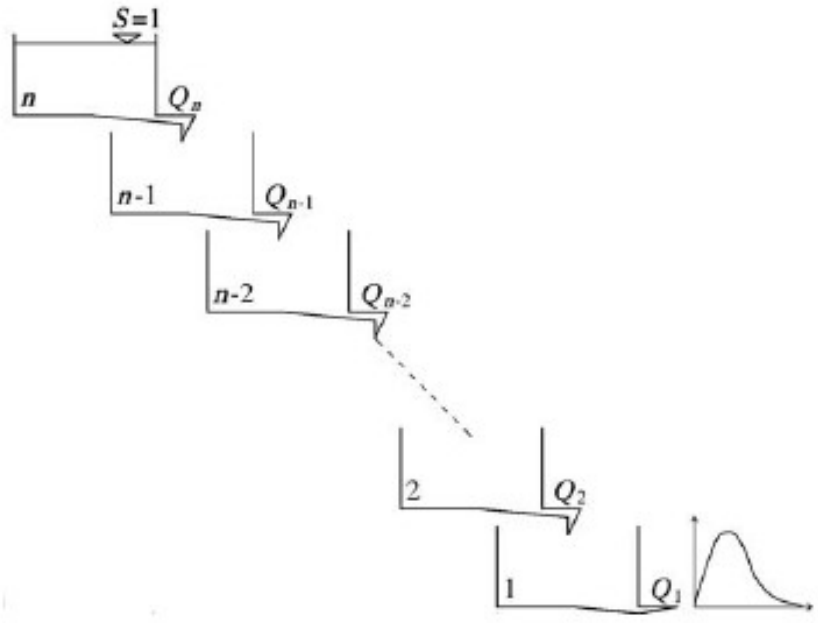


**Figure 6.3 Nash's cascade model structure (Agirre, 2005)**

The catchment is replaced by a series of $n$ reservoirs each having the storage characteristics $s = k.Q$ (equation 6.5), the outflow of the upper reservoir becoming the inflow of the next. Nash assumed that when the instantaneous input of rain ν (mms) takes place to the first reservoir, its level is raised by an amount sufficient to accommodate the increased storage and the discharge rises instantaneously from zero to $\nu / k$ ([S]) and diminishes with time according to the equation:

$$Q_1 = \frac{\nu}{k} e^{-t/k} \tag{6.6}$$

$Q_1$ then becomes the inflow to the second reservoir in which the level diminishes according to equation (6.6). After the rainfall input has passed through the $n$ reservoirs, the outflow from the nth reservoir is given by:

$$Q_n = \frac{\nu}{k.\Gamma(n)} e^{-t/k} (t/k)^{n-1} \tag{6.7}$$

where $\Gamma(n)$ is the gamma function equivalent to $(n-1)!$ (for further details, see Nash, 1957).

The ordinates of the Nash IUH are obtained by replacing ν by 1mm in equation (6.7), which leads to the gamma function equation:

$$u = \frac{1}{k.\Gamma(n)} e^{-t/k} (t/k)^{n-1} \tag{6.8}$$

This equation depends on the two parameters $n$ (number of reservoirs) and $k$ (storage coefficient) which can be determined using the Momentum Method (Chow, 1988). Calculating the 1st and 2nd moments leads to the following system:

$$\begin{cases} n.k = M_1 DR - M_1 ER \\ n.(n+1).k^2 = M_2 DR - M_2 ER - 2.n.k.M_1 ER \end{cases} \tag{6.9}$$

where $M_i DR$ is the i$^{th}$ moment of the direct runoff distribution and $M_i ER$ the ith moment of the excess rainfall distribution.

An analytic solution of equation (6.9) gives the $n$ and $k$ parameters for a given excess rainfall hyetograph and direct runoff hydrograph.

### 6.3.4 Unit hydrograph based on watershed morphology

The Geomorphological Unit hydrograph of Reservoirs (GUHR) (Lopez, 2005) which includes the watershed structure in its formulation is based on the traditional concept which aims to connect the watershed response to a cascade of linear reservoirs (as in the Nash IUH). The number and size of these reservoirs is defined by the subwatershed layout along the drainage network which leads to the geomorphologic approach of the unit hydrograph. Subwatersheds are defined as the portions of terrain flowing to the same point of the drainage network, and are labelled according the following numbering system (Lopez, 2005) (Figure 6.4):

- The first index starts from 1 and increases upstream, and represents channel or sub-watershed order.
- The second order is applied to channels of the same order and increases from left to right.

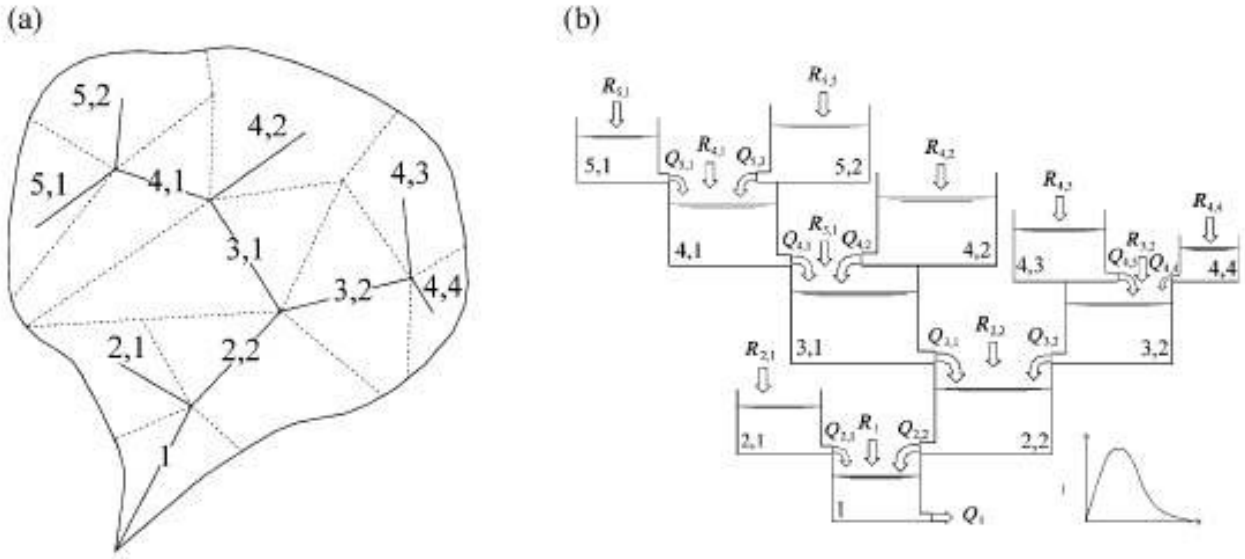


**Figure 6.4 Example of the used stream ordering system (a) and its associated conceptual reservoir model of a watershed (b) (Lopez, 2005)**

It should be noted that the watershed order (maximum order of the streams within the watershed) depends on the detail in which the drainage network is represented. Subwatersheds are then grouped according to their order, leading the representation shown in figure (6.5).

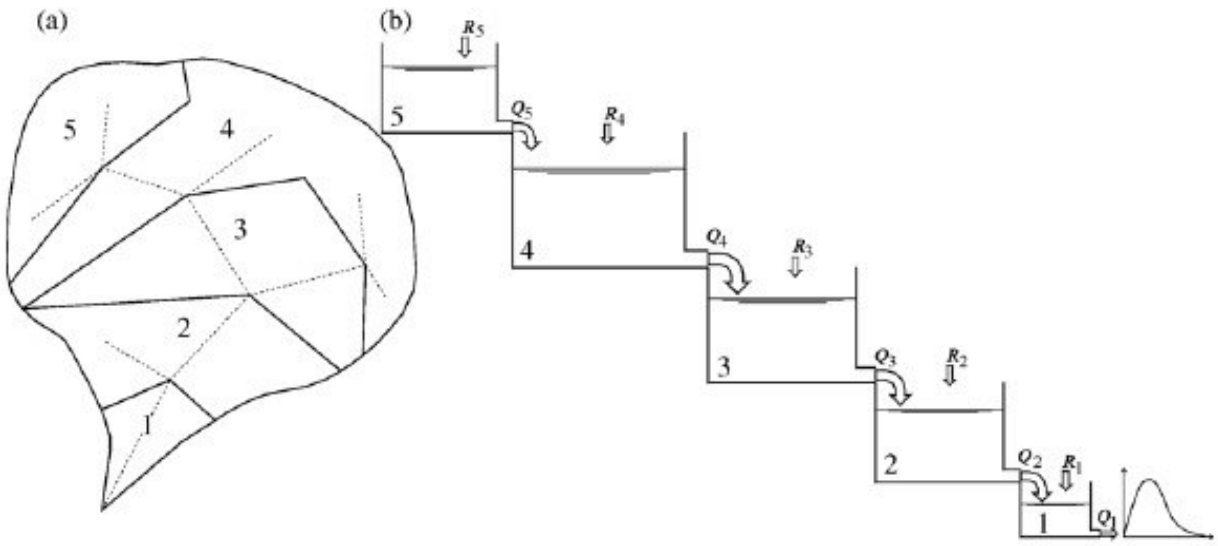


**Figure 6.5 Example of the used grouped stream ordering system (a) and its associated conceptual reservoir model of a watershed (b) (Lopez, 2005)**

The linear reservoir theory ( $S(t) = k.Q(t)$ ) (Chow, 1988) and continuity equation are then applied to each of the reservoirs considering a unique value for the storage coefficient $k$ (assumption of spatial uniformity in the watershed system). Grouping the different equations, re-ordering its terms and resolving the obtained system leads to the following formulation:

$$
\begin{array}{lllll}
(kD+1).Q_n(t) & & & & = R_n(t) \\
-Q_n(t) & +(kD+1).Q_{n-1}(t) & & & = R_{n-1}(t) \\
\vdots & \vdots & & & \vdots \\
\vdots & \vdots & & & \vdots \\
 & -Q_{i-1}(t) & +(kD+1).Q_i(t) & & = R_i(t) \\
 & \vdots & \vdots & & \vdots \\
 & \vdots & \vdots & & \vdots \\
 & & -Q_3(t) & +(kD+1).Q_2(t) & = R_2(t) \\
 & & & -Q_2(t) & +(kD+1).Q_1(t) = R_1(t)
\end{array}
\qquad (6.10)
$$

where $Q_i(t)$ and $R_i(t)$ are respectively the leaving flow and the intercepted rainfall of the i$^{th}$ reservoir.

According to the UH theory, effective rainfall is considered to be at a constant rate and uniformly distributed throughout the watershed. It is therefore accepted that the effective rainfall

depth falling over each subwatershed $R_i(t)$ depends on the ratio between the subwatershed area $A_i$ and the total catchment area $A_T$ :

$$R_i(t) = \frac{A_i}{A_T}.R_T(t) \tag{6.11}$$

where $R_T(t) = \frac{1}{\Delta t}$ for $0 \le t \le \Delta t$ and $R_T(t) = 0$ for $t \ge \Delta t$, $\Delta t$ being the UH duration.

The solution of the system leads to the following equation for $Q_1(t)$ the flow at the outlet:

$$Q_1(t) = \frac{1}{\Delta t}.\left[1 - \frac{e^{\frac{-t}{k}}}{A_T}.\left[\sum_{i=1}^{n}\left[\frac{1}{(i-1)!}\left(\frac{t}{k}\right)^{i-1}.\sum_{j=1}^{n}A_j\right]\right]\right] \text{ for } 0 \le t \le \Delta t \tag{6.12}$$

$$Q_1(t) = \frac{1}{\Delta t}.\left[\frac{e^{\frac{-(t-\Delta t)}{k}}}{A_T}.\left[\sum_{i=1}^{n}\left[\frac{1}{(i-1)!}\left(\frac{t-\Delta t}{k}\right)^{i-1}.\sum_{j=1}^{n}A_j\right]\right] - \frac{e^{\frac{-t}{k}}}{A_T}.\left[\sum_{i=1}^{n}\left[\frac{1}{(i-1)!}\left(\frac{t}{k}\right)^{i-1}.\sum_{j=1}^{n}A_j\right]\right]\right] \text{ for}$$

$$t \ge \Delta t \tag{6.13}$$

The parameter k is obtained from the effective rainfall hyetograph (ERH) and the direct runoff hydrograph (DRH) to which are applied the Momentum Method:

$$k = \frac{A_T(t_{DRH} - t_{ERH})}{\sum_{i=1}^{n} i.A_i} \tag{6.14}$$

where $t_{DRH}$ and $t_{ERH}$ are respectively the centroids of the DRH and the ERH.

The GUHR was recently developed (2005) and has been successfully tested on a small watershed (4.7 km2) in Northern Spain. There is nonetheless no sign of its application to a large catchment, hence its application to the study area.

## 6.4 Data processing

### 6.4.1 Flow separation

Hydrograph separation is an important component of the UH theory model application. Unfortunately, there is no satisfactory technique for extracting the direct runoff hydrograph from the total hydrograph (Beven, 2001, Bedient et al, 1992). Several techniques can be found in the literature (see Beven 1991), however all of them lack physical justification and are arbitrary (Nash, 1960). The only physically justifiable method to estimate baseflow would be to try to estimate the flow that might have occurred if the storm had not happened, but such a technique leads to direct runoff hydrographs with very long tails and too complicated when applied to complex storm events (Reed et al, 1975). Beven noted that the best method for dealing with hydrograph separation is to avoid it all together (Beven, 2001).

Considering the lack of a reference separation technique, constancy was privileged in this study, and the Nash method (Nash, 1960) was used in this study: a line was traced from the start of the rising limb (A) to a point on the recession curve (B) such that the time elapsed between the end of effective rainfall and the point B is equal to three times the lag time (see figure 6.6).

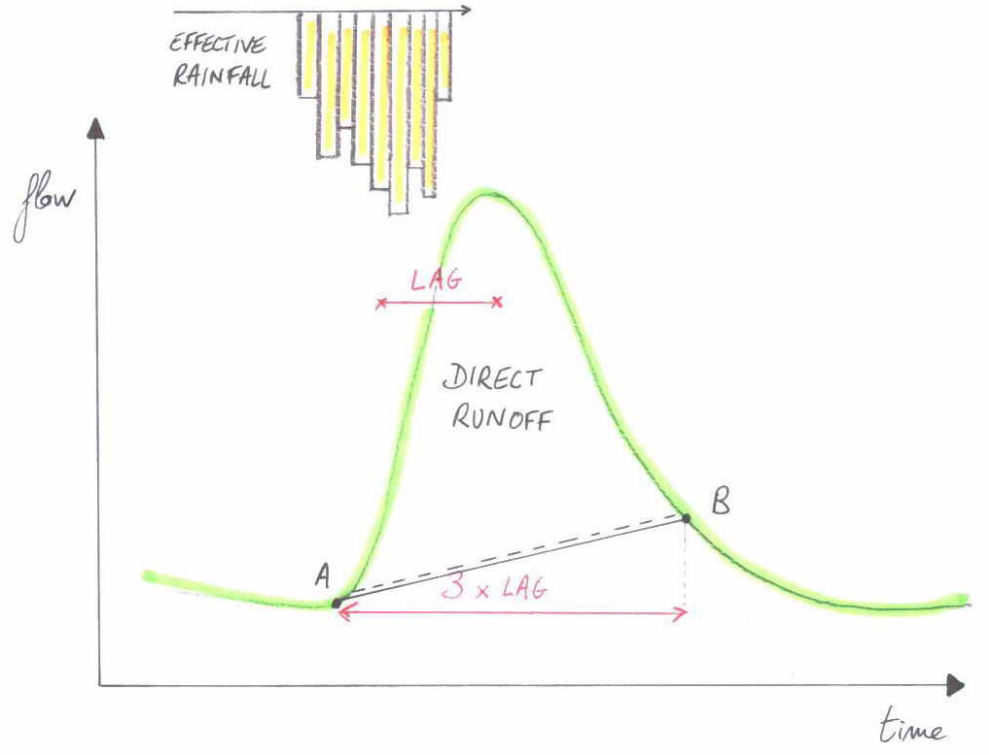


**Figure 6.6 Baseflow separation using Nash's method**

Before deciding to choose one of the flow separation methods, a comparison between the different available techniques was made and the results examined. Three different methods were used:

- Graphical method: a line is traced between point A and the point of the recession curve where the inflection occurs. This method depends on the user's appreciation and is therefore subjective. Nevertheless, as storm events lead to very particular hydrographs, a visual analysis is helpful allowing the user to spot specificities.
- Area method: similar to the Nash method, the distance between A and B is $N = A^{0.2}$ where $A$ is the catchment are in sq. miles (Ramirez, 2000). It is précised that this method is not suitable for small catchments and should be checked for many hydrographs before using.
- Nash's method.

Figure 6.7 shows the different direct runoff hydrographs obtained using the three separation methods (for the river Blackwater at Duarrigle):

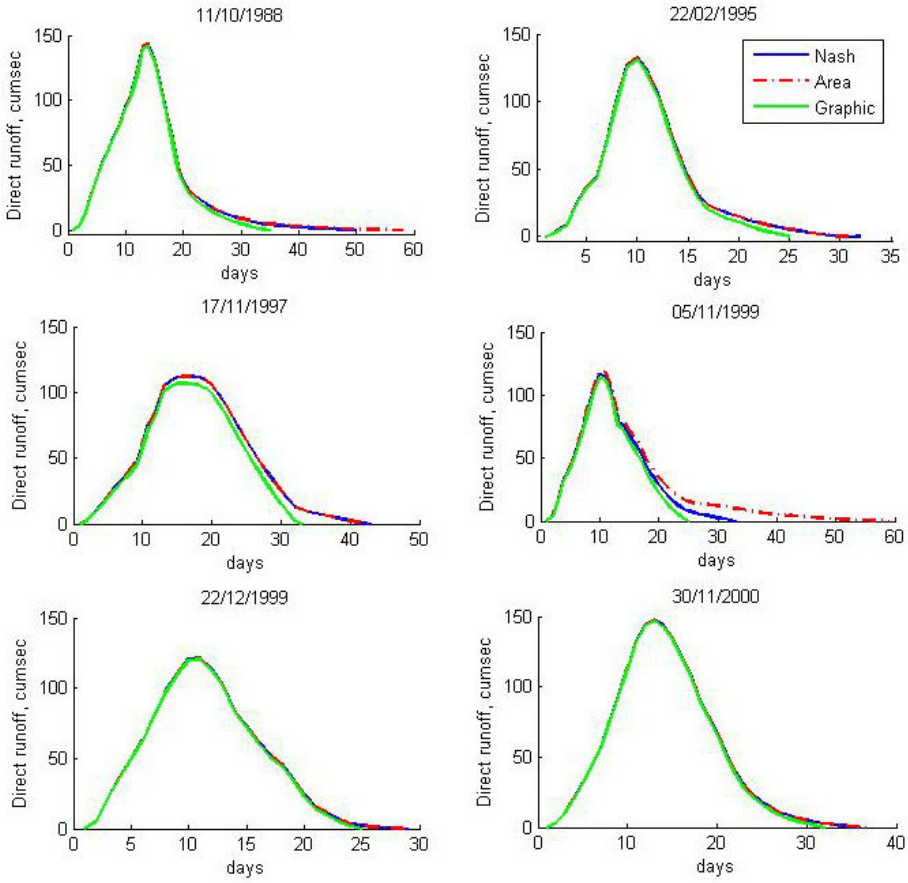


**Figure 6.7 Comparison of different baseflow separation method (Duarrigle)**

**Table 6-1 Comparison between Nash, Area and Graphic hydrograph separation methods**

| Storm events | Date | Error percentage (Nash / Area) | Error percentage (Nash / Graphic) |
|---|---|---|---|
| **1** | 11 Oct 1988 | 1.3 | 5.9 |
| **2** | 22 Feb 1995 | 0.3 | 6.5 |
| **3** | 17 Nov 1997 | 0 | 11.2 |
| **4** | 05 Nov 1999 | 19.9 | 9.5 |
| **5** | 22 Dec 1999 | 0 | 2.3 |
| **6** | 30 Nov 2000 | 0.2 | 2.5 |

As can be seen in figure 6.7, differences in derived hydrograph are slight and the Nash and Area methods' curve are usually the same. The Graphic method always gives a smaller direct runoff hydrograph. Table 6.1 shows the percentage of volume difference between the Nash method and the two other alternatives. Differences are small except for the 4$^{th}$ event, for which the difference in the derived direct runoff hydrograph volumes is significant (19% of difference in volumes between the Nash and Area methods). For this particular event, the Area method leads to a long tail hydrographs which is an undesirable characteristic. It is more acceptable to prefer the Nash derivation that gives a more acceptable hydrograph shape. Even if the 1$^{st}$ event also shows a long tail hydrograph for both Nash and Area methods, it does not appear to be a problem as the volume under the tail is very low, which is not the case in the 4$^{th}$ event.

### 6.4.2 Rainfall separation

The aim of the rainfall separation is to partition total rainfall into infiltration losses and net rainfall, which is the part that will be convoluted by the UH. Many different models in the past decades have considered the concept of infiltration loss-rate curves such as the Horton infiltration model (Chahinian, 2004), the Soil Conservation Service Curve Number method (SCS, 1972) or the Green-Ampt equation. Later developments provided grounds for the belief that a percentage-based method of rainfall separation was more appropriate (Houghton-Carr, 1999). In this study, preference was given to models not intending to describe the physical processes but rather objectively distributing the losses during the storm with recognition of the changing state of the catchment.

This method is adapted from the original method described in the Flood Estimation Handbook (FEH) (Institute of Hydrology, 1999) and consists in a variable loss rate changing with antecedent wetness and conditioned so that the volumes of net rainfall and direct runoff should be

equal (Webster *et al*, 2002). In the Decreasing Proportional Loss (DPL) model, the percentage runoff increases in proportion to the catchment wetness index (CWI) through the storm. The CWI index is defined as follows (FEH, 1999):

$$CWI = 125 + API - SMD \tag{6.14}$$

where *API* is the Antecedent Precipitation Index and *SMD* the Soil Moisture Deficit.

The API, expressed in mm, is the sum of the rainfall in *n* preceding days weighted exponentially such that the rainfall from the nth day has the smallest weight and the rainfall from the preceding day has the largest weight. Its general equation is (Anctil *et al*, 2003):

$$API_i(t) = \sum_{j=1}^{i} P_{t-j}.k^j \tag{6.15}$$

where *i* is the number of antecedent days considered, *k* the exponential decay constant and $P_d$ the rainfall on day *d* (mm).

The Flood Studies Report (Natural Environment Research council, 1975) and the FEH (IH, 1999) advice a length of recession of 5 days (i.e. $n = 5$) and make a modification to this equation so that it can fit the assumption that the rainfall occurs at the centroids of each day. Equation (6.16) is written taking into account this delay:

$$API = k^{0.5}.\left(P_{d-1} + k.P_{d-2} + k^2.P_{d-3} + k^3 P_{d-4} + k^4.P_{d-5}\right) \tag{6.16}$$

The constant k is determined assuming that the influence of the nth day's rainfall is reduced to approximately 1/20$^{th}$ of the original value ($k^{n-1/2} = 0.05$) (Reed, 1992), leading to $k = 0.5$.

The *SMD* is calculated using data provided by Mary Curley (Met Éireann) and computed with the Hybrid Soil Moisture Deficit Model which has been used by Met Éireann since May 2006. The SMD is calculated on a daily basis as:

$$SMD_t = SMD_{t-1} - RAIN + ET_a + DRAIN \tag{6.17}$$

where $ET_a$ is the actual evapotranspiration (mm/day), which is obtained by:

$$\begin{cases} AE = PE \\ AE = PE.\dfrac{SMD_{\max} - SMD_{t-1}}{SMD_{\max} - SMD_c} \end{cases} \tag{6.18}$$

depending on when $SMD \leq SMD_c$ or not.

The *critical SMD* ($SMD_c$) and the theoretical maximum value $SMD_{\max}$ are defined for each soil drainage class (well drained, moderately drained and poorly drained). Most of the Munster Blackwater catchment is covered with well-drained soils (see previous Chapter 3). Therefore the well drained soil drainage class is only considered and leads to the following values: $SMD_c = 0$ and $SMD_{\max} = 110mm$ (Schulte et al, 2005).

Potential Evapotranspiration (PE) (mm/day) is calculated according to the FAO Penman-Monteith Equation (for a reference grass crop at an assumed height of 0.12m) (Allen et al, 1998):

$$PE = \frac{0.408.\Delta(R_n - G) + \gamma \dfrac{900}{T + 273} u_2 (e_s - e_a)}{\Delta + \gamma(1 + 0.34.u_2)} \tag{6.19}$$

where $R_n$ is the net radiation at the crop surface (MJ/m².day), G is the ground heat flux density (MJ/m².day), T is the air temperature at 2m height (°C), $u_2$ the wind speed at 2m height (m/s), $e_s$ and $e_a$ the saturation vapor pressure and the actual vapor pressure respectively (kPa), $\Delta$ the slope of the vapor pressure curve (kPa/°C) and γ the psychometric constant (kPa/°C).

Considering the relative complexity of equation (6.19) and its high demand in field measurements, *PE*, and thus *AE* and *SMD* are available on a daily basis for the 14 Irish synoptic stations (see figure 6.8), the nearest to the Munster Blackwater being Cork Airport (synoptic station 955, Irish Grid Reference W709633). For three of the closest synoptic stations (Cork Airport, Shannon Airport and Rosslare) calculated data were analyzed and plotted for a period of a year. From figure 6.9 it appears that it is reasonable to adopt the SMD for Cork Airport as being suitable for the Blackwater catchment.

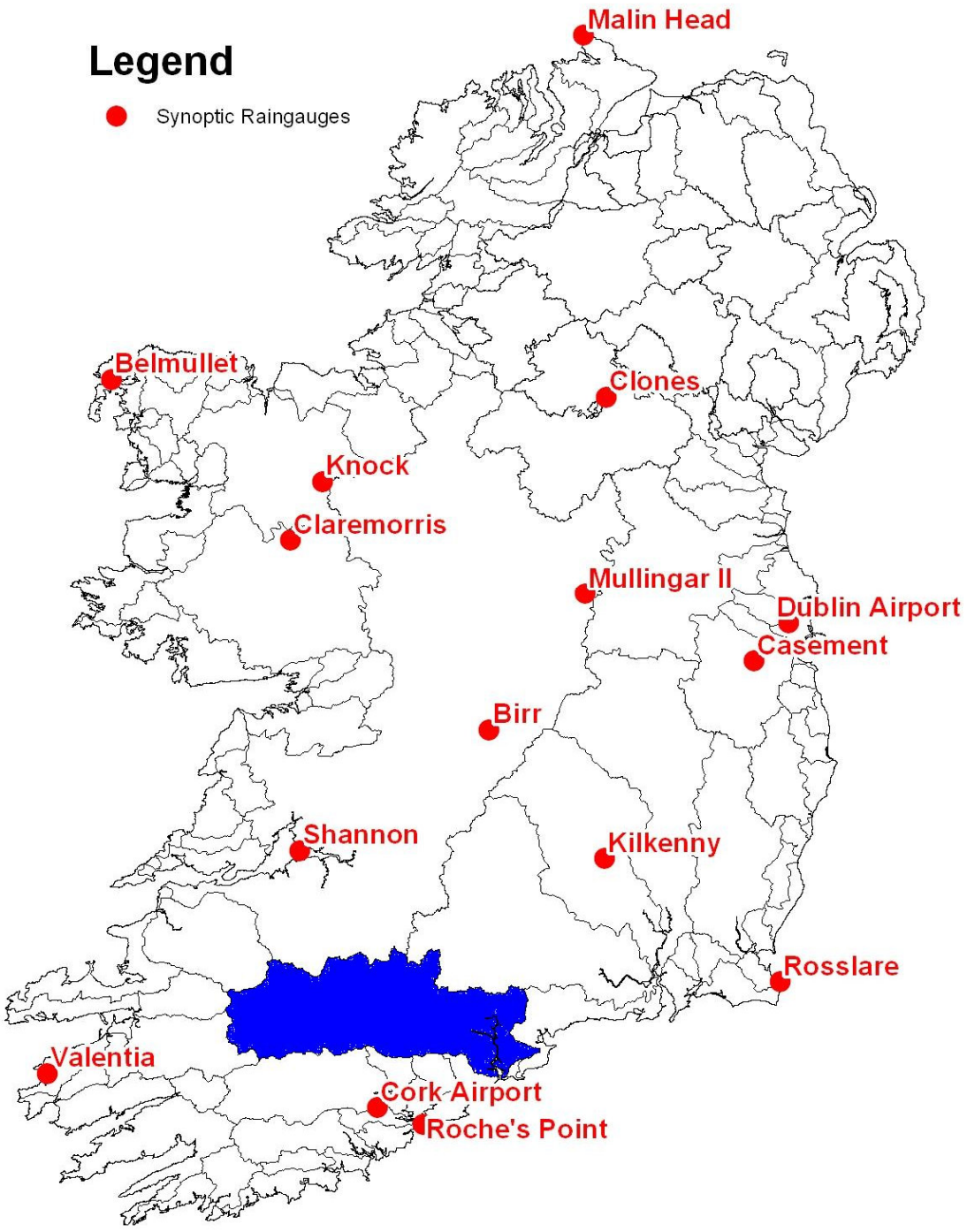


**Figure 6.8 Synoptic stations in Ireland**

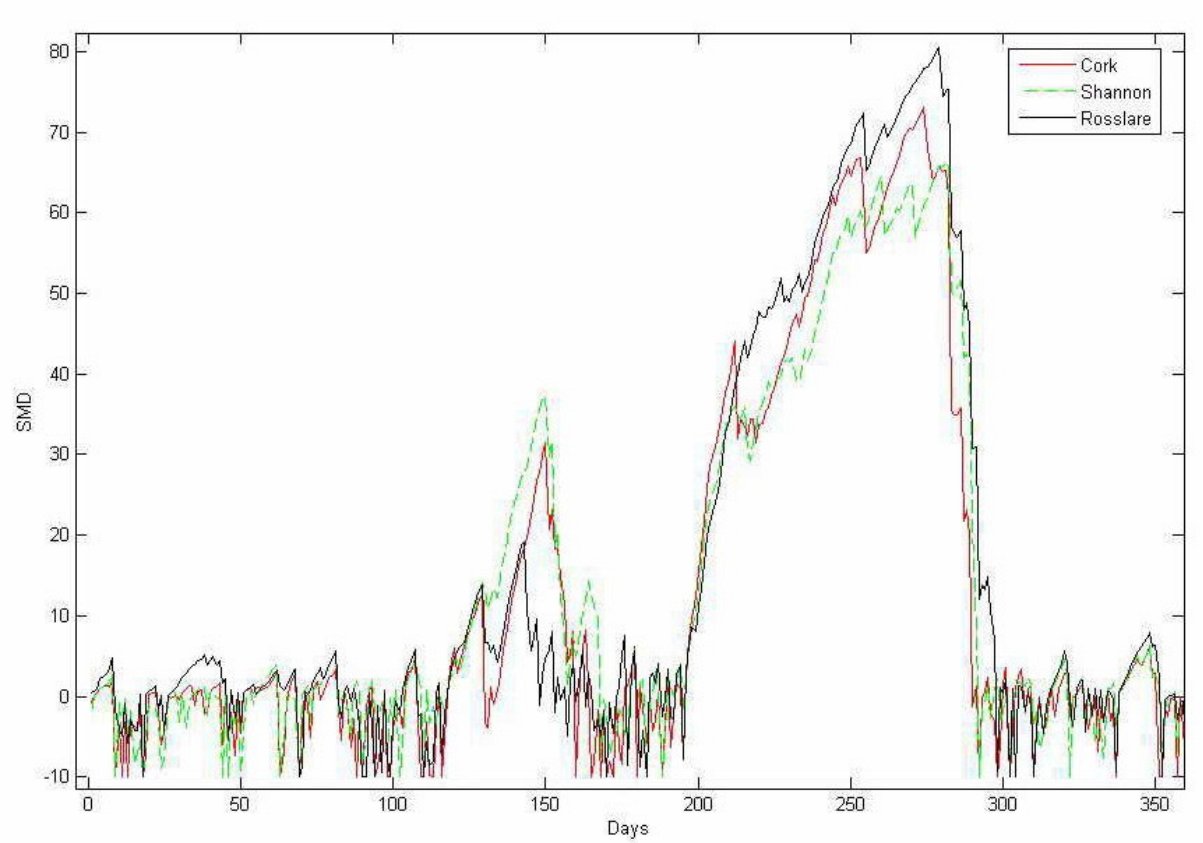


**Figure 6.9 Daily SMD values (mm/day) over the year 2005, for Cork, Shannon and Rosslare**

Both API and SMD (and therefore CWI) values are calculated on a daily basis which is not accurate enough to be used in a 1-hour step modeling. SMD and API are then readjusted by a continuous accounting procedure through the storm event. This is done by reducing SMD by the amount of any rain that has fallen in the previous time interval and by recalculating API as follows (Houghton-Carr, 1999):

$$API_t = API_{t-1}.(0.5)^{\frac{\Delta T}{24}} + P_{t-1}(0.5)^{\frac{\Delta T}{48}} \qquad (6.20)$$

where $\Delta T$ is the time step (usually 1 hour).

Using equations 6.21, it is then possible to calculate CWI from API and SMD at the end of every data interval and therefore the corresponding percentage runoff for each interval:

$$\begin{cases} F = \dfrac{Rapid\_Runoff\_Volume}{\sum_i rain_i * CWI_i} \\ PR_i = CWI_i .* F \end{cases} \tag{6.21}$$

where $rain_i$ and $CWI_i$ are respectively the rain and the CWI coefficient at the end of the i[th] data interval.

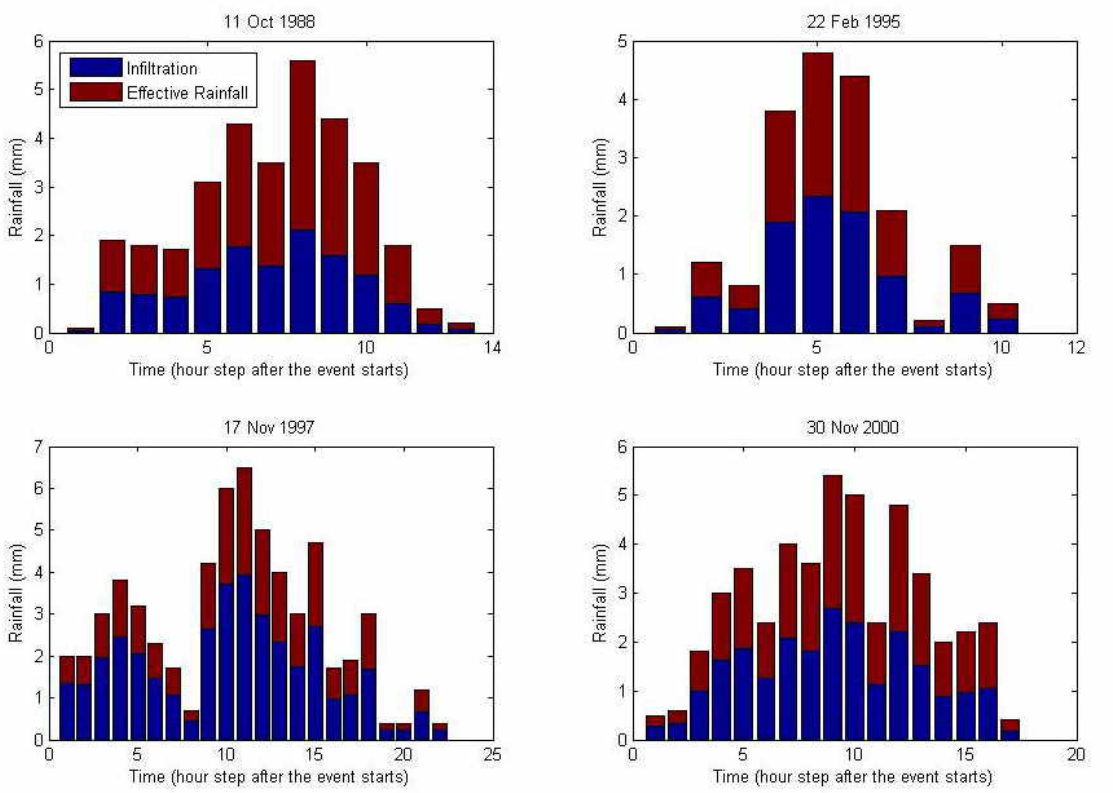


**Figure 6.10 Four examples of rainfall separation (CPL method)**

As a comparison, figure 6.11 shows the application of the Phi-Index method to the same four flood events that were plotted in figure 6.10. In this simple method, also called "constant loss rate method", the total rapid runoff volume is estimated and distributed uniformly across the storm pattern, considering that the infiltration rate is constant with time. This arbitrary rate is applied from the initiation of precipitation, and any rainfall which exceeds this rate contributes to the direct runoff hydrograph while the reminder goes into the losses. While this technique insures that the rainfall excess volume is exact, it does not reflect the time distribution of the effective rainfall.

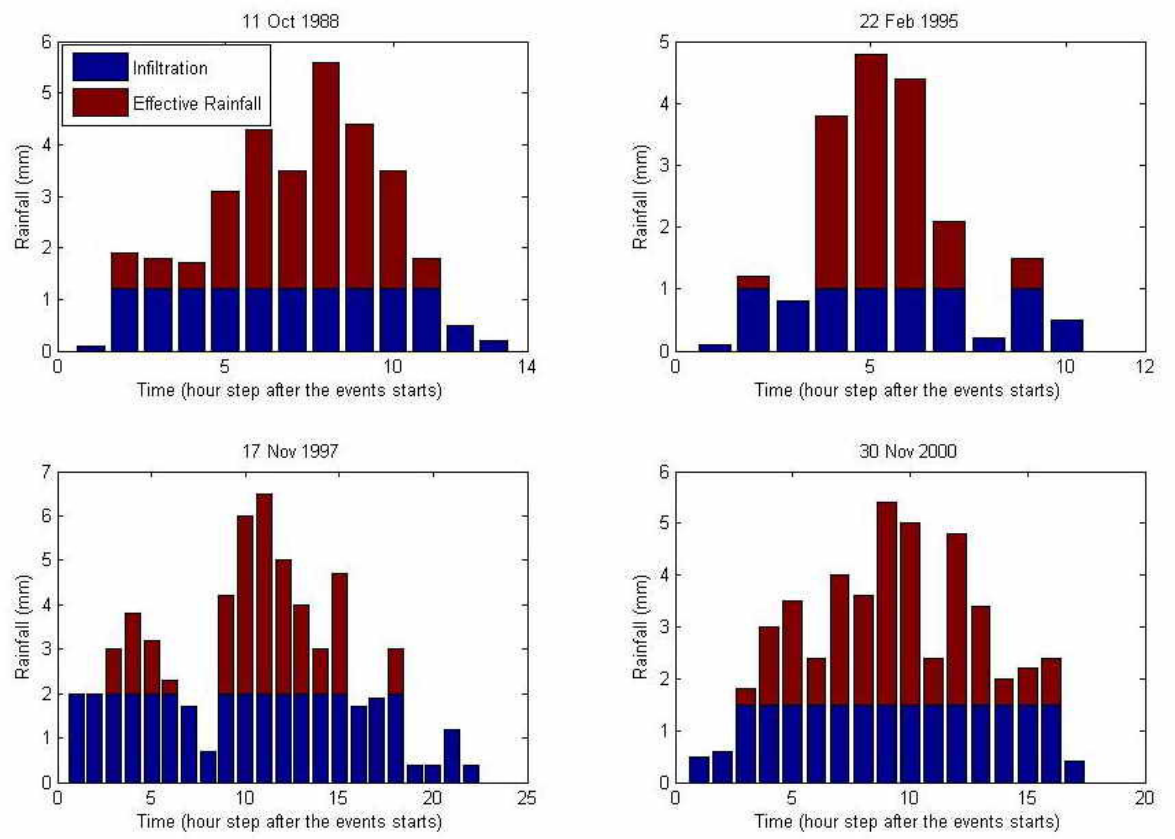


**Figure 6.11 Four examples of rainfall separation using the Phi-Index method**

### 6.4.3 Sub-watershed delineation for the GUHR

The definition of sub-watersheds was performed using the GIS Arc Map (ESRI, date) software. A Digital Elevation Model (DEM) with a 20 meters precision was created from Ordinance Survey of Ireland (OSI) digital contours maps and was used to derive the drainage network. It should be noted that the precision of the resulting drainage network depends on the number of contributing points considered to define a stream and that this number was fixed at 1500 in this study. The sub-watersheds were then obtained from the derived drainage network and those which had the same stream order were grouped together (see figure 6.12).

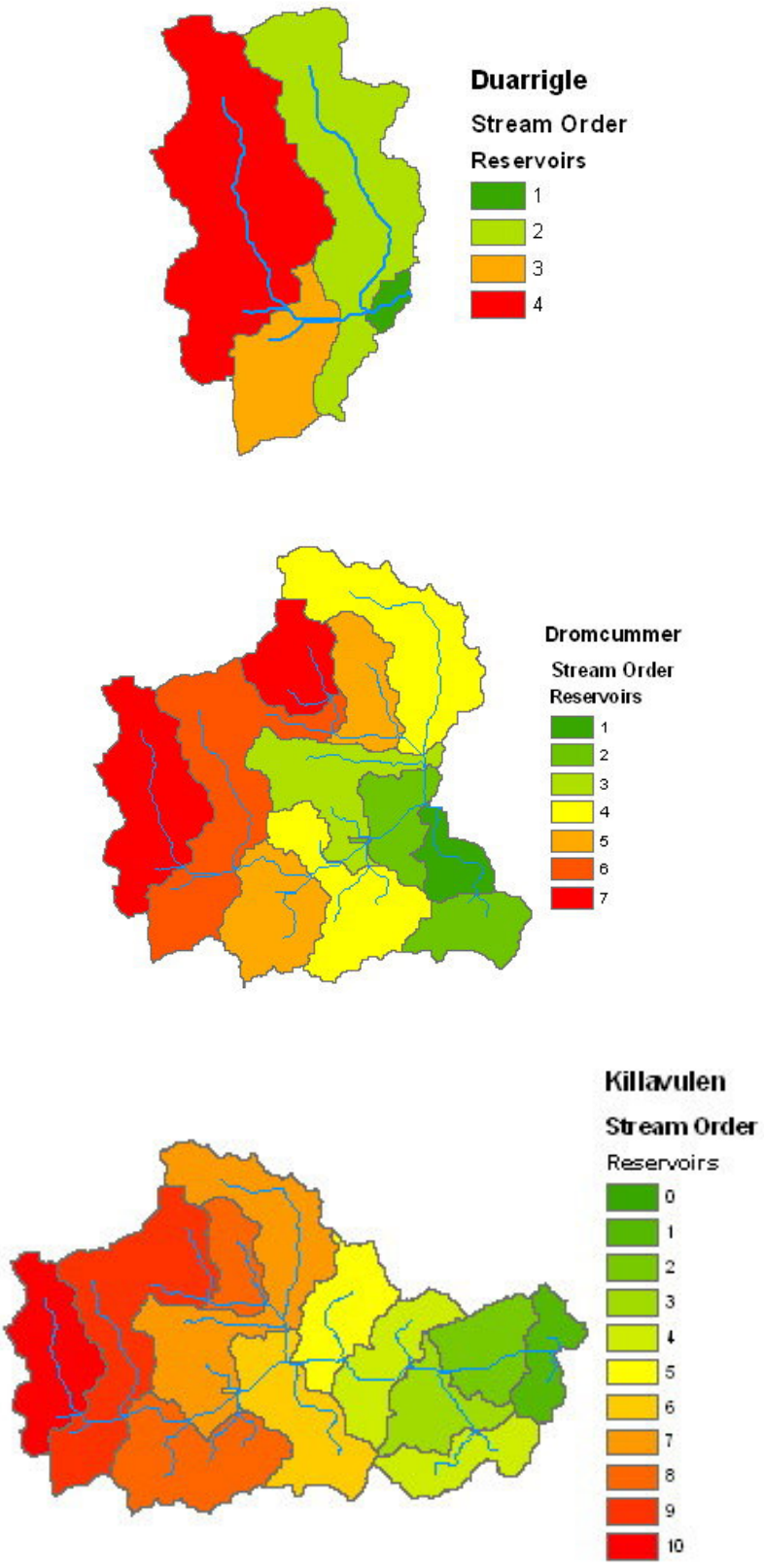


**Figure 6.12 Geomorphological sub-watershed delineation**

**Table 6-2 Sub-watersheds areas (m2) for the 3 sub-catchments**

| Reservoir order | Duarrigle | Dromcummer | Killavulen |
|---|---|---|---|
| **1** | 4.8 | 32.3 | 51.3 |
| **2** | 92.6 | 88.7 | 73.3 |
| **3** | 35.9 | 77.9 | 71.9 |
| **4** | 112.2 | 215.4 | 149.1 |
| **5** | --- | 122.9 | 85.2 |
| **6** | --- | 159.2 | 121.0 |
| **7** | --- | 165.3 | 232.9 |
| **8** | --- | --- | 183.3 |
| **9** | --- | --- | 212.2 |
| **10** | --- | --- | 112.2 |

## *6.5 A Graphic User Interface as an analysis tool*

A Graphic User Interface (GUI) was created in the Matlab (Mathworks, 1999) platform to run the different UH derivations (see figure 6.13). A plotting module built within this tool allows the user to plot both the rainfall and the flow discharge distribution together, to identify the corresponding rainfall events and peak hydrograph (see figure 6.14).

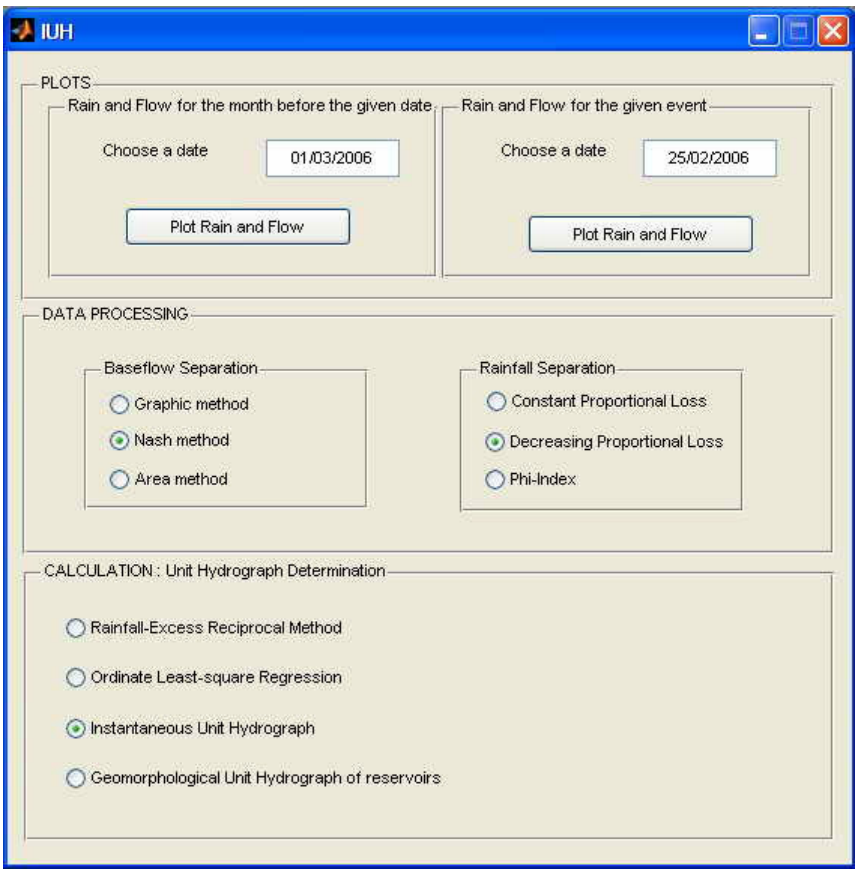


**Figure 6.13 Screenshot of the developed Graphic User Interface**

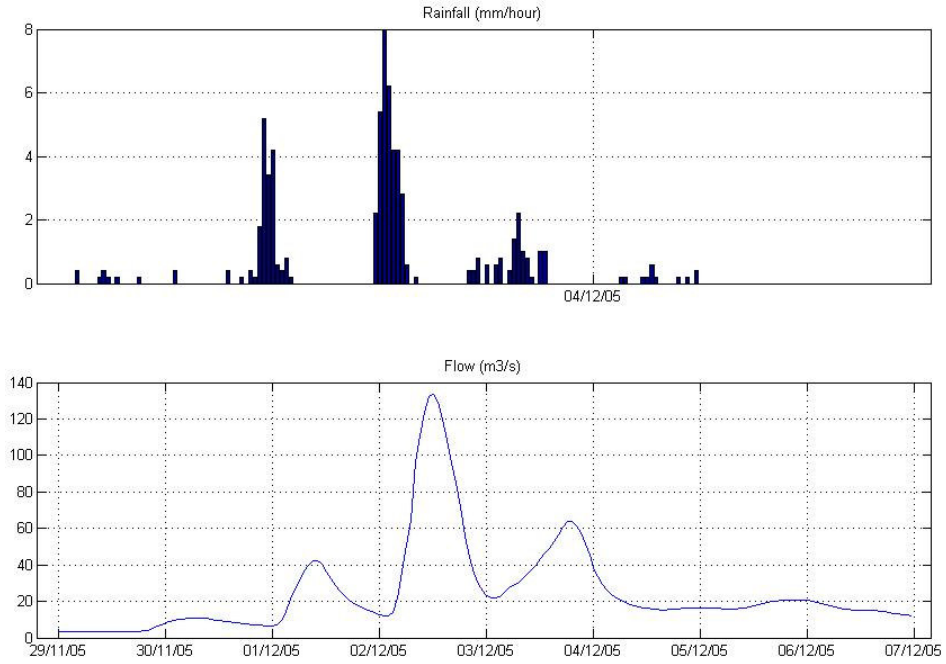


**Figure 6.14 Flow discharge and corresponding rain event (plotting module),Flood of the 2nd December 2005**

Data is processed by choosing among the different available methods (Graphic, Nash and Area methods for the baseflow separation and CPL, DPL and Phi-Index methods for the rainfall separation). The calculation module can be done using one of the four UH derivation methods (Rainfall-excess reciprocal method, least-square method, Nash IUH and the watershed morphology based method) and gives the UH as an output, with plots of calculated flow in comparison with actual observation.

## *6.6 Application and results*

### 6.6.1 Storm events selection

As the aim of the study is to model high flows, the catchment average hydrograph is derived from high flow events. The 25 most important events were therefore considered. Storm events were selected considering the quality of both rainfall and flow discharge data. For rain, the criteria is the availability with a precise enough time step (a 1-hour step was required). All the events which occurred after January 2005 are covered with the 15-minutes OPW data set. For events prior

to this date, the information had to be extracted from hard-copy daily hyetograph in Met Éireann headquarter in Dublin (see Chapter 4 – Rainfall Data). For the flow data, the shape of the direct runoff peak was studied and selected if the peak was well defined. As can be seen on figure 6.15 and table 6.3, only 8 events were considered suitable for the catchment average unit hydrograph construction.

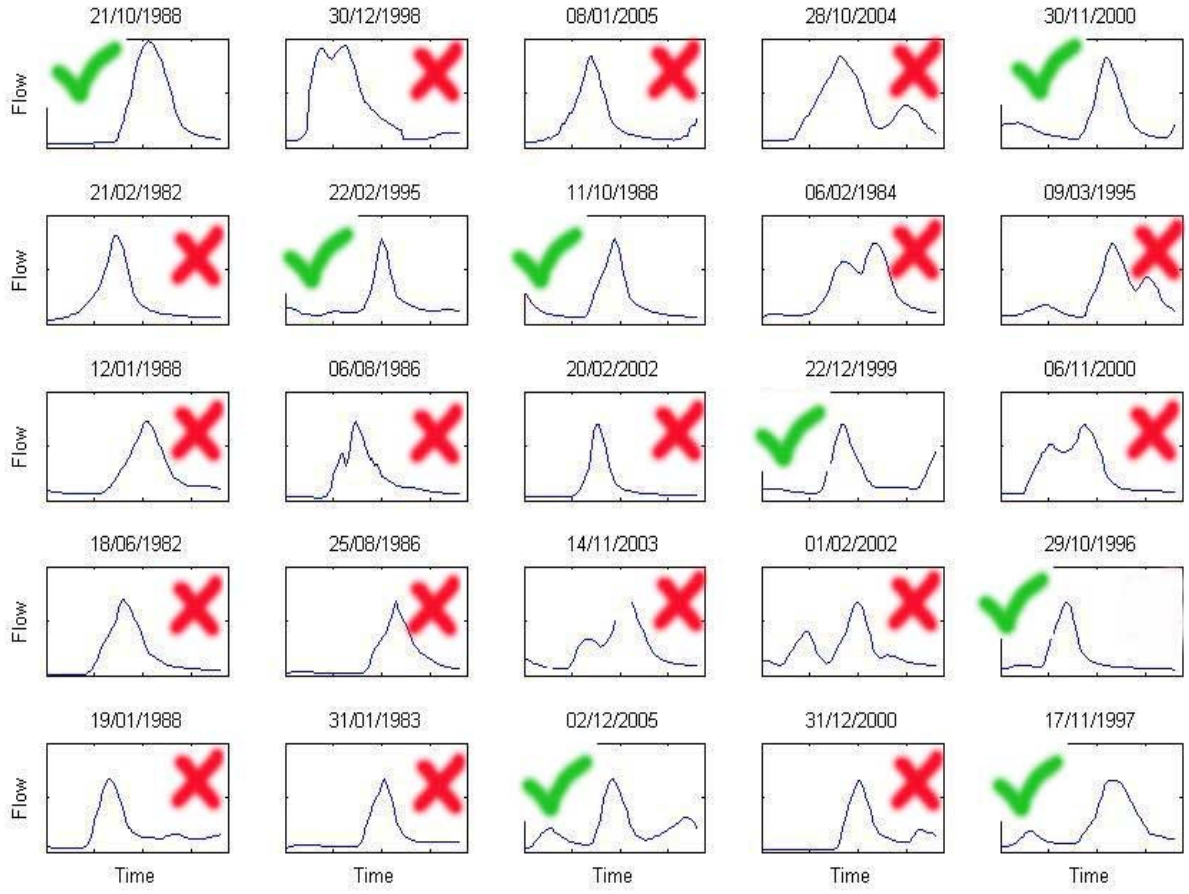


**Figure 6.15 The 25 highest floods in Duarrigle (selection of the suitable peaks).**

**Table 6-3 25 highest floods and those selected for the Catchment Average UH**

| Date | River Height (m) | Peak Flow discharge ($m^3/s$) |
|---|---|---|
| **21-Oct-88** | **3.818** | **195.5** |
| 30-Dec-98 | 3.714 | 186.9 |
| 8-Jan-05 | 3.464 | 166.9 |
| 28-Oct-04 | 3.462 | 166.7 |
| **30-Nov-00** | **3.439** | **164.9** |
| 21-Feb-82 | 3.416 | 163.1 |
| **22-Feb-95** | **3.327** | **156.3** |
| **11-Oct-88** | **3.324** | **156.1** |
| 6-Feb-84 | 3.212 | 147.6 |
| 9-Mar-95 | 3.202 | 146.8 |
| 12-Jan-88 | 3.169 | 144.3 |
| 6-Aug-86 | 3.167 | 144.2 |
| 20-Feb-02 | 3.114 | 140.3 |
| **22-Dec-99** | **3.095** | **139.0** |
| 6-Nov-00 | 3.094 | 138.8 |
| 18-Jun-82 | 3.083 | 138.0 |
| 25-Aug-86 | 3.050 | 135.7 |
| 14-Nov-03 | 3.043 | 135.1 |
| 1-Feb-02 | 3.042 | 135.1 |
| **29-Oct-96** | **3.040** | **135.0** |
| 19-Jan-88 | 3.034 | 134.5 |
| 31-Jan-83 | 3.032 | 134.4 |
| **2-Dec-05** | **3.020** | **133.5** |
| 31-Dec-00 | 2.986 | 131.1 |
| **17-Nov-97** | **2.979** | **130.6** |

The resulting catchment average UH is tested on floods which occurred during the period 2005-2006. Both simple and multiple peaks events with important enough direct runoff volumes were selected.

### 6.6.2 GUHR model modification

As can be seen on figure 6.16, the original GUHR model formulation lead to poor results, and the large size of the studied catchments (245km$^2$ to 1292km$^2$) was likely to be responsible.

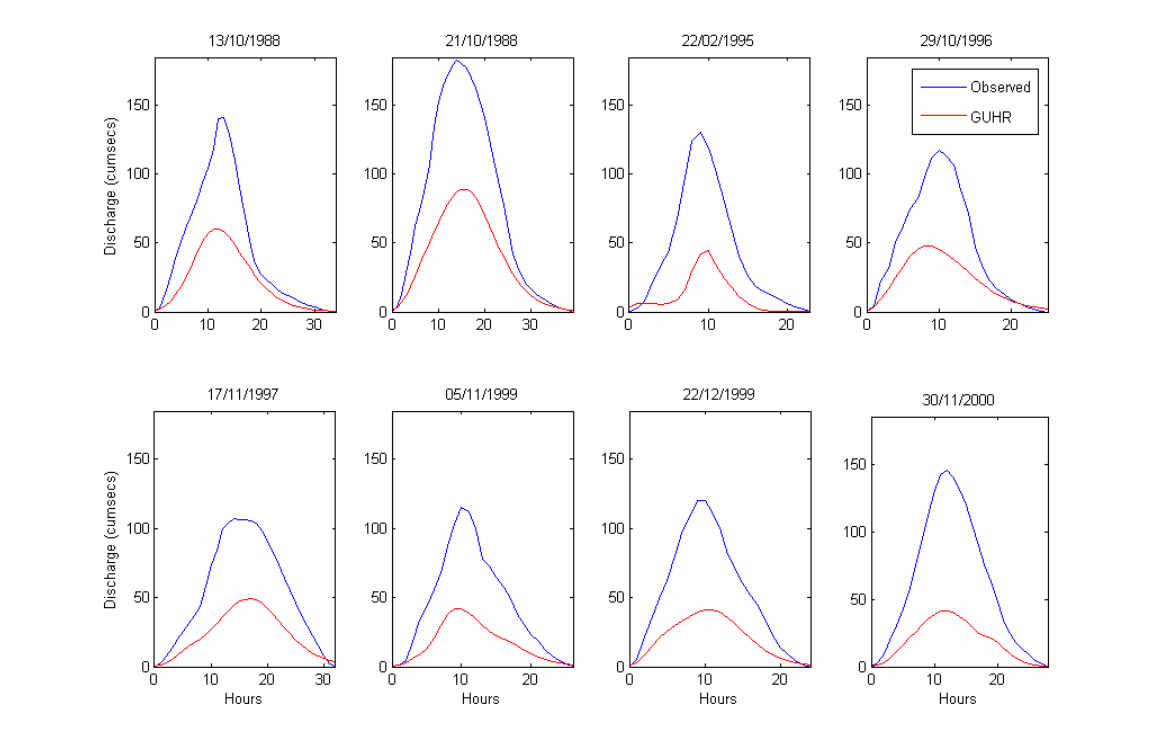


**Figure 6.16 Example of the original GUHR model in Duarrigle**

It was therefore decided to keep the mathematical structure of the model (equations 6.12-13) which is founded on acceptable theory and to modify the reservoir determination method that did not fit the Munster Blackwater catchment. The number of reservoirs and their sizes were directly derived from the data using an optimization process during a "calibration phase". In order to make the optimization process easier, two simplification morphology assumptions were made:

- The i+1$^{th}$ reservoir has to be greater than the i$^{th}$ reservoir.
- Sizes of two consecutives reservoirs are linearly related as $S_{i+1} = S_i.C$, where $C$ is a constant coefficient greater than 1

The optimization was first run to obtain the reservoir number and then to fix the $C$ coefficient (see table 6.4), which lead to the reservoir structure for each sub-catchment (see table 6.5).

**Table 6-4 Number and size of reservoirs for the modified GUHR**

| Sub-catchment | Number of Reservoir | C |
|---|---|---|
| **Duarrigle** | 5 | 1.325 |
| **Dromcummer** | 6 | 1.175 |
| **Killavullen** | 6 | 1.425 |

**Table 6-5 Sub-watersheds areas ($m^2$) for the 3 sub-catchments with the modified GUHR**

| Reservoir Order | Duarrigle | Dromcummer | Killavulen |
|---|---|---|---|
| **1** | 24.6 | 90.7 | 54.1 |
| **2** | 29.6 | 99.8 | 75.8 |
| **3** | 35.5 | 109.8 | 106.1 |
| **4** | 42.6 | 120.7 | 148.6 |
| **5** | 51.1 | 132.8 | 208.1 |
| **6** | --- | 146.1 | 291.3 |

In the remainder of this chapter, GUHR refers to the above modified GUHR.

### 6.6.3 Model evaluation

The simulated hydrographs are graphically observed in order to evaluate the agreement between observed and modelled values. For a more precise evaluation, the Nash and Sutcliffe Efficiency (NSE) indicator (Nash, 1970) was calculated:

$$NSE = 1 - \frac{\sum_{i=1}^{n} \left(Q_{i,OBS} - Q_{i,SIM}\right)^2}{\sum_{i=1}^{n} \left(Q_{i,OBS} - \overline{Q_{OBS}}\right)} \tag{6.21}$$

where $Q_{i,OBS}$ and $Q_{i,SIM}$ are the observed and simulated flow values, and $Q_{OBS}$ the average value of the observed flow over the full event time period.

The normalization of the variance of the observed time series of flows results in relatively higher values of NSE in catchments with higher dynamics and lower values of NSE in catchments with lower dynamics. An efficiency of lower than zero indicates that the mean value of the observed time series would have been a better predictor than the model (Krause, 2005). As the differences between the observed and predicted values are calculated as squares values, larger values are overestimated whereas lower values are minimized. That makes the NSE an appropriate

efficiency indicator for flood hydrographs analysis, in which more importance is given to the flow peak area.

Basic linear regression can also be used in order to see the correlation between the observed and calculated time series. In this case, the slope coefficient (coefficient *a* if the line equation is $y = ax + b$) indicates the fit between the two time series (a slope coefficient equal to one would mean that the results are perfected) and $R^2$ (coefficient of determination) indicates the strength of this fit.

### 6.6.4 Catchment Average UH derivation

The three different UH approaches (the ordinates method, the Nash IUH and the GUHR) are applied to each of the 3 sub-catchments in the Blackwater for 8 storm events. These 8 storms were selected for their high peak flows (among the 25 highest flows) but have different characteristics in term of rainfall duration, peak discharge and percentage runoff, which leads to obviously different UHs that reflect the heterogeneity of the catchment response. The 8 resulting unit hydrographs are then averaged to obtain the catchment average UH (CAUH).

The application of each approach is shown graphically and is evaluated using the NSE indicator.

#### 6.6.4.1 Duarrigle

Table 6.6 lists the 8 floods used to derive the UH in Duarrigle, with the corresponding rain event characteristics, flow response and volumes.

**Table 6-6 Storm events selection in Duarrigle – CAUH derivation**

| Events | Date | rainfall duration (hours) | peak discharge (m3/s) | rainfall volume (mm) | direct runoff volume (mm) | Percentage Runoff |
|---|---|---|---|---|---|---|
| **1** | 11-Oct-88 | 12 | 156.1 | 60.9 | 23.1 | 0.379 |
| **2** | 21-Oct-88 | 18 | 195.5 | 51.9 | 42.6 | 0.822 |
| **3** | 22-Feb-95 | 14 | 156.3 | 70.5 | 14.0 | 0.199 |
| **4** | 28-Oct-96 | 11 | 135.0 | 71.7 | 17.4 | 0.242 |
| **5** | 17-Nov-97 | 18 | 130.6 | 88.1 | 24.4 | 0.277 |
| **6** | 5-Nov-99 | 17 | 129.7 | 46.8 | 17.5 | 0.375 |
| **7** | 22-Dec-99 | 13 | 139.0 | 107.2 | 19.0 | 0.177 |
| **8** | 30-Nov-00 | 19 | 164.9 | 124.7 | 25.1 | 0.201 |

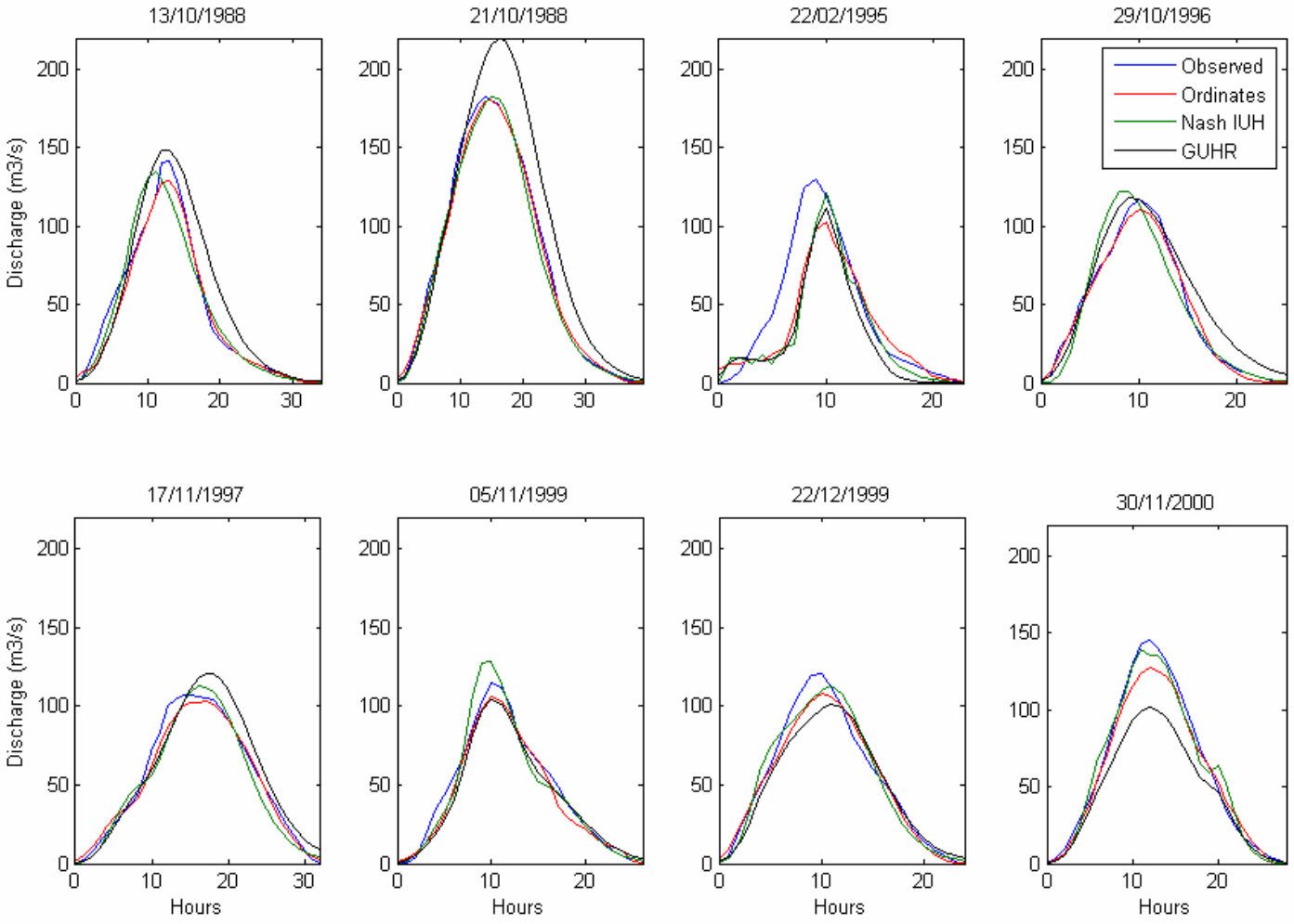


Figure 6.17 shows the application of the three different methods, in comparison with the observed direct runoff flow. Calculated and observed values are compared in table 6.7 which also gives NSE values for each event.

**Figure 6.17 Observed and simulated direct runoff hydrographs in Duarrigle – CAUH derivation**

**Table 6-7 Time to peak, Peak discharge and NSE for the 8 events - Duarrigle**

| Events | Observed | | Ordinates | | | IUH | | | GUHR | | |
|---|---|---|---|---|---|---|---|---|---|---|---|
| | Time to peak (hours) | Peak Discharge (m3/s) | Time to peak (hours) | Peak Discharge (m3/s) | NSE | Time to peak (hours) | Peak Discharge (m3/s) | NSE | Time to peak (hours) | Peak Discharge (m3/s) | NSE |
| **1** | 14 | 141.23 | 14 | 129.42 | 0.9781 | 12 | 134.37 | 0.9406 | 13 | 148.65 | 0.8562 |
| **2** | 15 | 182.82 | 16 | 180.38 | 0.9962 | 16 | 182.28 | 0.9897 | 17 | 219.09 | 0.8636 |
| **3** | 10 | 130.43 | 11 | 103.17 | 0.7543 | 11 | 121.53 | 0.6896 | 11 | 111.8 | 0.6875 |
| **4** | 11 | 117.13 | 11 | 110.24 | 0.9904 | 9 | 121.75 | 0.9163 | 10 | 117.81 | 0.9157 |
| **5** | 15 | 106.79 | 18 | 103.67 | 0.9847 | 17 | 112.71 | 0.9543 | 18 | 120.49 | 0.9257 |
| **6** | 11 | 114.97 | 11 | 105.78 | 0.9725 | 11 | 128.25 | 0.9464 | 11 | 103.95 | 0.9615 |
| **7** | 11 | 120.34 | 11 | 108.37 | 0.9710 | 12 | 113.28 | 0.9629 | 12 | 100.98 | 0.9279 |
| **8** | 13 | 145.3 | 13 | 126.89 | 0.9757 | 12 | 138.99 | 0.9796 | 13 | 101.24 | 0.8181 |

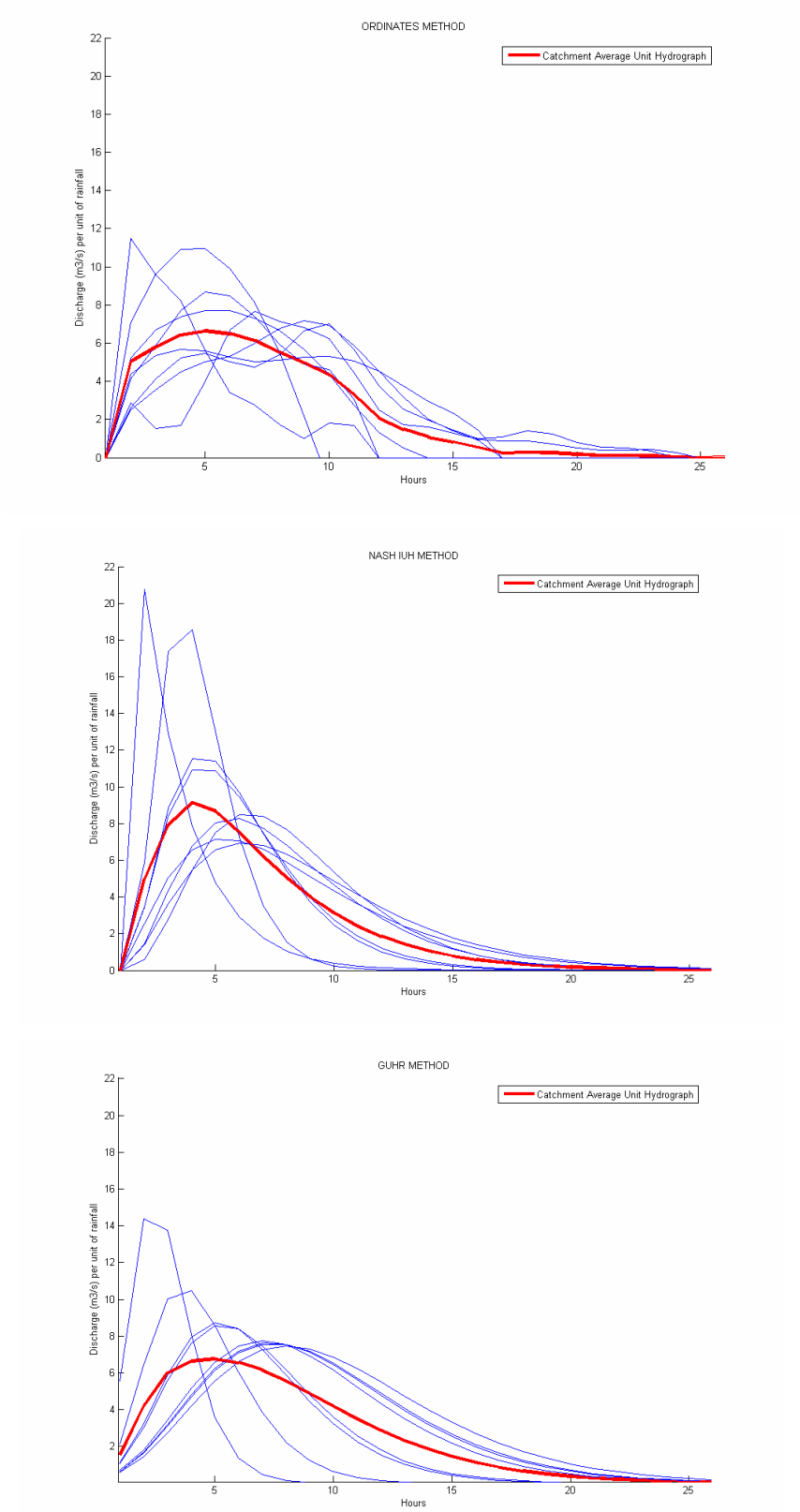


**Figure 6.18 Averaging the Unit Hydrograph with the 3 different methods - Duarrigle**

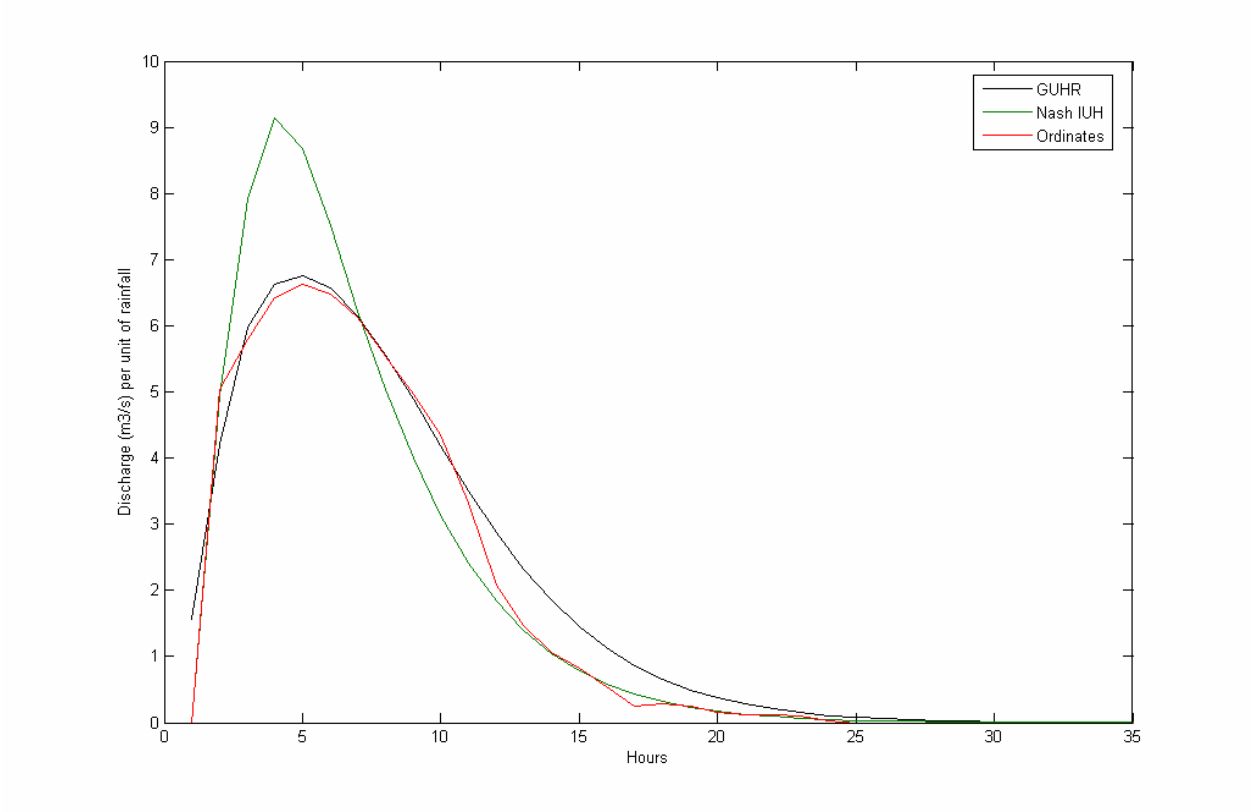


**Figure 6.19 3 Unit Hydrographs for Duarrigle**

### 6.6.4.2 Dromcummer

Table 6.8 lists the 8 floods used to derive the UH in Dromcummer, with the corresponding rain event characteristics, flow response and volumes.

**Table 6-8 events selection in Dromcummer – CAUH derivation**

| Events | Date | rainfall duration (hours) | peak discharge (m3/s) | rainfall volume (mm) | direct runoff volume (mm) | PR |
|---|---|---|---|---|---|---|
| **1** | 11-Oct-88 | 8 | 262.1 | 68.3 | 10.2 | 0.149 |
| **2** | 21-Oct-88 | 12 | 238.9 | 66.7 | 11.1 | 0.166 |
| **3** | 22-Feb-95 | 13 | 270.7 | 70.2 | 18.6 | 0.265 |
| **4** | 28-Oct-96 | 17 | 234.5 | 46.0 | 16.9 | 0.367 |
| **5** | 17-Nov-97 | 11 | 258.5 | 91.8 | 13.0 | 0.142 |
| **6** | 5-Nov-99 | 17 | 277.5 | 111.1 | 16.6 | 0.150 |
| **7** | 22-Dec-99 | 19 | 196.8 | 20.5 | 11.9 | 0.579 |
| **8** | 30-Nov-00 | 16 | 61.2 | 30.3 | 3.9 | 0.129 |

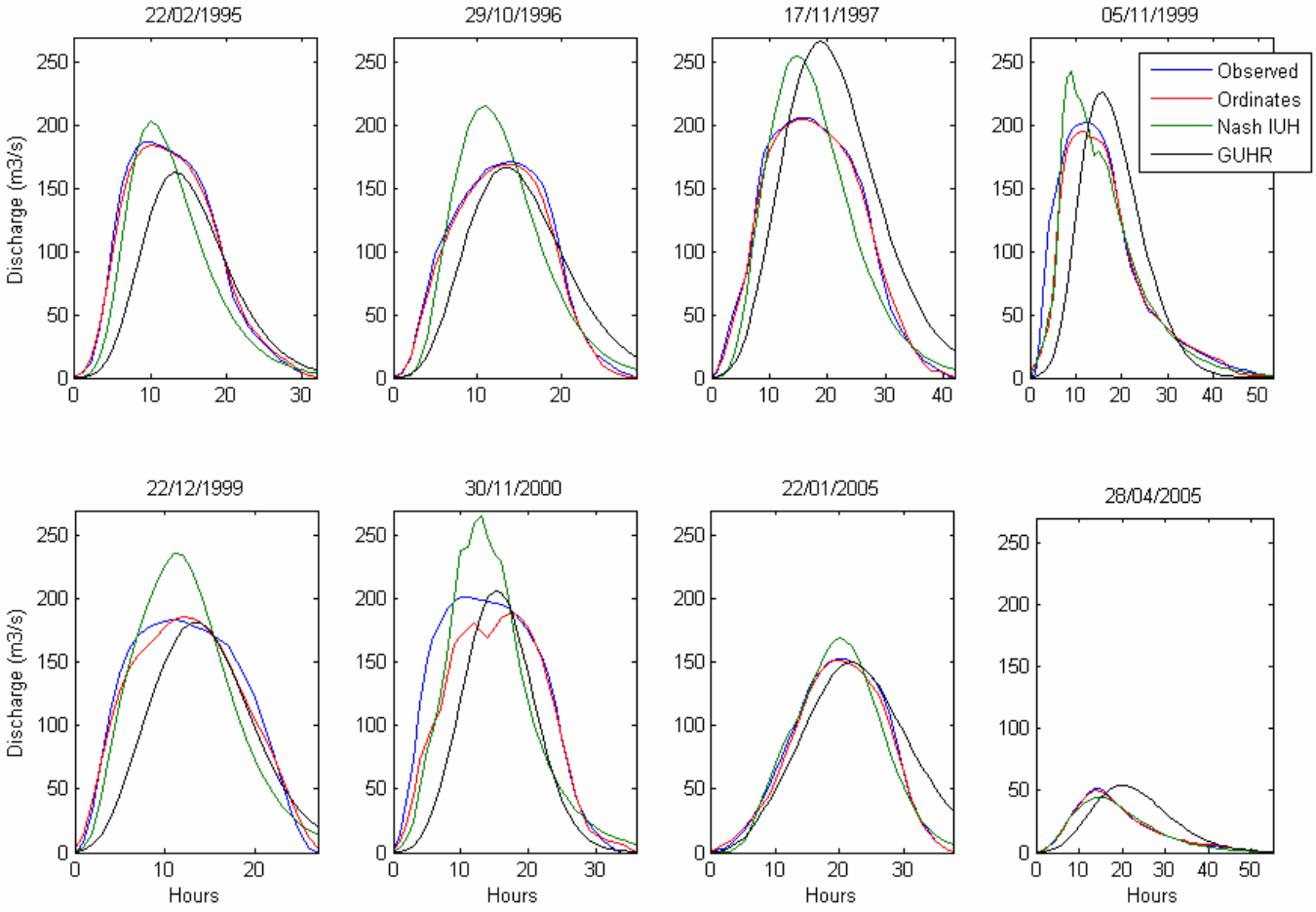


**Figure 6.20 Observed and simulated direct runoff hydrographs in Dromcummer – CAUH derivation**

Figure 6.20 shows the application of the three different methods, in comparison with the observed direct runoff flow. Calculated and observed values are compared in table 6.9 which also gives NSE values for each event.

**Table 6-9 Time to peak, Peak discharge and NSE for the 8 events - Dromcummer**

| Events | Observed | | Ordinates | | | IUH | | | GUHR | | |
|---|---|---|---|---|---|---|---|---|---|---|---|
| | Time to peak (hours) | Peak Discharge (m3/s) | Time to peak (hours) | Peak Discharge (m3/s) | E | Time to peak (hours) | Peak Discharge (m3/s) | E | Time to peak (hours) | Peak Discharge (m3/s) | E |
| **1** | 11 | 187.53 | 11 | 184.46 | 0.9966 | 11 | 203.17 | 0.8814 | 14 | 162.52 | 0.6599 |
| **2** | 15 | 171.87 | 15 | 169.46 | 0.9942 | 12 | 215.26 | 0.8012 | 14 | 166.69 | 0.8016 |
| **3** | 17 | 206.38 | 17 | 204.88 | 0.9966 | 16 | 255.55 | 0.8816 | 20 | 266.51 | 0.6474 |
| **4** | 14 | 202.67 | 12 | 195.27 | 0.9460 | 10 | 243.12 | 0.9175 | 17 | 226.13 | 0.5508 |
| **5** | 12 | 184.33 | 13 | 185.92 | 0.9795 | 12 | 235.86 | 0.8008 | 14 | 181.76 | 0.6216 |
| **6** | 11 | 201.55 | 19 | 188.72 | 0.8951 | 14 | 265.44 | 0.7258 | 16 | 206.71 | 0.4696 |
| **7** | 21 | 152.4 | 21 | 152.13 | 0.9955 | 21 | 169.24 | 0.9638 | 23 | 149.96 | 0.8584 |
| **8** | 15 | 51.52 | 15 | 49.881 | 0.9987 | 16 | 44.838 | 0.9799 | 21 | 54.308 | 0.3476 |

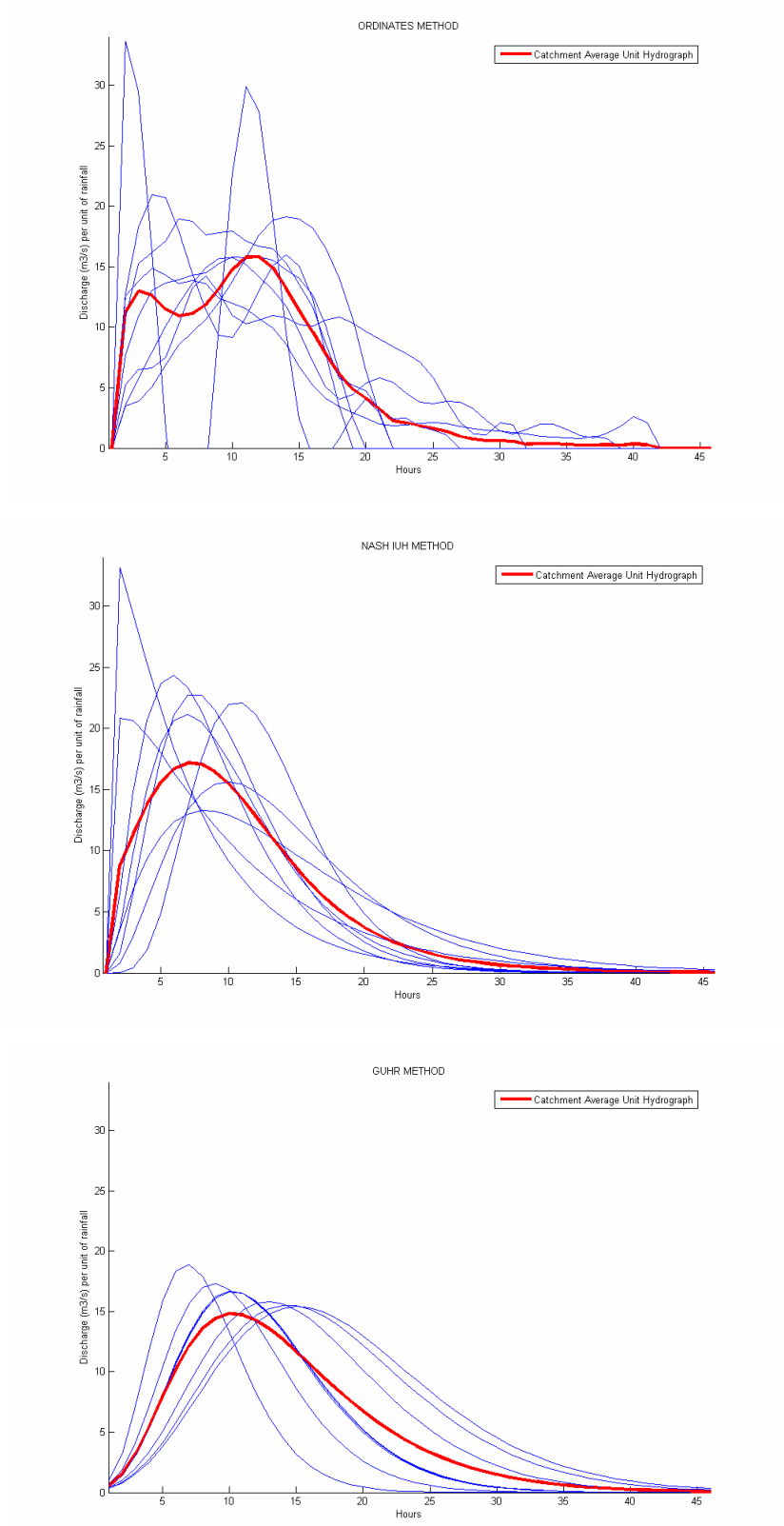


**Figure 6.21 Averaging the Unit Hydrograph with the 3 different methods - Dromcummer**

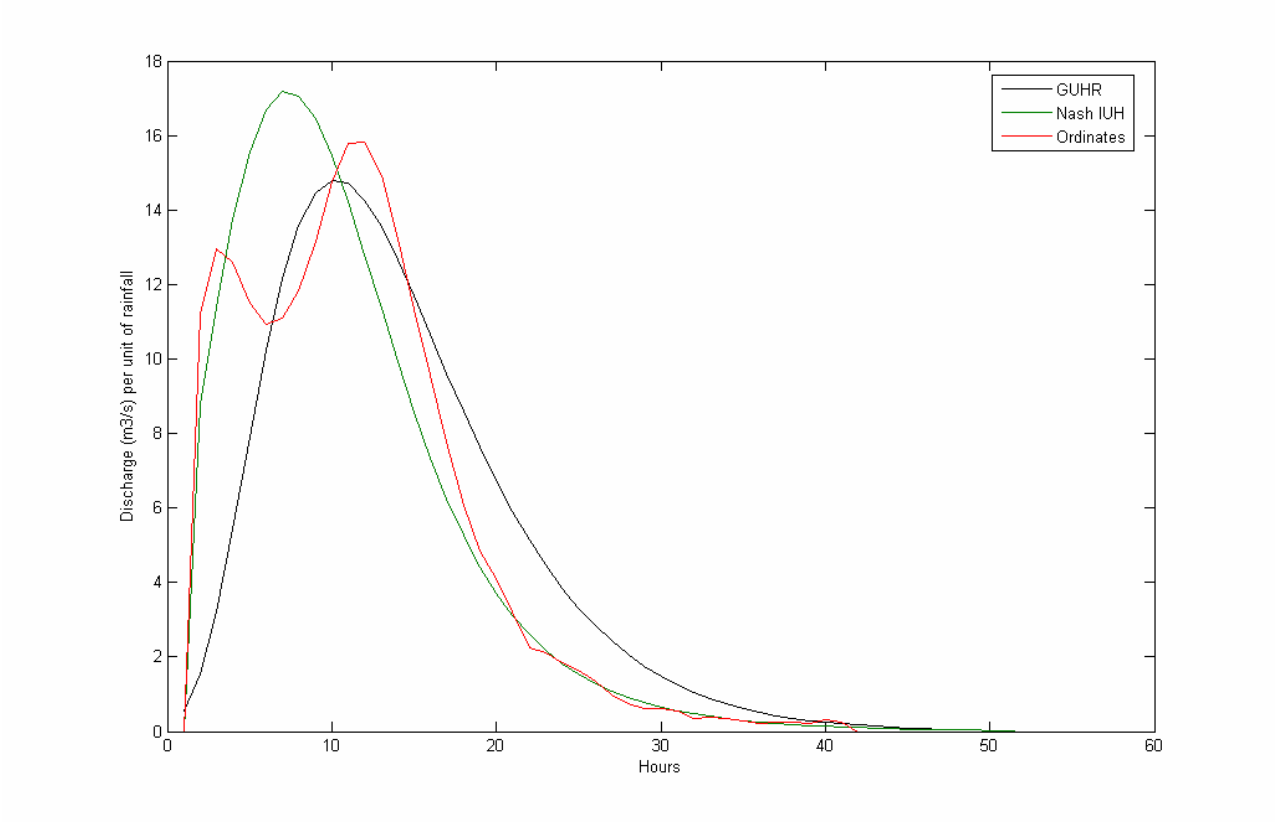


**Figure 6.22 3 Unit Hydrographs in Dromcummer**

### 6.6.4.3 Killavullen

Table 6.10 lists the 8 floods used to derive the UH in Killavulen, with the corresponding rain event characteristics, flow response and volumes.

**Table 6-10 events selection in Killavulen – CAUH derivation**

| Events | Date | Rainfall duration (hours) | Peak discharge (m3/s) | Rainfall volume (mm) | Direct runoff volume (mm) | Percentage Runoff |
|---|---|---|---|---|---|---|
| **1** | 12-Oct-88 | 17 | 302.5 | 74.8 | 14.6 | 0.195 |
| **2** | 22-Oct-88 | 19 | 437.4 | 55.8 | 21.7 | 0.388 |
| **3** | 23-Feb-95 | 14 | 302.6 | 63.3 | 8.6 | 0.136 |
| **4** | 29-Oct-96 | 12 | 223.7 | 71.4 | 6.0 | 0.084 |
| **5** | 18-Nov-97 | 22 | 336.9 | 70.5 | 13.7 | 0.195 |
| **6** | 5-Nov-99 | 25 | 218.9 | 42.3 | 10.1 | 0.239 |
| **7** | 22-Dec-99 | 16 | 290.7 | 86.9 | 10.1 | 0.116 |
| **8** | 01-Ded-00 | 17 | 357.7 | 108.4 | 12.9 | 0.119 |

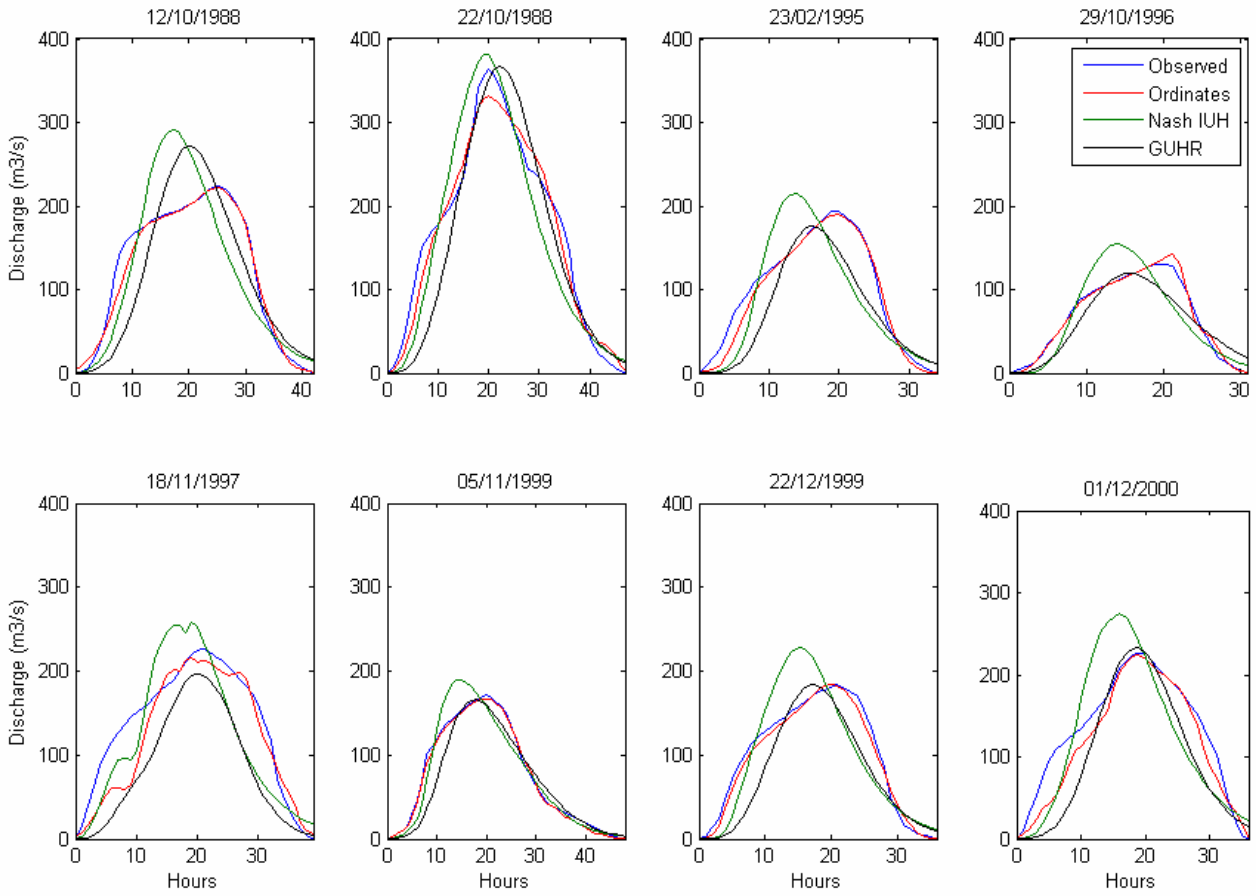


**Figure 6.23 Observed and simulated direct runoff hydrographs in Killavulen – CAUH derivation**

Figure 6.23 shows the application of the three different methods, in comparison with the observed direct runoff flow. Calculated and observed values are compared in table 6.11 which also gives NSE values for each event.

**Table 6-11 Time to peak, Peak discharge and NSE for the 8 events - Killavullen**

| Events | Observed | | Ordinates | | | IUH | | | GUHR | | |
|---|---|---|---|---|---|---|---|---|---|---|---|
| | Time to peak (hours) | Peak Discharge (m3/s) | Time to peak (hours) | Peak Discharge (m3/s) | E | Time to peak (hours) | Peak Discharge (m3/s) | E | Time to peak (hours) | Peak Discharge (m3/s) | E |
| **1** | **26** | **223.04** | **26** | **222.12** | **0.9812** | **18** | **290.68** | **0.6013** | **21** | **271.48** | **0.6799** |
| **2** | **21** | **363.67** | **21** | **331.22** | **0.9727** | **20** | **380.82** | **0.8580** | **23** | **366.54** | **0.8473** |
| **3** | **20** | **193.95** | **21** | **189.45** | **0.9747** | **15** | **214.34** | **0.5605** | **17** | **175.87** | **0.6688** |
| **4** | **21** | **130.72** | **22** | **141.77** | **0.9876** | **15** | **154.89** | **0.7251** | **16** | **118.94** | **0.8408** |
| **5** | **22** | **226.18** | **20** | **216.01** | **0.8313** | **20** | **257.91** | **0.6172** | **21** | **196.69** | **0.3543** |
| **6** | **21** | **171.26** | **21** | **166.9** | **0.9963** | **15** | **189.17** | **0.9193** | **19** | **165.91** | **0.8933** |
| **7** | **22** | **183.92** | **21** | **184.34** | **0.9868** | **16** | **227.85** | **0.6531** | **18** | **183.66** | **0.7251** |
| **8** | **20** | **226.69** | **20** | **223.48** | **0.9025** | **17** | **274.12** | **0.5067** | **20** | **232.52** | **0.5985** |

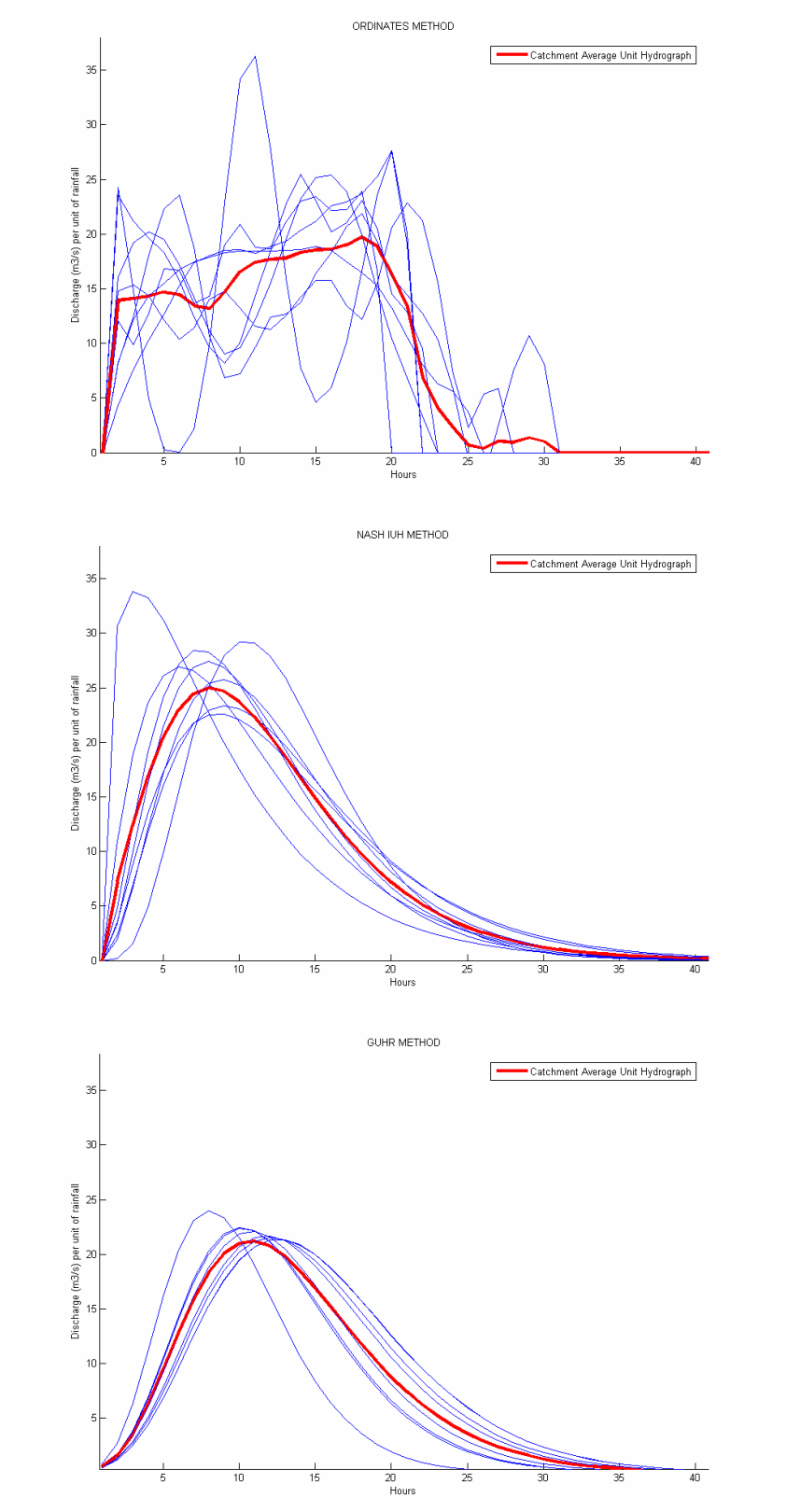


**Figure 6.24 3 Unit Hydrographs in Killavulen**

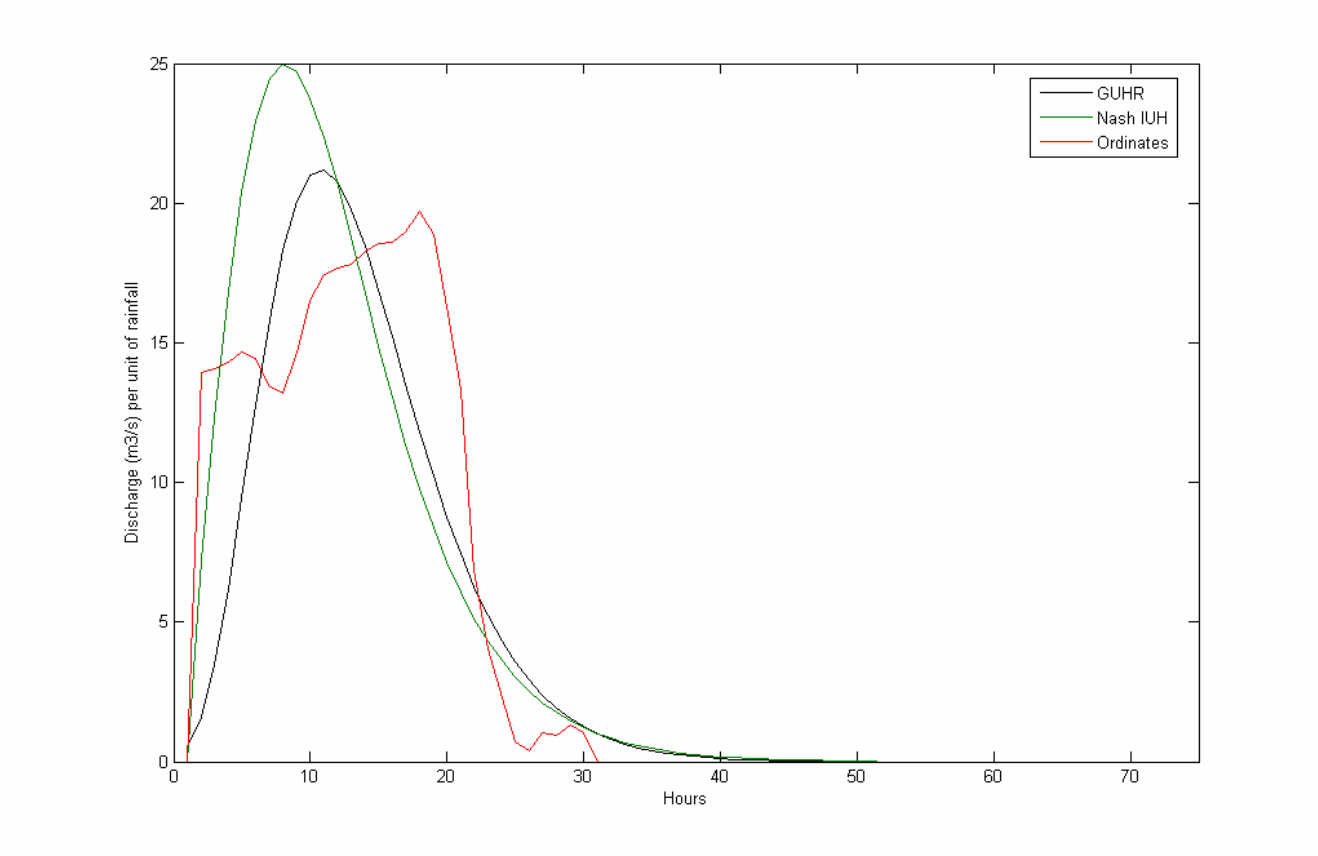


**Figure 6.25 3 Unit Hydrographs in Killavulen**

### 6.6.4.4 Interpretation of the results

Averaged NSE values (see table 6.12) show that the calculated direct runoff flow time series obtained with the Ordinates Method (OM) give more accurate results than with the Nash IUH or the GUHR. This is due to the fact that this method only uses the matrix inversion coupled with data exploitation, and the UH construction is undertaken with the objective that its convolution with the effective rainfall hyetograph will lead to the exact observed time series. The slight error comes from the UH smoothing process and the NSE value would be 1 if this step was not applied. On the other hand, this good agreement between the calculated and the observed time series is not necessarily an advantage as the method produces poorly shaped unit hydrographs (showing oscillation or negative values even after the smoothing process, see figure 6.18 for example) that reflects the unrealistic nature of the solution.

**Table 6-12 Average NSE values for the CAUH derivation phase**

| | Ordinates | Nash IUH | GUHR |
|---|---|---|---|
| **Duarrigle** | 0.9529 | 0.9224 | 0.8695 |
| **Dromcummer** | 0.9753 | 0.869 | 0.6196 |
| **Killavulen** | 0.9541 | 0.6801 | 0.701 |

The two other methods based on cascade of reservoirs leads to lower NSE but produces well shaped UHs, with only slight differences between the different events (see figure 6.18 for example), which is not the case with the Ordinates Method. The averaging process is therefore more justifiable than in this first method. The NSE indicator results show that the Nash IUH generally gives a greater efficiency indicator than the GUHR.

In each of the 3 sub-catchments, the CAUH obtained with the Nash IUH method has the highest peak value and the shortest time to peak (see table 6.13). The GUHR method produces CAUHs that appear to be between the Nash IUH and the Ordinates Method.

**Table 6-13 Peak value and time to peak for the CAUH**

| | Ordinates | | Nash IUH | | GUHR | |
|---|---|---|---|---|---|---|
| | Peak value (m3/s per unit of rainfall) | Time to peak (hours) | Peak value (m3/s per unit of rainfall) | Time to peak (hours) | Peak value (m3/s per unit of rainfall) | Time to peak (hours) |
| **Duarrigle** | 7.68 | 5 | 9.14 | 4 | 6.75 | 5 |
| **Dromcummer** | 15.81 | 12 | 17.17 | 7 | 14.8 | 10 |
| **Killavullen** | 19.72 | 18 | 24.97 | 8 | 21.18 | 11 |

In order to compare the different calculated UHs on a same scale, hydrographs were expressed in flow per unit of draining area. To do so, UHs were divided by the corresponding catchment area in $km^2$. Normalized average UHs are shown in figure 6.26, for each of the three UH derivation methods.

It can be seen that the Duarrigle UH always has a significantly higher peak than the two other stations. It can also be noted that its time to peak is smaller, and that its shape is steeper. When important precipitations occur, the river flow in Duarrigle will respond quicker than in the downstream stations, by rising quickly up to a high value, but lowering to its normal flow at a same fast rate. This response type is explained by the size of the river before Duarrigle. The river is indeed rising only 20 kilometres upstream and behaves more as a stream than a river up to this point. With a narrow river channel (in both width and depth), and a smaller catchment area, the contributing runoffs have higher intensities and flow is more quickly risen up.

A high likeness is observable between Dromcummer and Killavulen UHs, for each of the three methods. Even if the UH is a bit steeper (higher peak value and lower time to peak) in Dromcummer, it seems that river flow have a similar response type to precipitation in the two stations. The difference between Duarrigle and the two other stations is due to the flood wave attenuation which only significantly applies to Dromcummer and Killavulen.

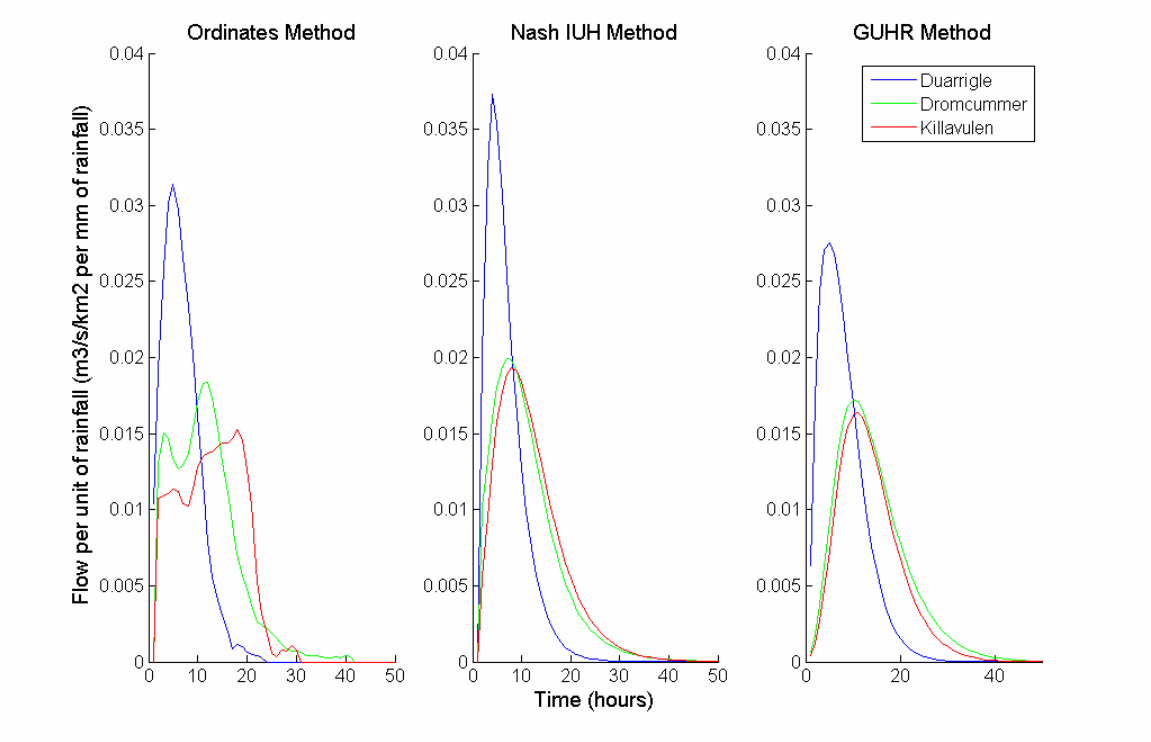


**Figure 6.26 Comparison of the normalized average unit hydrographs**

## 6.6.5 Application to other floods: simulation

The derived UHs are applied to flood events (both simple and multiple peak events) in the three different sub-catchments. Events are selected for their high peak flows and also to reflect the heterogeneity of the sub-catchment.

The NSE indicator is calculated for each simulation, as well as the linear regression coefficient in order to observe the level of agreement between calculated and observed flow peaks, which is the most important criteria in flood hydrograph prediction.

### 6.6.5.1 Duarrigle

Table 6.14 lists the 12 floods used to test the computed average UHs in Duarrigle, with the corresponding rain event characteristics, flow response and volumes.

**Table 6-14 Storm events selection in Duarrigle – Simulation**

| Events | Date | rainfall duration (hours) | peak discharge (m3/s) | rainfall volume | direct runoff volume | PR |
|---|---|---|---|---|---|---|
| **1** | 22-Jan-05 | 18 | 104.5 | 41.5 | 19.6 | 0.471 |
| **2** | 12-Feb-05 | 63 | 125.4 | 73.2 | 37.6 | 0.514 |
| **3** | 30-Mar-05 | 9 | 21.1 | 11.6 | 2.9 | 0.253 |
| **4** | 6-Apr-05 | 47 | 38.5 | 43.0 | 13.5 | 0.314 |
| **5** | 17-Apr-05 | 16 | 35.8 | 29.7 | 4.1 | 0.140 |
| **6** | 28-Apr-05 | 14 | 37.9 | 28.7 | 4.5 | 0.158 |
| **7** | 27-May-05 | 36 | 56.5 | 59.9 | 18.9 | 0.316 |
| **8** | 24-Jul-05 | 18 | 40.5 | 48.1 | 5.2 | 0.109 |
| **9** | 2-Dec-05 | 12 | 133.3 | 56.6 | 16.6 | 0.294 |
| **10** | 13-Jan-06 | 19 | 122.3 | 56.6 | 22.1 | 0.390 |
| **11** | 19-Apr-06 | 19 | 28.8 | 22.0 | 4.5 | 0.207 |
| **12** | 22-May-06 | 20 | 104.1 | 64.2 | 20.4 | 0.318 |

Table 6.15 and figure 6.27 gives a comparison between observed and calculated values, regarding to the three methods. Times to peak and peak values are calculated as well as NSE indicator.

**Table 6-15 Time to peak, Peak discharge and NSE for the 12 simulated events - Duarrigle**

| | Observed | | Ordinates | | | Nash IUH | | | GUHR | | |
|---|---|---|---|---|---|---|---|---|---|---|---|
| Events | Time to peak (hours) | Peak Discharge (m3/s) | Time to peak (hours) | Peak Discharge (m3/s) | E | Time to peak (hours) | Peak Discharge (m3/s) | E | Time to peak (hours) | Peak Discharge (m3/s) | E |
| **1** | 18 | 87.937 | 16 | 88.153 | 0.98244 | 16 | 91.715 | 0.97042 | 17 | 85.302 | 0.95471 |
| **2** | 52 | 110.68 | 55 | 83.774 | 0.56254 | 54 | 90.712 | 0.58758 | 55 | 80.532 | 0.49418 |
| **3** | 8 | 16.909 | 10 | 19.036 | 0.80999 | 10 | 20.541 | 0.80591 | 10 | 17.592 | 0.81021 |
| **4** | 8 | 33.1 | 13 | 32.054 | 0.61932 | 14 | 33.112 | 0.63019 | 14 | 30.884 | 0.54122 |
| **5** | 10 | 29.665 | 10 | 22.677 | 0.91298 | 9 | 23.468 | 0.93491 | 11 | 21.022 | 0.83361 |
| **6** | 11 | 32.446 | 10 | 23.966 | 0.89439 | 9 | 24.636 | 0.8822 | 11 | 22.31 | 0.87744 |
| **7** | 14 | 51.011 | 13 | 57.417 | 0.89098 | 13 | 58.454 | 0.89166 | 13 | 54.419 | 0.87784 |
| **8** | 16 | 36.6 | 14 | 26.855 | 0.70372 | 14 | 27.933 | 0.68615 | 14 | 25.558 | 0.78123 |
| **9** | 11 | 117.44 | 10 | 105.36 | 0.95826 | 10 | 113.87 | 0.94115 | 11 | 96.927 | 0.91645 |
| **10** | 14 | 104.07 | 17 | 100.85 | 0.8334 | 17 | 104.69 | 0.83236 | 17 | 99.216 | 0.75055 |
| **11** | 12 | 23.278 | 11 | 19.276 | 0.81724 | 11 | 20.151 | 0.8007 | 11 | 17.989 | 0.85759 |
| **12** | 15 | 93.839 | 14 | 90.441 | 0.73764 | 14 | 90.875 | 0.72961 | 18 | 86.899 | 0.61679 |

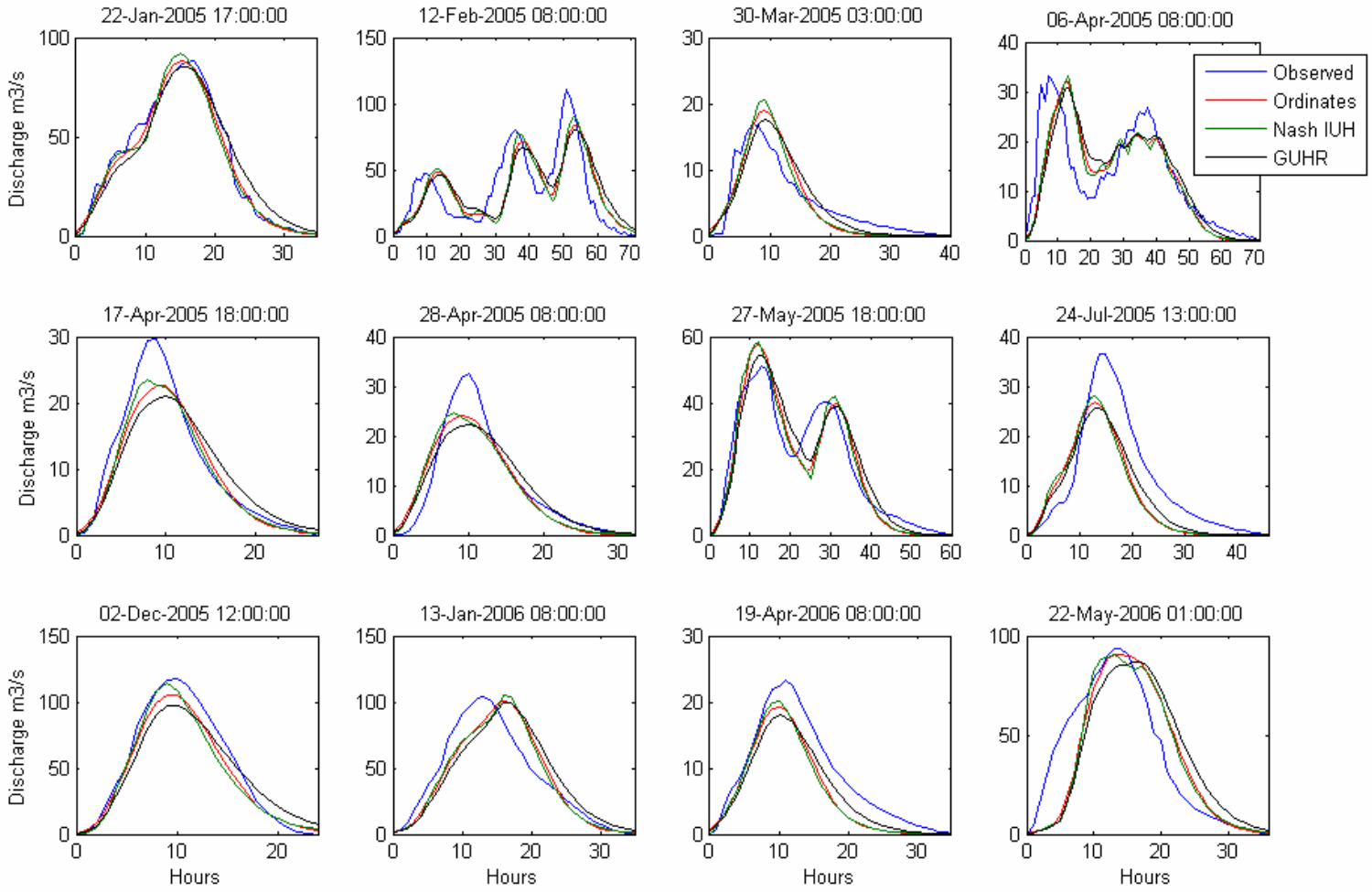


**Figure 6.27 Observed and simulated flow in Duarrigle**

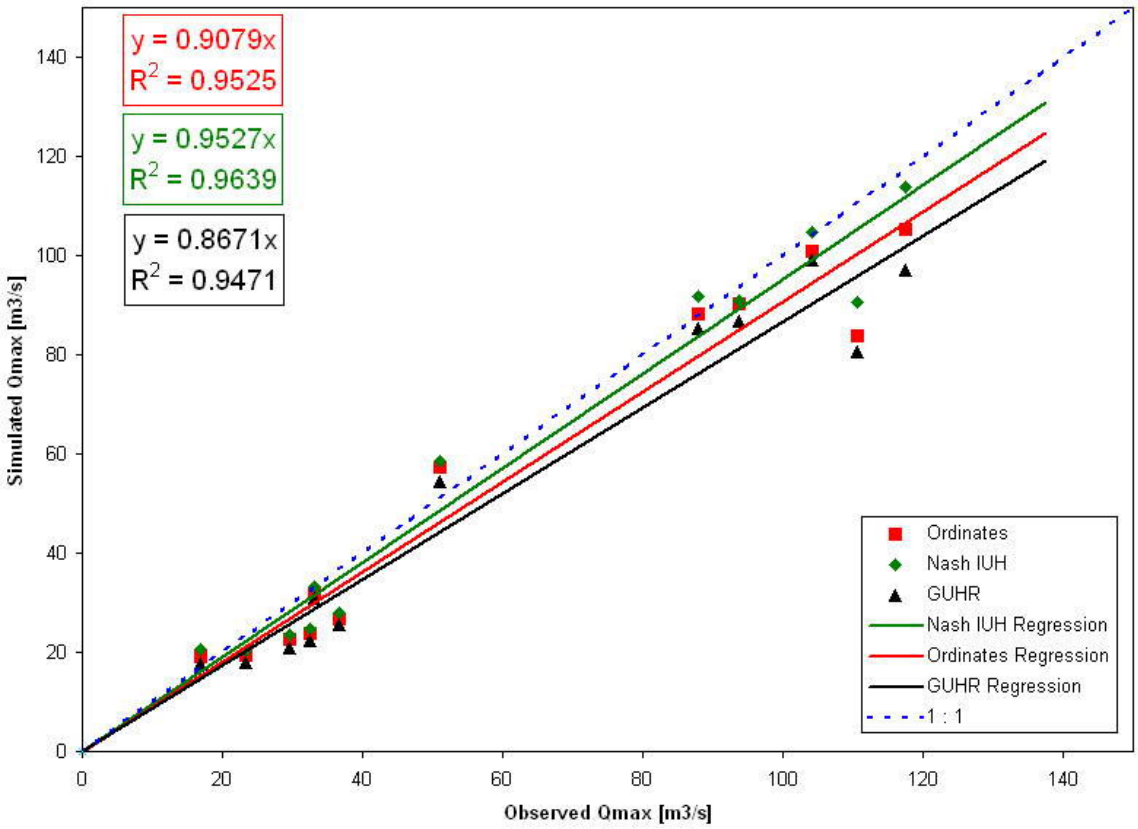


**Figure 6.28 Simulated and observed peak discharge (direct runoff) – Duarrigle**

A rapid graphic analysis of figure 6.27 tells us that the application of the 3 CAUH gives really good results for a range of floods events.

The convolution of multi-peaks events (events 2, 4 and 7) also shows good agreement between the calculated and observed even if the two lowest values of NSE, are obtained for the events 2 and 4 (see table 6.15). The results obtained for the flood event 2 are good both in hydrograph shape and peak value but shifted in time, which leads to the low NSE value. The peak height prediction is nevertheless still acceptable.

In each of the 12 events, the highest calculated direct runoff flow is obtained with the Nash IUH, followed by the GUHR and eventually the ordinates method UH. The linear regression applied to the relationship between the observed and calculated peak flows (figure 6.28) gives the best $R^2$ (0.9639) to the Nash IUH, followed by the ordinates UH (0.9525) and eventually the GUHR (0.9471). The average NSE for the 12 events put the ordinates first (0.8012), almost equaled by the Nash IUH (0.8077), both before the GUHR (0.7759).

### 6.6.5.2 Dromcummer

Table 6.16 lists the 12 floods used to test the computed average UHs in Dromcummer, with the corresponding rain event characteristics, flow response and volumes.

**Table 6-16 Storm events selection in Dromcummer – Simulation**

| Events | Date | rainfall duration (hours) | peak discharge (m3/s) | rainfall volume (mm) | direct runoff volume (mm) | PR |
|---|---|---|---|---|---|---|
| **1** | 22-Jan-05 | 19 | 196.8 | 20.5 | 11.7 | 0.570 |
| **2** | 18-Apr-05 | 17 | 41.9 | 27.2 | 2.4 | 0.090 |
| **3** | 2-Dec-05 | 12 | 228.7 | 52.4 | 10.9 | 0.207 |
| **4** | 12-Feb-05 | 60 | 176.3 | 50.9 | 20.1 | 0.394 |
| **5** | 30-Mar-05 | 10 | 30.4 | 11.0 | 1.4 | 0.126 |
| **6** | 7-Apr-05 | 53 | 65.9 | 34.7 | 8.7 | 0.250 |
| **7** | 28-Apr-05 | 16 | 61.2 | 30.3 | 3.9 | 0.128 |
| **8** | 28-May-05 | 40 | 76.2 | 57.7 | 9.8 | 0.171 |
| **9** | 24-Jul-05 | 21 | 76.5 | 50.1 | 5.1 | 0.102 |
| **10** | 13-Jan-06 | 20 | 243.9 | 56.7 | 18.2 | 0.321 |
| **11** | 19-Apr-06 | 19 | 34.6 | 16.3 | 1.5 | 0.093 |
| **12** | 22-May-06 | 20 | 220.8 | 61.3 | 12.6 | 0.206 |

Table 6.17 and figure 6.29 gives a comparison between observed and calculated values, regarding to the three methods. Times to peak and peak values are calculated as well as NSE indicator.

**Table 6-17 Time to peak, Peak discharge and NSE for the 12 simulated events, Dromcummer**

| | Observed | | Ordinates | | | Nash IUH | | | GUHR | | |
|---|---|---|---|---|---|---|---|---|---|---|---|
| Events | Time to peak (hours) | Peak Discharge (m3/s) | Time to peak (hours) | Peak Discharge (m3/s) | E | Time to peak (hours) | Peak Discharge (m3/s) | E | Time to peak (hours) | Peak Discharge (m3/s) | E |
| **1** | 20 | 151.2 | 19 | 132.3 | 0.9054 | 19 | 145.0 | 0.8476 | 21 | 133.6 | 0.8832 |
| **2** | 25 | 30.3 | 19 | 32.7 | 0.4362 | 17 | 36.2 | 0.1221 | 20 | 31.9 | 0.7613 |
| **3** | 10 | 180.7 | 16 | 156.3 | 0.7010 | 12 | 174.2 | 0.8108 | 15 | 151.8 | 0.2070 |
| **4** | 58 | 152.6 | 56 | 100.9 | 0.7637 | 58 | 115.1 | 0.7961 | 61 | 107.6 | 0.7143 |
| **5** | 13 | 24.1 | 17 | 19.1 | 0.8854 | 13 | 21.8 | 0.9168 | 16 | 19.0 | 0.8757 |
| **6** | 41 | 54.9 | 18 | 52.4 | 0.7680 | 15 | 56.8 | 0.7601 | 18 | 50.7 | 0.7995 |
| **7** | 15 | 51.4 | 15 | 51.7 | 0.9351 | 14 | 54.0 | 0.8922 | 17 | 48.4 | 0.9441 |
| **8** | 32 | 66.1 | 19 | 80.2 | 0.8217 | 16 | 83.4 | 0.7600 | 20 | 75.4 | 0.9344 |
| **9** | 21 | 74.1 | 21 | 63.9 | 0.9017 | 18 | 70.4 | 0.8805 | 21 | 63.0 | 0.8651 |
| **10** | 17 | 204.2 | 18 | 227.3 | 0.8713 | 19 | 243.9 | 0.9110 | 22 | 219.4 | 0.6487 |
| **11** | 14 | 25.5 | 18 | 17.9 | 0.4717 | 19 | 20.2 | 0.5643 | 22 | 18.2 | 0.1212 |
| **12** | 16 | 185.3 | 19 | 166.1 | 0.6066 | 17 | 168.3 | 0.7421 | 20 | 151.9 | 0.1496 |

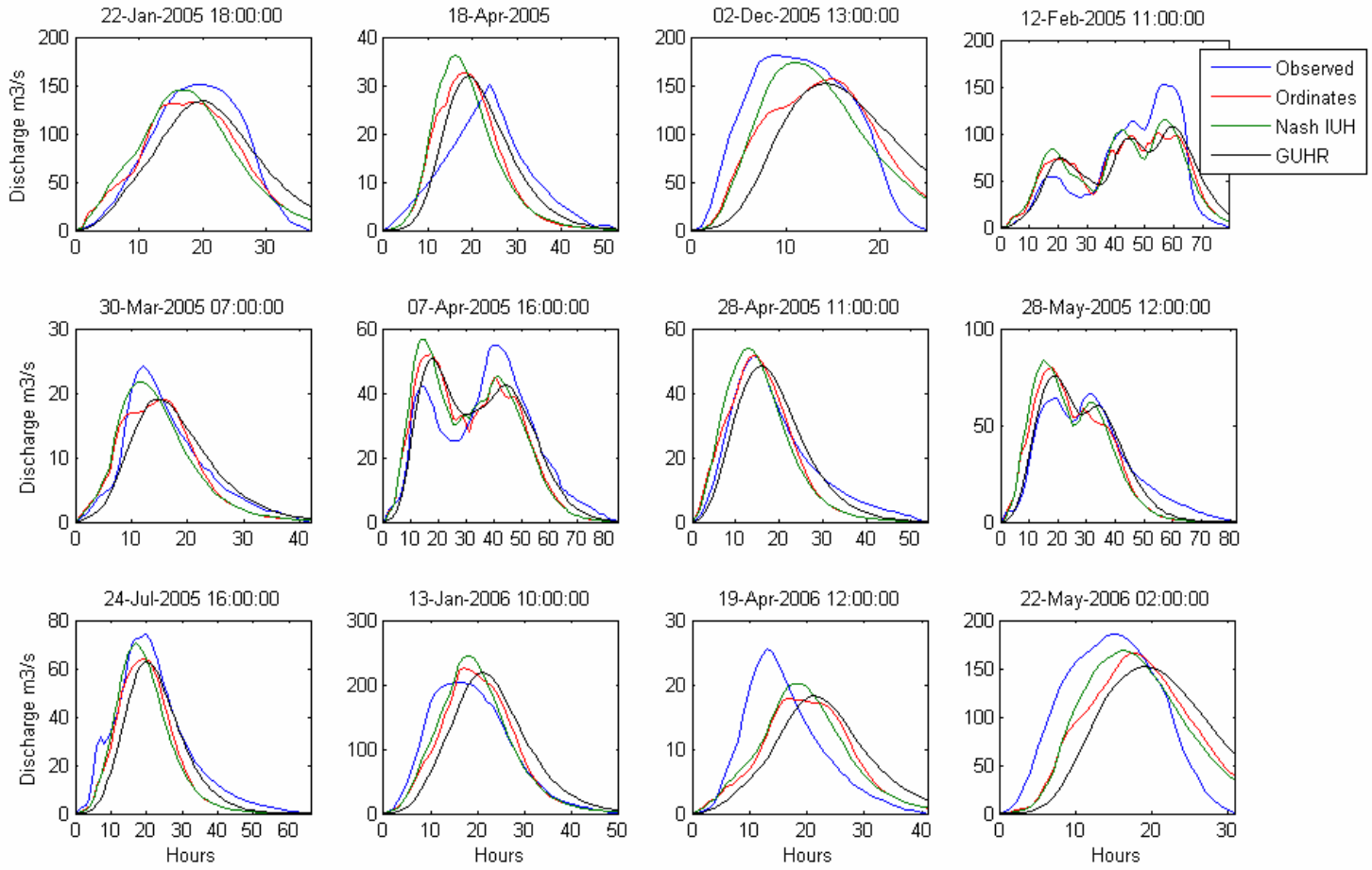


**Figure 6.29 Observed and simulated flow in Dromcummer**

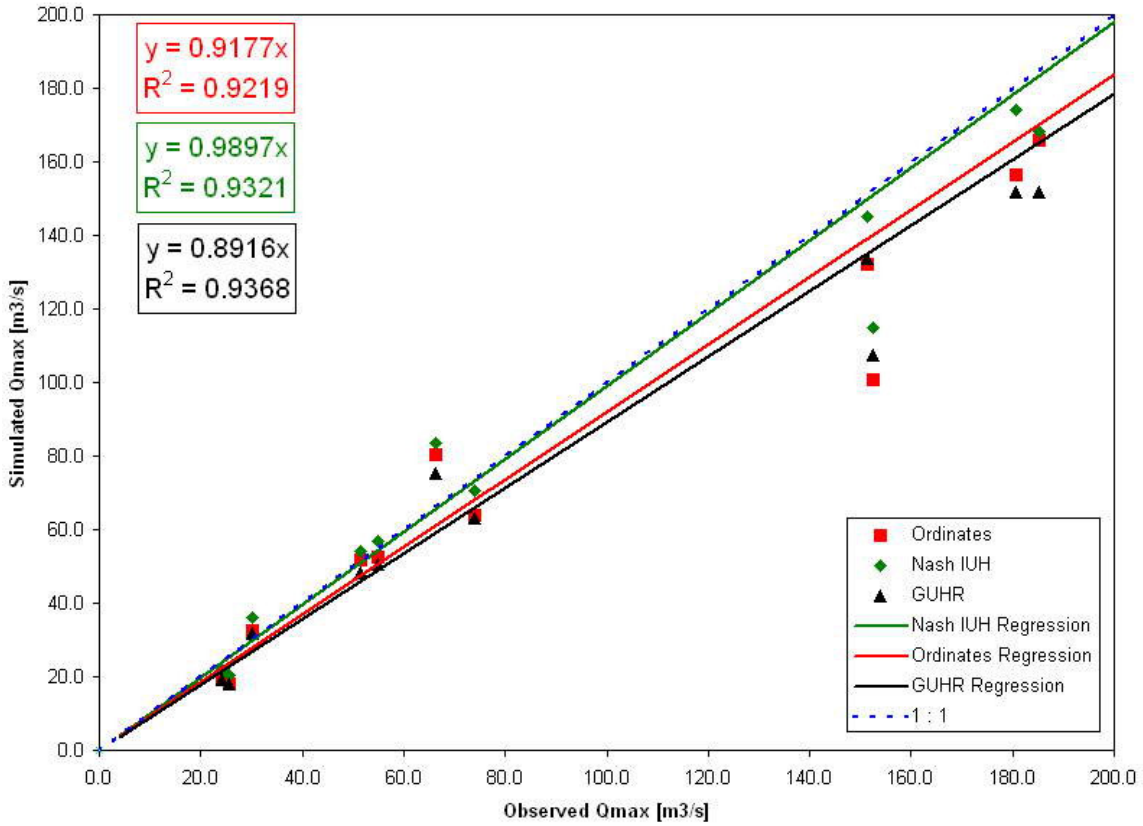


**Figure 6.30 Simulated and observed peak discharge (direct runoff) - Dromcummer**

The difference in derived CAUH is reflected in the three different simulations as the Nash always produces the highest peak with the lowest time to peak.

The difference in shape in the events 2 (figure 6.29) is likely to be caused from a bad quality flow data (interpolation for example) more than by the application of the UH convolution.

Events 3 and 12 (figure 6.29) show very low NSE values because of the fact that the recession limb of the simulated hydrographs are not steep enough. Even if underestimating, the calculated peak flow values are nonetheless acceptable with Nash IUH (respectively 96% and 90% of the observed values).

The low slope coefficient (0.8916) of the linear regression (figure 6.30) for the GUHR reflects the general underestimation produced by the application of this UH.

### 6.6.5.3 Killavullen

Table 6.18 lists the 12 floods used to test the computed average UHs in Duarrigle, with the corresponding rain event characteristics, flow response and volumes.

**Table 6-18 Storm events selection in Killavulen – Simulation**

| Events | Date | rainfall duration (hours) | peak discharge (m3/s) | rainfall volume (mm) | direct runoff volume (mm) | PR |
|---|---|---|---|---|---|---|
| **1** | 23-Jan-05 | 18.8 | 235.59 | 17.2 | 8.6 | 0.499 |
| **2** | 12-Feb-05 | 57.8 | 199.2 | 47.0 | 15.6 | 0.331 |
| **3** | 22-Mar-05 | 38.8 | 98.691 | 31.0 | 4.1 | 0.132 |
| **4** | 7-Apr-05 | 52.8 | 106.5 | 32.8 | 6.0 | 0.184 |
| **5** | 18-Apr-05 | 47.8 | 91.291 | 27.7 | 3.2 | 0.118 |
| **6** | 28-May-05 | 33.8 | 112.34 | 57.4 | 7.4 | 0.129 |
| **7** | 24-Jul-05 | 22.8 | 124.01 | 47.2 | 3.6 | 0.076 |
| **8** | 10-Sep-05 | 27.8 | 64.635 | 24 | 2.5 | 0.103 |
| **9** | 24-Oct-05 | 50.8 | 188.97 | 35.4 | 9.5 | 0.268 |
| **10** | 30-Oct-05 | 63.8 | 248.31 | 41.5 | 17.2 | 0.415 |
| **11** | 3-Nov-05 | 77.8 | 261.65 | 61.9 | 18.3 | 0.296 |
| **12** | 1-Jan-06 | 15.8 | 215.51 | 40.2 | 6.2 | 0.155 |

Table 6.19 and figure 6.31 gives a comparison between observed and calculated values, regarding to the three methods. Times to peak and peak values are calculated as well as NSE indicator.

**Table 6-19 Time to peak, Peak discharge and NSE for the 12 simulated events - Killavulen**

| | Observed | | Ordinates | | | Nash IUH | | | GUHR | | |
|---|---|---|---|---|---|---|---|---|---|---|---|
| Events | Time to peak (hours) | Peak Discharge (m3/s) | Time to peak (hours) | Peak Discharge (m3/s) | E | Time to peak (hours) | Peak Discharge (m3/s) | E | Time to peak (hours) | Peak Discharge (m3/s) | E |
| **1** | 26 | 150.6 | 21 | 143.9 | 0.9251 | 19 | 157.1 | 0.7600 | 21 | 134.9 | 0.8514 |
| **2** | 55 | 147.4 | 53 | 131.28 | 0.6300 | 57 | 130.0 | 0.7284 | 59 | 108.5 | 0.5336 |
| **3** | 13 | 66.4 | 22 | 65.216 | 0.7867 | 14 | 64.3 | 0.9506 | 17 | 55.6 | 0.7538 |
| **4** | 37 | 70.5 | 22 | 51.971 | 0.1931 | 16 | 58.4 | 0.4133 | 19 | 50.1 | 0.1094 |
| **5** | 16 | 62.2 | 25 | 48.205 | 0.4606 | 19 | 58.6 | 0.7251 | 21 | 49.8 | 0.3907 |
| **6** | 12 | 92.6 | 23 | 89.185 | 0.6045 | 17 | 93.7 | 0.6857 | 20 | 81.4 | 0.4399 |
| **7** | 19 | 104 | 23 | 62.475 | 0.7154 | 19 | 72.0 | 0.8581 | 21 | 61.8 | 0.6849 |
| **8** | 19 | 50.2 | 22 | 34.001 | 0.6497 | 27 | 32.0 | 0.6645 | 29 | 26.7 | 0.5432 |
| **9** | 19 | 129.9 | 23 | 116 | 0.8072 | 18 | 127.1 | 0.9709 | 20 | 109.4 | 0.7926 |
| **10** | 23 | 174.3 | 28 | 198.04 | 0.6890 | 20 | 182.8 | 0.8021 | 22 | 158.2 | 0.6062 |
| **11** | 41 | 158.1 | 38 | 142.7 | 0.7404 | 32 | 155.3 | 0.6342 | 34 | 132.8 | 0.6787 |
| **12** | 16 | 148.9 | 21 | 112.22 | 0.6333 | 15 | 132.9 | 0.9158 | 18 | 113.5 | 0.6233 |

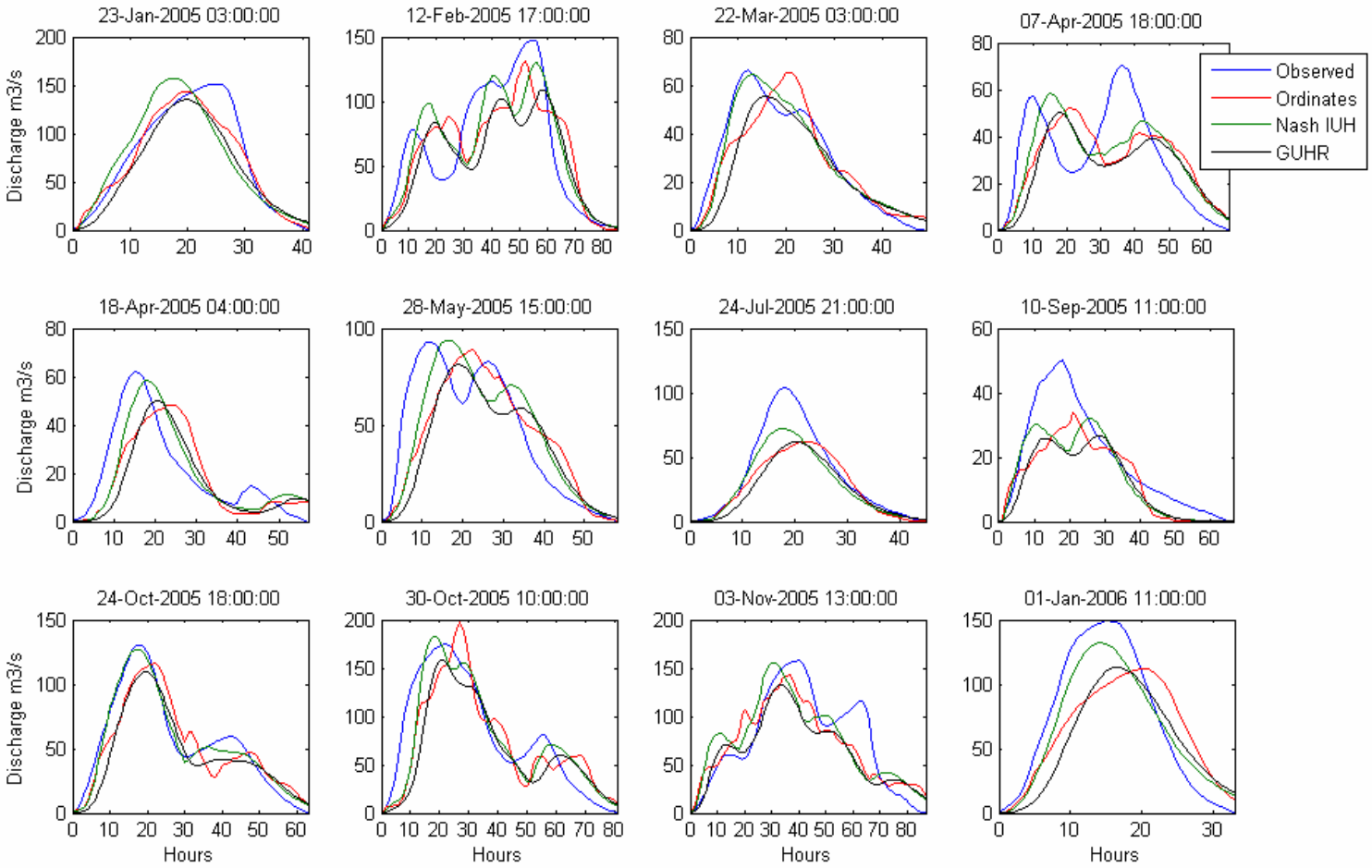


**Figure 6.31 Observed and simulated flow in Killavulen**

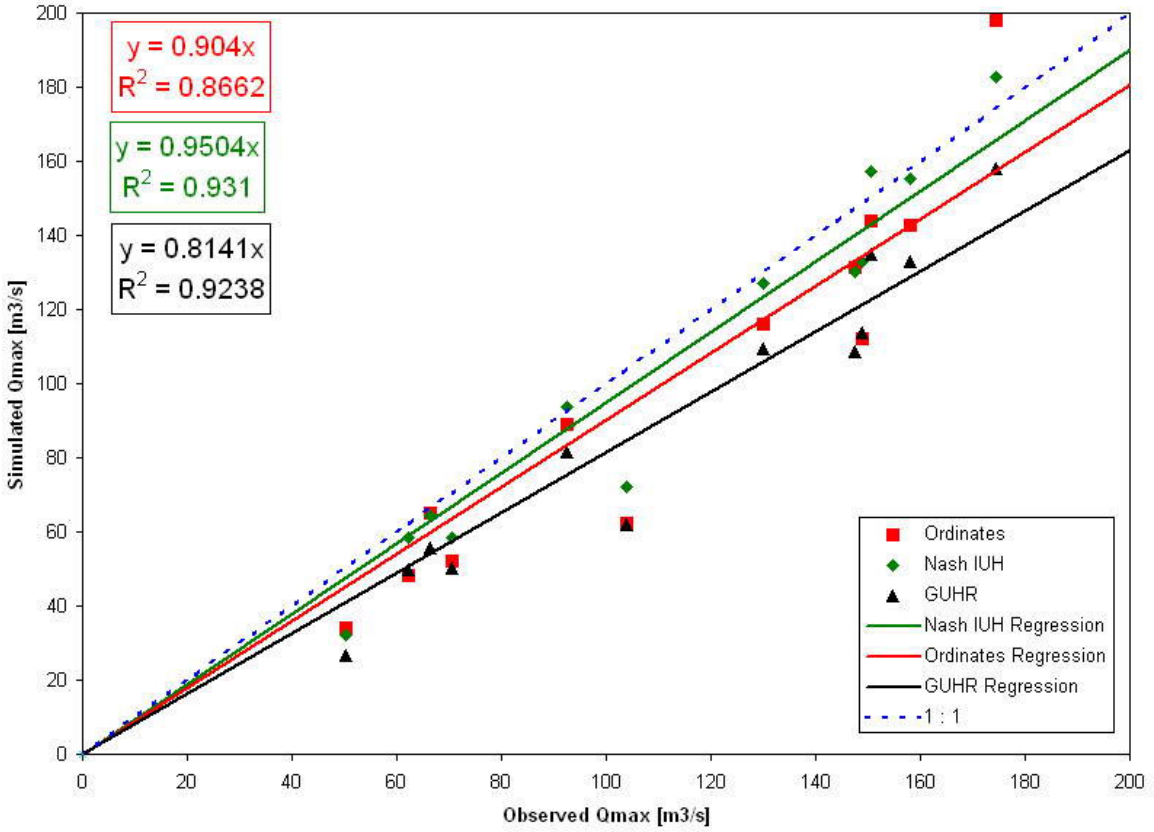


**Figure 6.32 Simulated and observed peak discharge (direct runoff) - Killavulen**

A rapid graphic analysis of the results for the Killavulen sub-catchments shows that the results are not as good as in the two first sub-catchments, which is also confirmed with the lower average NSE values (respectively 0.6529, 0.7591 and 0.5840 for the ordinates UH, the Nash IUH and the GUHR).

The second peak in the event 4 is largely underestimated with the three different models. Events 8 simulations produce truncated direct runoff hydrographs, with bad results near the peaks but still acceptable values on the two limbs. In most of the events, the times to peak are badly simulated (see table 6.19).

### 6.6.5.4 Interpretation of the results

The application of the CAUHs to the three nested sub-catchments shows generally good agreement between it observed and modelled flow time series. Looking to the calculated NSE values, it appears that the results are best for Duarrigle, good for Dromcummer and least accurate for Killavulen (where average NSE values are respectively 0.7980, 0.7215 and 0.6654). The accuracy of prediction decreases as the size of the catchment increases. With an average NSE close from 0.8, results in Duarrigle (245 $km^2$ of surface area) are considered as being good, while results in both Dromcummer (861 $km^2$ of surface area) and Killavulen (1292 $km^2$ of surface area) could be seen as reasonable. This tendency is not as obvious in the $R^2$ slope coefficients calculated from the linear regression applied to the relationship between observed and calculated peak flows. It can then be concluded that the increasing error that we observed when moving to higher area catchments mainly comes from the whole hydrograph shape and timing more than from the peak flow value determination. The methods applied are therefore still acceptable for the prediction of peak values.

When zooming to the sub-catchment scale, the same conclusion is made for the three areas: Nash IUH provides the best modelling, followed by the ordinates method and the GUHR. This conclusion comes from both graphical and indicator analysis. NSE values are indeed higher for Nash IUH, which is also the method that produces slope coefficient (for the linear regression) closest from 1 (see figures 1.25, 1.27 and 1.29). The Nash IUH indeed gives higher prediction than the two other methods, which are therefore generally closer from the observed values. The difference between the three CAUHs is more noticeable in Dromcummer (figure 6.29) and in Killavulen (figure 6.31) than in Duarrigle (figure 6.27) where the three convolutions give similar results. The gap is particularly important in Killavulen where the average NSE indicators are respectively 0.7592, 0.6529 and 0.5840 for the Nash IUH, the ordinates method and the GUHR. When results are still considered as being good with the Nash IUH, the two other methods have to low NSE values.

## 6.7 Discussion

In this chapter, 3 different unit hydrograph methods (the ordinate least-squares method, the Nash instantaneous unit hydrograph and the geomorphological unit hydrograph of reservoirs) were applied to three sub-catchments of the Munster Blackwater catchment. In each sub-catchment, three catchment average unit hydrographs (CAUH) were derived from 8 selected flood events and were then applied to 12 other events. In both phases, baseflow and effective rainfall separation were respectively undertaken using the Nash method (in order to have constancy in the procedure) and the decreasing proportional loss method (in order to reflect the time distribution of the effective rainfall).

First applications of the GUHR, which had been developed for its application to small catchments, showed poor results in Duarrigle, Dromcummer and Killavulen. It was decided that the original sub-watershed delineation process was not suitable for large catchments, and a modification was therefore made, in which the different reservoirs characteristics were extracted from the available data. An interesting work would be to test the original GUHR model on a smaller subcatchment (approximately 10 $km^2$) in order to test its applicability to the Blackwater River.

During the CAUH derivation phase, the best fitting results were obtained with the ordinates method, which only uses data exploitation and matrix inversion processes. The two other methods are parameterized (respectively two and one parameters for the Nash IUH and the GUHR). However, it should be noted that the ordinates method produces realistic solutions only when applied to single peak events, and produces a high variability in term of UH shape, which makes the averaging phase more uncertain. The two other methods show constancy in the UH derivation, and can be applied to any kind of flood events. In the three sub-catchments, the CAUH obtained with the Nash IUH method is greater and steeper than the two other.

The simulation phase showed that calculation lead to best results when the sub-catchment area was smaller. Efficiency estimations indicate that results can be considered as being good in Duarrigle, but lower in Dromcummer and Killavulen. From these results, it can be concluded that the general UH theory should not be applied to sub-catchments draining too much important surface area. This conclusion is in agreement with the common belief that the UH theory should not be applied to catchments larger than 500 square kilometres (Shaw, 1994, pp433). The different basic hypotheses made by the unit hydrograph theory are indeed more and more questionable when the size of the studied area is growing. The assumption that the effective rainfall is constant over the catchment and uniformly distributed in time appears to be unfounded for big catchments, hence the low efficiency obtained for Dromcummer and Killavulen. An interesting work would be

to apply the same techniques to smaller sub-catchments within the Duarrigle sub-catchment, in order to observe whether or not the results would be better.

A comparison between the three UH approaches lead to the conclusion that the Nash IUH was the better method to be used. The results indeed showed better correlation between calculated and observed flow time series in comparison with the ordinates and GUHR methods which produced greater underestimations of the peak values. Calculated NSE values and linear regression $R^2$ make the Nash IUH the best predicting method, followed by the ordinates method and the GUHR. This order in efficiency is also noticeable in Dromcummer and Killavulen sub-catchments, where the Nash IUH gives best simulations for both peak flow value and time to peak. A better understanding of the CAUH behaviour would have probably been obtained if the simulation had been calculated for more than 12 storms. Unfortunately, the available 1hour-step data set was not available for a long enough period of time.

Finally, it should be noted that the Ordinates method and the Nash IUF represent opposite ends of the Unit Hydrograph theory spectrum, the former being analysis, the latter synthesis. The Ordinates method is indeed purely based on data exploitation while the Nash IUH, with its Gamma distribution, imposes a particular limited functional form. In the particular case of the Blackwater River, this parametrically economic Gamma distribution proved to lead to creditable results. The modified GUHR method, like the Nash IUH, is following a Gamma distribution, and is therefore creating smoothed, infinite tail hydrographs. It is nevertheless positioned between the two previous techniques, between analysis and synthesis, as its parameters are calculating through a calibration phase that uses rainfall and flow data.

# Chapter 7 Conclusion

## 7.1 Conclusions

With the installation of a 32 tipping bucket raingauges network in the catchment, which provides precise time-scaled information about precipitation, the Munster Blackwater Valley has seen its rainfall survey scheme significantly improved. From the rainfall analysis, the different rainfall patterns and two main trends over the Munster Blackwater catchment were identified. An intensity gradient from West to East was noticeable at all the different observations scales (cumulative, monthly, daily and hourly rainfall). Coupled with this first factor is the impact of elevation, which is clearly linked with higher depths of rainfall. These two relationships describe the rainfall spatial variation, and explain some of the changes in river flows from West to East, where flows per unit of area are lower. A particular meteorological phenomenon, called the orographic effect was also identified as potentially responsible for a particularly wet area in the extreme East of the catchment. The analysis also produced accurate information about the rainfall time variation, and the way rainfall events usually occur.

Particular attention was given to the 2006 rainfall data, when significantly low values were recorded. A drought assessment in comparison with known Irish droughts was undertaken and lead to the conclusion that the 2006 and 1976 droughts were comparable. It was also concluded that 2006 rainfall data should be used in the future as a mean of comparison to determine the importance of a given drought.

In the second part of the thesis, rainfall and river flow data were used as input in a rainfall-runoff model based on different unit hydrograph approaches. The Ordinates method, purely data-analysis-based, the synthetic Nash Instantaneous Unit Hydrograph, and the "in between" Geomorphological Unit Hydrograph of Reservoirs (GUHR) showed good results when applied to excess rainfall volumes. Simulated and observed river flow values were compared for a selection of flood events, in three river stations along the Blackwater River. It was concluded, after looking at efficiency indicators, that the parameterized Gamma distribution of the Nash Instantaneous Unit Hydrograph was the best modelling method. This synthetic method is applicable to a wider range of rain events than the Ordinates Method, and provides better simulation than the GUHR. A difference was also noticeable regarding the size of the sub-catchment, and it appeared that the three Unit Hydrograph approaches lead to better results in Duarrigle, the smallest of the three sub-catchments, where the calculated average Nash-Sutcliffe Efficiency indicator (NSE) was approximately 0.8. Results were still considered reasonable but lower in both Dromcummer (the

intermediary nested sub-catchment) and Killavulen (the largest sub-catchment), with respectively 0.72 and 0.66 as average NSEs.

Even if the Unit Hydrograph is sometimes considered as being a simple rainfall-runoff solution, its application to the Munster Blackwater catchment showed good results in flood hydrographs simulations. Choosing this metric approach to construct direct runoff hydrographs from excess rainfall volumes appeared to be relevant, and suitable to the Blackwater River flow response type. Accordance between calculated and observed values were indeed better than with some more complicated models that have already been applied to this same catchment.

## *7.2 Recommendations for further research*

The different analyses undertaken in this thesis have highlighted different points that should be considered for further research. These recommendations mainly apply to the rainfall analysis, and to the rainfall-runoff modelling effort.

### 7.2.1 Rainfall analysis

- At the time of the writing, rainfall data was only available up to July 2006. As the summer 2006 was a drought period, an interesting piece of research would be to run the drought assessment with some more updated data, and to compare the results with previous drought (e.g. 1976).

- Statistical analysis of monthly, daily and hourly rainfall showed good accordance between observed depths and known probability distributions. It lets us believe that the Blackwater rainfall data could be used as an input for rainfall prediction model. Particular attention could be given to the use of an artificial neural network.

- Finally, the increasing data set of hourly rainfall could be used to explore the rainfall disagregation, from daily or weekly data to smaller increments. If well calibrated, such a work could significantly improve the quality of the different data sources.

### 7.2.2 Rainfall-Runoff modelling

- In the rainfall-runoff modelling, priority was given to rainfall separation and the Unit Hydrograph derivation. The baseflow separation was undertaken with a widely accepted but still simple method. Accuracy would certainly be improved by integrating a precise module for the baseflow element that could take into account the Catchment Wetness

Index, the different infiltration processes and the contribution to the river channel flows from the adjacent saturated soils.

- The application of Geomorphological Unit Hydrograph of Reservoirs, with its original reservoirs delineation process, appeared not to be suitable for large watershed as the one studied in this thesis (245 to 1265 $km^2$). As it was originally developed and successfully tested for a small catchment (4.7 $km^2$, in North Spain), its applicability to the Blackwater catchment should be re-considered with a smaller watershed within the Duarrigle sub-catchment (~ 10 $km^2$).

- The quality of the results quality from simulation with the three unit hydrograph techniques (Ordinates method, Nash IUH and the modified GUHR) appeared to decrease with the size of the sub-catchment. In order to comfort the idea that the Unit Hydrograph will provide better results with smaller drainage areas, the same technique should be applied to smaller nested sub-catchments and the upper threshold of catchment size for unit hydrograph analysis should be delineated.

- For each of the three watersheds, the Catchment Average Unit Hydrographs were derived from 8 events and were then applied to 12 different events for simulation purposes. These numbers were chosen due to the sort dataset of 1-hour rainfall (from January 2005 to July 2006). A better understanding of the application of the catchment unit hydrographs will certainly be obtained if a wider range of events could be studied.

- Finally, the investigation of built-in metric unit hydrograph based rainfall-runoff models should be considered. A particular attention should be given to the IHACRES (Identification of a unit Hydrograph And Component flows from Rainfall, Evaporation and Streamflow data) that promises to give good results for the Munster Blackwater Catchment.

# References

Agirre U., Lopez J.J., Gimena F.N., Goni M., 2005. Application of a unit hydrograph based on subwatershed division and comparison with Nash's instantaneous unit hydrograph, Catena 64(2005), pp 321-332.

Ahmad S., Simonovic S.P., 2005. An artificial neural network model for generating hydrograph from hydro-meteorological parameters, Journal of Hydrology 315 (2005), pp 236-251.

Allen, R.G., Pereira, L.S., Raes, D. and Smith, M. 1998. Crop evapotranspiration. Guidelines for computing crop water requirements. FAO irrigation and drainage paper 56, 227 pages.

Anctil F., Michel C., Perrin C., Andreassian V., 2003, A soil moisture index as an auxiliary ANN input for stream flow forecasting, Journal of Hydrology 286 (2004), pp 155-167

ASCE Task Committee on Application of Artificial Neural Networks in Hydrology, 2000. Artificial Neural Networks in Hydrology. I: Preliminary concepts, Journal of Hydrology (2000), 2, pp 115-123.

ASCE Task Committee on Application of Artificial Neural Networks in Hydrology, 2000. Artificial Neural Networks in Hydrology. II: Hydrologic applications, Journal of Hydrology (2000), 2, pp 124-137.

Bedient P.B., Huber W.C., 1992, Hydrology and Floodplain analysis, 2nd edition, New York, Addison–Wesley Publishing Company.

Beven K.J., 2001, Rainfall-Runoff Modelling, The Primer, John Wiley and Sons, Ltd, Chichester, England, 360pp.

Beven K.J., Kirkby M.J., 1979. A physically based, variable contributing area model of basin hydrology. Hydrological Sciences Bulletin, 24(1), pp 43-69.

Beven K.J., 1984. Infiltration into a class of vertically non-uniform soils. Hydrological Sciences Journal, 29(4), pp 425-434.

Beven K., 1989. Changing ideas in hydrology -- The case of physically-based models. Journal of Hydrology, 105(1-2), pp 157-172.

Boorman D.B, Reed D.W., 1981. Derivation of a catchment average unit hydrograph, report 71, Institute of Hydrology.

Brutsaert W., 2005. Hydrology, an Introduction, Cambridge University Press, pp605.

Cameron D., 2006. An application of the UKCIP02 climate change scenarios to flood estimation by continuous simulation for a gauged catchment in the northeast of Scotland, UK (with uncertainty), Journal of Hydrology, 328, pp 212-226.

Chahinian N., Moussa R., Andrieux P., Voltz M., 2004, Comparison of infiltration models to simulate flood events at the field scale, Journal of Hydrology 306 (2005) pp191-214.

Yen B.C, Lee K.T, 1997. Unit Hydrograph derivation for ungauged Watersheds by Stream-Order Laws, Journal of Hydrologic Engineering 2(1997), pp 1-9.

Chow V.T., Maidment D.R., Mays W., 1988. Applied Hydrology, McGraw-Hill International Editions, Civil Engineering Series.

Corcoran G., 2004. Development and examination of flood warning systems for the Munster Blackwater at Mallow. M.Eng.Sc Thesis, University College Cork, Cork, 145 pp.

Croke B., Cleridou N., Kolovos A., Vardavas I., Papamastorakis J., 2000. Water resources in the desertification-threatened Messara Valley of Crete: estimation of the annual water budget using a rainfall-runoff model, Environmental Modelling and Software 15(2000), pp 387-402.

Croke B., 2006. A technique for deriving an average even unit hydrograph from streamflow – only data for ephemeral quick-flow dominant catchments, Advances in Water Resources 29 (2006), pp 493-502.

Dawson C.W., Abrahart R.J., Shamseldin A.Y., Wilby R.L., 2006. Flood estimation at ungauged sites using artificial neural networks, Journal of Hydrology 319(2006), pp 391-409.

Dooge J.C., 1959. A General Theory of the Unit Hydrograph, Journal of Geophysical Research, 64(2), pp 241-256.

Dufour C., 1995. Analysis of thirty-one years of hourly rainfall at Cork, Ireland, Higher Diploma Thesis, University College of Cork.

Fenton M., Guero P., McKeogh E., Leahy P., Kiely G., 2006. Flood Studies Update Programme, Work Group 3 – Flood Hydrograph Analysis, Work Package 3.2, Flood Event Analysis.

Gallart F., Latron J., Llorens P., Beven K., 2006. Using internal catchment information to reduce the uncertainty of discharge and baseflow predictions, in press, Water Resources.

Gupta V.K., Waymire E., Wang C.T., 1980. A representation of an instantaneous unit hydrograph from geomorphology, Water Resource Research, 16(5), pp 855-862.

Houghton-Carr H., 1999, Restatement and application of the Flood Studies Report rainfall-runoff method, Flood Estimation Handbook Volume 4, Institute of Hydrology.

Ivanov V.Y., Vivoni E.R., Bras R.L., Entekhabi, D., 2004. Preserving high-resolution surface and rainfall data in operational-scale basin hydrology: a fully-distributed physically-based approach. Journal of Hydrology, 298(1-4),pp 80-111.

Jakeman A.J., Littlewood I.G., Whitehead P.G., 1990. Computation of the instantaneous unit hydrograph and identifiable component flows with application to two small upland catchments, Journal of Hydrology, 117, pp 275-300.

Kildore L. J., 1997, Developpement and evaluation of a GIS-based spatially distributed unit hydrograph model, Thesis submitted to the Faculty of the Virginia Polytechnic Institute and State University

Kirkby M.J., 1975. Hydrograph modelling strategies. In: R. Peel, M. Chisholm and P. Hagget (Editors), Processes in Physical and Human Geography. Heinemann, London, pp 69-90.

Kokkonen T.S, Jakeman A.J., 2001. A Comparison of metric and conceptual approaches in rainfall-runoff modeling and its implications, Water Resources Research 37(9), pp 2345-2352.

Krause P., Boyle D.P., Base F., 2005. Comparison of different efficiency criteria for hydrological model assessment, Advances in Geosciences, 5 pp 89-97.

Kumar S.A.R., Sudheer K.P., Jain S. K., Agarwal P.K., 2004. Rainfall-runoff modelling using artificial neural networks: comparison of network types.
*Hydrol. Processes,* 2004**, 19,** No. 6, pp 1277-1291.

Lamb R., Beven K.J., Myrabo S., 1997. Discharge and water table predictions using a generalized TOPMODEL formulation, Hydrological Processes, 11, pp 1145-1168.

Leahy P., Kiely G., Corcoran G., 2006. Minimal input artificial neural networks for flood forecasting, Water Management Journal, in review.

Lee K.L., Chang C.H., 2005. Incorporating subsurface-flow mechanism into geomorphology-based IUH modeling, Journal of Hydrology, 311 (2005), pp 91-105.

Lee K.L., Yen B.C., 1997. Geomorphology and Kinematic-Wave-Based Hydrograph Derivation, Journal of Hydraulic Engineering, 123 (1997), pp 73-80.

Linsley R.K., Kolher M.A., Paulhus J.L.H., 1988. Hydrology for Engineers, SI Metric Edition, McGraw-Hill Book Company.

Lopez J.J., Gimena F.N., Goni M., Agirre U., 2005. Analysis of a unit hydrograph model based on watershed geomorphology represented as a cascade of reservoirs, Agricultural Water Management 77(2005), pp 128-143.

Lopez J.J., Gimena F.N., Goni M., Agirre U., 2005. Application of a unit hydrograph based on subwatershed division and comparison with Nash's instantaneous unit hydrograph, Catena 64 (2005), pp 312-332.

MacCárthaigh M., 1996. An assessment of the 1995 drought : including a comparison with other known drought years, EPA, Wexford.

McCuen R.H., 2004. Hydrologic Analysis and Design, Third Edition, Pearson Prentice Hall Editions.

McCullough W., Pitts W.H., 1943. A logical calculus of the ideas immanent in nervous activity, Bull. Math. Biophys., 1943, 5, pp 115-133.

Nash J.E., 1957. The form of the instantaneous unit hydrograph. Int. Assoc. Sci. Hydrol. 45(3), pp 114-l 21.

Nash J.E., 1960. A unit hydrograph study, with particular reference to British catchments, Proc Inst Civ Eng 17, pp 249-282.

Nash J.E., Sutcliffe J.V., 1970. River flow forecasting through conceptual models, Part I, A discussion of principles, Journal of Hydrology, 10, pp 282-290.

Pedruco P., Indicative flood forecasting in Ireland, 2005. M.Sc Thesis, Imperial College of Science, Technology and Medicine, London, 152 pp.

Rajurka M.P., Kothyari U.C., Chaube U.C., 2004. Modeling of the daily rainfall-runoff relationship with artificial neural network. J. Hydrol., 2004, 285, pp 96-113.

Raymond I.J., Coon G.C., 2003. True Form of Instantaneous Unit Hydrograph of Linear Reservoirs, Journal of Irrigation and Drainage Engineering, pp 11-17.

Reed D. W., 1992. Triggers to server floods: Extreme rainfall and antecedent wetness, Water resources and reservoir engineering, Thomas Telford, London, 1992.

Rodriguez-Iturbe I., Valdes J.B., 1979. The geomorphologic structure of hydrologic response, Water Resources Research, 15(6), pp 1409-1420.

Sahoo G.B., Ray C., DeCarlo E.H., 2006. Use of neural network to predict flash flood and attendant water qualities of a mountainous stream Oahu, Hawaii, Journal of Hydrology (2006), 327, pp 525 538.

Scanlon T.M., Raffensperger J.P., Hornberger G.M., Clapp R.B., 2000. Shallow subsurface storm flow in a headwater catchment: observations and modeling using a modified TOPMODEL, Water Resources Research, 36, 9, pp 2575-2586.

Scanlon T.M., Kiely G., Quishi X., 2004. A nested catchment approach for defining the hydrological controls on phosphorus transport, Journal of Hydrology, 291(3-4), pp 218-231.

Schulte R.P.O., Diamond J., Finkele K., Holden N.M. and Brereton A.J., 2005, Predicting the Soil Moisture Conditions of Irish Grasslands. Irish Journal of Agricultural Research 44, pp 95-110.

Shaw M.S., 1994. Hydrology in Practice, Third Edition, Chapman and Hall Editions.

Sherman L.K., 1932. Stream flow from rainfall by the unit-graph method, Engrg. News Rec., 108, pp 501-505.

Smith R.M.S, Evans D.J, Wheater H.S., 2005. Evaluation of two hybrid metric-conceptual models for simulating phosphorus transfer from agricultural land in the River Enborne, a lowland UK catchment, Journal of Hydrology, 304(2005), pp 366-380.

Soil Conservation Service (SCS), 1972. National Engineering Handbook, Section 4, Hydrology. U.S. Dept. of Agriculture (available from U.S. Government Printing Office), Washington, DC.

Steinmann E., 2005. An Investigation of Flood Forecasting using a Physically-Based Rainfall-Runoff Model, M.Eng.Sc Thesis, University College Cork, Cork, 119 pp.

Tilford K.A., Sen K., Chatterton J. B., Whitlow C., 2003. Environment Agency /DEFRA R&D Technical Report W5C-013/5/TR.

Wagener T., Wheater H. S., Gupta H.V., 2004, Rainfall-Runoff Modeling in Gauged and Ungauged Catchments, Imperial College Press, London, England, 306 pp.

Wagener T., lees M.J., Wheater H. S., 2000. Incorporating predictive uncertainity into a rainfall-runoff modeling system. Proceedings of Hydroinformatics 2000 Conference, on CD, Iowa, USA.

Webster P., Ashfaq A., 2002, Comparison of UK flood event characteristics with design guidelines, Water and Maritime Engineering 156 (2003), pp 33-40.

Wheater H.S., Jakeman A.J. and Beven K.J., 1993. Progress and direction in rainfall-runoff modelling. In: A.J. Jakeman, M.B. Beck and M.J. McAleer (Editors), Modelling change in environmental systems. John Wiley & Sons, pp. 101-132.

Wilson E.M., 1990. Engineering Hydrology, Fourth Edition, McMillan Education Ltd Editions.

# Appendix A

**Matlab Code for the rainfall and baseflow separation**

```
%[RF,effective_rain]=RAINFALL_SEPARATION(R,F,flow_points,rain_points)
%INPUT
%stat=duar/drom/kill
%R=rainfall data vector
%F=flow data vector
%flow_points=start of the rising limb, peak, end of the runoff
hydrograph
%rain_points=start and en of the rain event
%OUTPUT
%RF= Response Flow
%effective rain=rain - losses

function
RF,effective_rain]=RAINFALL_SEPARATION(R,F,flow_points,rain_points)
if stat=='duar'
    cd 'C:\matwork\duarigle';
    load ('duar_rain.mat');
    rain_stat=rain_duar;
    cd 'C:\matwork\duarigle\OPW'
    load UH_IUH.mat
    area=245;
elseif stat=='drom'
    cd 'C:\matwork\drom';
    load ('drom_rain.mat');
    rain_stat=rain_drom;
    cd 'C:\matwork\drom\OPW'
    load UH_IUH.mat
    area=861;
elseif stat=='kill'
    cd 'C:\matwork\killavulen';
    load ('kill_rain.mat');
    rain_stat=rain_kill;
    cd 'C:\matwork\killavulen\OPW'
```

```
    load UH_IUH.mat
    area=1292;
end
%x=[x1,x2,x3]=start,peak,end
[flow_points(1,3).Position(1),flow_points(1,2).Position(1),flow_points(1
,1).Position(1)];
%Y=[y1,y2]
Y=[flow_points(1,3).Position(2),flow_points(1,2).Position(2),flow_points
(1,1).Position(2)];

%--------- LAG TIME ----------------------------------
r1_date=rain_points(1,2).Position(1,1);r1=floor(r1); %time of first rain
r2_date=rain_points(1,1).Position(1,1);r2=floor(r2); %time of last rain
r1= (r1_date - R(1,1)) / (1/24) +2; %index of R where the first rain is
r2= (r2_date - R(1,1)) / (1/24) +1; %index of R where the last rain is
%rain is extracted from R
for i=r1:r2
    rain(i-r1+1,1)=R(i,1);
    rain(i-r1+1,2)=R(i,2);
end
%rain_centroid : = (t1rain1 + t2rain2 + t3rain3 + ...) /
(rain1+rain2+rain3+...)
%(centroid is a kind of barycenter)
for i = 1 :length(rain)
    tR(i) = rain(i,1)*rain(i,2);
end
rain_centroid= (sum(tR)) / (sum(rain(:,2)));
rain_centroid= floor( rain_centroid/(1/24) ) * (1/24);

for i=1:length(R)
    if datestr(F(i,1),'dd-mmm-yyyy
HH:MM:SS')==datestr(rain_centroid,'dd-mmm-yyyy HH:MM:SS')
        rain_centroid_index=i;break
    end
end
%lag time = (flow peak) - (rain centroid)
LAG = flow_points(1,2).Position(1) - rain_centroid;
```

```
LAG = floor( LAG/(1/24) )* (1/24); % to make it multiple of (1/24 JD = 1
hour)
%1 index unit = 1 hour = 1/24 JD
LAG_index= LAG / (1/24);
end_index=r2 + 4*LAG_index;
%-----------------------------------------------------------------

xi=[flow_points(1,3).Position(1):1/24:F(end_index,1)];%every hour
between x1 and x2
if xi(end)~=F(end_index,1) %because of the approximation 1/24=0.0417
xi=[xi,F(end_index,1)];
end

x=[flow_points(1,3).Position(1),F(end_index,1)];
Y=[flow_points(1,3).Position(2),F(end_index,2)];
yi = interp1(x,Y,xi); %interpolates the line between the two points =
baseflow

resp_flow=zeros(length(F),2);
for i=1:length(F)     %date
    resp_flow(i,1)=F(i,1);
end
%resp_flow=the peak with the whole time period
%RF=the peak only
for i=[flow_points(1,3).DataIndex:end_index]
        resp_flow(i,2)=F(i,2)-yi(i-flow_points(1,3).DataIndex +1);
        RF(i-flow_points(1,3).DataIndex+1,1)=resp_flow(i,1);
        RF(i-flow_points(1,3).DataIndex+1,2)=resp_flow(i,2);
end

%flow_centroid : = (t1RF1 + t2RF2 + t3RF3 + ...) / (RF1+RF2+RF3+...)
for i = 1 :length(RF)
   tRF(i) = RF(i,1)*RF(i,2);
end
RF_centroid= (sum(tRF)) / (sum(RF(:,2)));
RF_centroid= floor( RF_centroid/(1/24) ) * (1/24);
```

```
total_rain_volume=sum(rain(:,2));
peakflow_mm(:,1)=RF(:,1);
peakflow_mm(:,2)=1000*RF(:,2)*3600/(area*10.^6); %peakflow in mm (not in
m3/s)
total_peakflow_volume=sum(peakflow_mm(:,2));

PR = total_peakflow_volume / total_rain_volume ;%the percentage runoff

%-------- option_rainfall = DECREASING PROPORTIONAL LOSS --------------
%the calculation are made for 9am to 9am days
if str2num(datestr(rain(1,1),'HH'))<9
event_start_9am=datenum(datestr(rain(1,1),'dd/mm/yyyy'),'dd/mm/yyyy')+9/
24 -1 ;
else
event_start_9am=datenum(datestr(rain(1,1),'dd/mm/yyyy'),'dd/mm/yyyy')+9/
24;
end
%event_start_9am is "9am time" before the event starts
five_days_before= event_start_9am - 5; %still at 9am

l=length(rain_stat);
for i=1:l
    if rain_stat(i,1)==five_days_before
        i1=i;break
    end
end
for i=i1:l
    if rain_stat(i,1)==event_start_9am
        i2=i;break
    end
end
for i=i1:i2
    antecedent_rain(i-i1+1,1)=rain_stat(i,1);
    antecedent_rain(i-i1+1,2)=rain_stat(i,2);
end

for i=1:5 % P(1)=rainfall one day ago, P(i)=rainfall i days ago ...
    P(6-i)=sum(antecedent_rain(24*(i-1)+1:24*i,2));
```

```
end
%API5 is the API5 value on the starting day at 9am
API5=0.5*(P(1)+0.5*P(2)+(0.5.^2)*P(3)+(0.5.^3)*P(4)+(0.5.^4)*P(5));
API=[];
l=length(rain_stat);
for i=1:l
    if rain_stat(i,1)==event_start_9am
        i3=i;break
    end
end
%-------------------------------------------------------------------
R1=rain_points(1,2).Position(1,1);
start_rain_fixed=floor(R1)+floor((R1-floor(R1))/(1/24))*1/24;
R1=start_rain_fixed;%time of first rain FIXED
R2=rain_points(1,1).Position(1,1);
enddate_rain_fixed=floor(R2)+floor((R2-floor(R2))/(1/24))*1/24;
R2=enddate_rain_fixed;%time of last rain FIXED
%-------------------------------------------------------------------
for i=i3+1:l
    if abs(rain_stat(i,1)-R2)<1/1440
        i4=i;break
    end
end
API(1,1)=event_start_9am;
API(1,2)=API5;
smd(1,1)=event_start_9am;
smd(1,2)=SMD( datestr(event_start_9am,'dd/mm/yyyy') );
for i=i3+1:i4
    API(i-i3+1,1)=rain_stat(i,1);
    API(i-i3+1,2)=API(i-i3,2)*(0.5.^(1/24))+rain_stat(i-
1,2)*(0.5.^(1/48));
    smd(i-i3+1,1)=rain_stat(i,1);
    smd(i-i3+1,2)=max(smd(i-i3+1-1,2)-rain_stat(i,2),0);
end
for i=i3:i4
    RR(i-i3+1,1)=rain_stat(i,1);
    RR(i-i3+1,2)=rain_stat(i,2);
    CWI(i-i3+1,1)=API(i-i3+1,1);
```

```
    CWI(i-i3+1,2)=125+API(i-i3+1,2)+smd(i-i3+1,2);%CWI= API + 125 (+SMD)
    RCWI(i-i3+1,1)=API(i-i3+1,1);
    RCWI(i-i3+1,2)=CWI(i-i3+1,2)*RR(i-i3+1,2);
end
Fa= total_peakflow_volume / (sum(RCWI(:,2))) ;
for i=1:length(CWI)
    PR2(i,1)=CWI(i,1);
    PR2(i,2)=CWI(i,2)*Fa;
end
for i=1:length(CWI)
    if CWI(i,1)==rain(1,1)
        i5=i;break
    end
end
for i=i5:length(PR2)
    effective_rain(i-i5+1,1)=PR2(i,1);
    effective_rain(i-i5+1,2)=PR2(i,2)*RR(i,2);
    infiltration(i,2)=(1-PR2(i,2))*RR(i,2);
end
```

# Appendix B

**Matlab code for the event Unit Hydrograph Derivation**

```
%function DER stands for (UH) derivation
%stat=duar/drom/kill
%RF=Response flow=direct runoff
%effective_rain=rainfall - losses
%OUTPUT=UNIT HYDROGRAPH with OR ,Nash IUH and GUHR

function [U_ord,U_nas,U_mor]=DER(stat,RF,effective_rain)
%UNIT HYDROGRAPH DERIVATION = ORDINATES METHOD ------------------------
Y=RF(:,2);
p=length(effective_rain); %p=number of rainfall imputs
m=length(Y); %m=length of the peak hydrograph
n=m-p+1; %n=size oh the UH
X=zeros(m,n);
%convolution
for j=1:n
    for i=1:p
        X(i+j-1,j)=effective_rain(i,2);
    end
end
U=inv(X'*X)*X'*Y;%U=Unit hydrograph, obtained by the least square method
UH_ord=U;
YY=X*UH_ord;
uh=U;
%smoothing process
uh_smoo=[0;uh;0];
ls=length(uh_smoo)-1;
for i=1:ls-2
uh_smoo(ls-i)=(uh_smoo(ls-i-1)+uh_smoo(ls-i)+uh_smoo(ls-i+1))/3;
end
for i=2:length(uh_smoo)-1
uh_smoo(i)=(uh_smoo(i-1)+uh_smoo(i)+uh_smoo(i+1))/3;
end
UH_ord_smoo=uh_smoo(2:end-1,1);
```

```
YYY=X*UH_ord_smoo;
RF_ord=YYY;

%----BASIC METHOD ----------------------------------------------------
RF_mm(:,2)=1000*RF(:,2)*3600/(area*10.^6);
tot_peak_vol=sum(RF_mm(:,2));
UH_bas=RF(:,2)/tot_peak_vol;
%convolution
for i=1:length(effective_rain)
    for j=1:length(UH_bas)
        resp_basic(j+i-1,i)=effective_rain(i,2)*UH_bas(j);
    end
end
for i=1:length(resp_basic)
    Y_basic(i)=sum(resp_basic(i,:));
end
RF_bas=Y_basic;

%-----NASH IUH ---------------------------------------------------------
M1RF=0;%1st moment of storm runoff=SR=RF
M2RF=0;
SR(:,1)=(RF(:,1)-RF(1,1))*24;
SR(:,2)=RF(:,2);
for i=1:length(SR)
    SQT(i)=SR(i,1)*SR(i,2);
    SQT2(i)=(SR(i,1).^2)*SR(i,2);
end
M1RF=(sum(SQT)) / (sum(SR(:,2)));
M2RF=(sum(SQT2)) / (sum(SR(:,2)));

SR_area=sum(SR(:,2))*1; %toal area under the graph, in (m3/s).h
SR_arm=SR(:,1)+0.5;
for i=1:length(SR)
    num_SR1(i)=SR_arm(i)*SR(i,2)*1; %1st moment numerator in h*m3/s*h
    num_SR2(i)=(SR_arm(i).^2)*(SR(i,2)*1);
end
M1SR=sum(num_SR1)/SR_area; %first moment in h.
M2SR=sum(num_SR2)/SR_area; %second moment in h^2
```

```
M1eff=0;M2eff=0;
P=effective_rain;
P(:,1)=(P(:,1)-P(1,1))*24;
P(:,2)=P(:,2)/(1000*3600)*(area*10.^6); %in cumsec

for i=1:length(P)
    SPT(i)=P(i,1)*P(i,2);
    SPT2(i)=(P(i,1).^2)*P(i,2);
end
M1eff=(sum(SPT)) / (sum(P(:,2)));
M2eff=(sum(SPT2)) / (sum(P(:,2)));

P_area=sum(P(:,2))*1; %toal area under the graph, in (m3/s).h
P_arm=P(:,1)+0.5;

for i=1:length(P)
    num_P1(i)=P_arm(i)*P(i,2)*1; %1st moment numerator in h*m3/s*h
    num_P2(i)=(P_arm(i).^2)*(P(i,2))*1;
end

M1P=sum(num_P1)/P_area; %first moment in h.
M2P=sum(num_P2)/P_area; %second moment in h^2

k=0;n=0;
%application of the moments method
k=( M2RF - M2eff -2*(M1RF - M1eff)*M1eff - (M1RF-M1eff).^2 ) / ( M1RF -
M1eff) ;
n=( M1RF - M1eff) / k;
%check the results for k and n
k2=( M2SR - M2P -2*(M1SR - M1P)*M1P - (M1SR-M1P).^2 ) / ( M1SR - M1P) ;
n2=( M1SR - M1P) / k2;

XX=[0:50];%truncated at 50 hours. no infinite tail
for i=1:length(XX)
    UH_nas(i)=1/(k*gamma(n)) * exp (-XX(i)/k) * (XX(i)/k).^(n-1);
    UH_nas2(i)=1/(k2*gamma(n2)) * exp (-XX(i)/k2) * (XX(i)/k2).^(n2-1);
```

```
end
UH_nas3=UH_nas*(area*10.^6)/(1000*3600);

%checking
for i=1:length(P(:,2))
    for j=1:length(UH_nas)
        Resp(j+i-1,i)=P(i,2)*UH_nas(j);
    end
end
for i=1:length(Resp)
    RESP(i)=sum(Resp(i,:));
end
RF_nas=RESP;
UH_nas=UH_nas3;

%-----GUHR ----------------------------------------------------------
n=length(A); %number of reservoirs
GUHR=[];
for i=1:n
    iA(i)=i*A(i);
end
K=sum(A)*(M1RF-M1eff)/sum(iA);
dt=1;
for t=1:50 % for t >dt
    for i=1:n
        for j=i:n
            inter2(j)= 1/(gamma_paul(j-i))*( ((t-dt)/K).^(j-i)) *
sum(A(j:end) );
        end
        inter1(i)=1 / (gamma_paul(i-1)) * (t/K).^(i-1) *
sum(inter2(i:n));
        inter3(i)=1 / (gamma_paul(i-1)) * (t/K).^(i-1) * sum(A(i:end));
    end
        GUHR(t)=1/dt*( exp(-(t-dt)/K)/sum(A)*sum(inter1) - exp(-
t/K)/sum(A)*sum(inter3) );
end
Resp_GUHR2=[];RESP_GUHR2=[];
for i=1:length(effective_rain)
```

```
      for j=1:length(GUHR)
            Resp_GUHR2(j+i-1,i)=effective_rain(i,2)*GUHR(j);
      end
end
for i=1:length(Resp_GUHR2)
   RESP_GUHR2(i)=sum(Resp_GUHR2(i,:));
end
UH_mor=GUHR;
RF_mor=RESP_GUHR2;
```

# Appendix C

**Matlab Code for the Unit Hydrograph Simulation**

```
%[RF_nas,RF_ord,RF_mor]=SIM(stat,RF,effective_rain,A_ord,A_nas,A_mor)
%function SIM stands for simulation
%stat=duar/drom/kill
%RF=Response flow=direct runoff
%effective_rain=rainfall - losses
%A_ord,A_nas,A_mor are the respective UHs
%OUTPUT=Response Flows with OR ,Nash IUH and GUHR

function
[RF_nas,RF_ord,RF_mor]=SIM(stat,RF,effective_rain,A_ord,A_nas,A_mor)
%-------------------------------------------------------------------------
%Unit hydrograph convolution : ORDINATES METHOD
X=[];UH=[];
UH=A_ord';
p=length(effective_rain); %p=number of rainfall imputs
n=length(UH);
m=n+p-1; %n=size oh the UH
X=zeros(m,n);
for j=1:n
    for i=1:p
        X(i+j-1,j)=effective_rain(i,2);
    end
end
RF_ord=X*UH;
%--------------------Unit hydrograph convolution : NASH IUH METHOD
UH=[];X=[];UH=A_nas';
p=length(effective_rain); %p=number of rainfall imputs
n=length(UH);
m=n+p-1; %n=size oh the UH
X=zeros(m,n);
for j=1:n
    for i=1:p
        X(i+j-1,j)=effective_rain(i,2);
```

```
    end
end
RF_nas=X*UH;
%----------------------Unit hydrograph convolution : GUHR METHOD
UH=[];X=[];UH=A_mor';
p=length(effective_rain); %p=number of rainfall imputs
n=length(UH);
m=n+p-1; %n=size oh the UH
X=zeros(m,n);
for j=1:n
    for i=1:p
        X(i+j-1,j)=effective_rain(i,2);
    end
end
RF_mor=X*UH;
%------------------------plots the different simulation results
figure(222), plot(RF(:,2),'b'),hold on,
plot(RF_ord,'r')
plot(RF_nas,'g')
plot(RF_mor,'k')
legend('Observed','Odrinates','Nash IUH','GUHR')
hold off
```